PREDICTION OF COOLING OF THE NOCTURNAL ENVIRONMENT USING TWO ATMOSPHERIC MODELS

By

PAUL HEINZ HEINEMANN

A DISSERTATION PRESENTED TO THE GRADUATE SCHOOL
OF THE UNIVERSITY OF FLORIDA IN
PARTIAL FULFILLMENT OF THE REQUIREMENTS
FOR THE DEGREE OF DOCTOR OF PHILOSOPHY

UNIVERSITY OF FLORIDA

1985

ACKNOWLEDGEMENTS

I would like to extend my deepest thanks to my major professor, Dr. J. David Martsolf, for making this project challenging and worthwhile, and for his guidance and support. I would also like to thank the members of my committee, Dr. James Henry, Dr. James Jones, and Dr. John Gerber, for their assistance and insights whenever needed. Dr. Michael Burke was also of great help in the early part of this program.

Many thanks also go to "the team," Ferris Johnson, Gene Hannah, Mike Baker, Fred Stephens, Bob Dillon, Dana Shaw, Doyle Davidson, Cathy Weaver, Debra Cox, Susan Oswalt, Cheri Lazar, Ellen McMullan, Eileen Grimes, John Orthoefer, Carol Vaughn, and Gary Venn, for any and all help they have given me.

Finally, my love and thanks go to my parents, for letting me make life's important decisions with support and guidance, but without interference.

TABLE OF CONTENTS

LIST OF TABLES

LIST OF FIGURES

Page

LIST OF SYMBOLS

symbol	meaning	units
B	background radiative flux	$W\ m^{-2}$
b	distance from central location to surrounding stations	m
C_a	air volumetric specific heat	$J\ K^{-1}\ m^{-3}$
C_g	soil heat capacity	$kJ\ C^{-1}\ m^{-3}$
C_p	air heat capacity	$kJ\ C^{-1}\ m^{-3}$
c_p	air specific heat	$kJ\ kg^{-1}\ C^{-1}$
C_s	soil specific heat	$kJ\ kg^{-1}\ C^{-1}$
e	ambient vapor pressure	mb
e_s	saturation vapor pressure	mb
f	coriolis parameter	s^{-1}
H	air layer sensible heat flux	$W\ m^{-2}$
H_o	heat flux removed from surface by turbulence	$W\ m^{-2}$
h	parameter related to height of nocturnal boundary layer	m
I	long wave atmospheric back radiation	$W\ m^{-2}$
k	von Karmann constant	dimensionless
K_h	convective heat transfer coefficient	$m^2\ s^{-1}$
K_h	turbulent exchange coefficient for heat	$m^2\ s^{-1}$

K_m	turbulent exchange coefficient for momentum	$m^2\ s^{-1}$
k_m	1.18	
K_s	thermal conductivity	$W\ m^{-1}\ C^{-1}$
L	monin length	m
l	parameter that characterizes size of turbulent eddy	m
p	atmospheric pressure	kpa
p	input variable or parameter to be analyzed (sensitivity)	
p_o	pressure at a central location	mb
R	surface radiative flux	$W\ m^{-2}$
R	ideal gas constant	$J\ kg^{-1}\ K^{-1}$
R_c	critical Richardson Number	dimensionless
Ri	Richardson Number	dimensionless
R_n	net radiation	$W\ m^{-2}$
S	solar insolation	$W\ m^{-2}$
S	soil heat flux	$W\ m^{-2}$
s	wind shear	$m\ s^{-1}/m$
T	temperature	K or C
T_d	dew point temperature	K or C
T_s	soil temperature	K or C
T_1	temperature in first upper air layer	K or C
t	time	s
U	relative humidity	dimensionless
U_9	9 m wind speed	$m\ s^{-1}$
U_*	friction velocity	$m\ s^{-1}$

u, v	east-west and north-south wind components	$m\ s^{-1}$
W_1	wind velocity in first upper air layer	$m\ s^{-1}$
w	mixing ratio	dimensionless
x, y, z	spatial coordinates	m
x	R/C_p	dimensionless
y	output variable to be analyzed (sensitivity)	
z	depth or height	m
z_o	roughness length	m
z_1	height of surface air layer	m
α	undefined	
β	derived value for linear wind profile	
ρ	air density	$kg\ m^{-3}$
θ	potential temperature	K
σ	Stephan-Boltzmann constant	$W\ m^{-2}\ K^{-4}$
ε	emissivity	dimensionless
ϕ	geographic latitude	degrees
ω	angular velocity of earth's rotation	s^{-1}

Abstract of Dissertation Presented to the Graduate School of the University of Florida in Partial Fulfillment of the Requirements for the Degree of Doctor of Philosophy

PREDICTION OF COOLING OF THE NOCTURNAL ENVIRONMENT USING TWO ATMOSPHERIC MODELS

By

Paul Heinz Heinemann

December 1985

Chairman: J. David Martsolf
Major Department: Horticultural Science (Fruit Crops)

Two atmospheric models were used to predict nocturnal cooling in a vegetated environment. The results from both models were compared with the observed temperatures to determine which model predicted the cooling curve more accurately. Blackadar's Boundary Layer Model (BLM) was tested against the original Satellite Frost Forecast System prediction model, called the P-model. Upper air soundings obtained from the National Weather Service computer network and local characteristics of the nocturnal environment were processed into Boundary Layer Model input files. Ground station measurements were used as input to the P-model, and remotely-sensed temperatures from Geostationary Operational Environmental Satellite (GOES West) were used as input to a modified P-model. The models were run on a real-time basis on the eve of 23 advective and radiative nights. Model output was analyzed for two Florida locations, Gainesville and Ruskin.

The BLM predicted temperatures with more precision than both the P-model and the modified P-model for both sites. The 95% confidence intervals from t-tests run to determine significant difference between predicted minus observed and zero averaged ± 1.7 C for the BLM at Gainesville, ± 2.9 C for the P-model and modified P-model at Gainesville, ± 1.4 C for the BLM at Ruskin, and ± 4.6 C for the modified P-model at Ruskin. A BLM-predicted temperature bias of + 3.35 C at the Gainesville site was attributed to the interpolation procedure that produced a sounding for Gainesville from the Waycross and Ruskin soundings.

Temperature predictions have a direct application to horticultural users in frost protection management decisions. Prediction of temperature versus time provides information on when critical temperatures are being reached, the duration of those temperatures, and the minimum temperature.

INTRODUCTION

Temperature predictions aid in frost protection decisions, providing the horticultural user warnings of critical temperatures. Frost night temperature forecasts are usually limited to minimum temperature, but prediction of cooling rates in small time increments would be much more beneficial. A predicted cooling curve could provide the user with not only minimum temperature, but also time of occurrence of mimimum temperature, time of occurrence of critical temperature, and duration of critical temperature. The high cost of heating oil, wind machine fuel, and limited water in Florida are incentives to conserve these resources. Readily available temperature predictions may enable a horticulturist to save hours' worth of fuel or water during the winter.

Frost protection originated thousands of years ago (Martsolf, 1979b), but temperature prediction efforts are documented in more recent history (Georg, 1971). The earliest prediction formulae date back to the late 1800s. The incentive to develop methods of local temperature predictions began with agricultural needs, after severe freeze damage to agricultural crops occurred in the western states. Early predictions employed simple empirical formuli, but much more elaborate theoretical and empirical methods have been used ever since.

The Federal-State Frost Warning Service has been providing frost night temperature predictions on an operational basis for over 50 years. The Satellite Frost Forecast System (SFFS) was developed as an aid to that

service (Figure 1). SFFS provided satellite-sensed temperature maps of Florida and computer-produced temperature predictions for several locations in the state to National Weather Service forecasters in Ruskin, Florida, where the frost forecasts were made. The computer-produced predictions were calculated from a model that simulated the surface energy balance under nocturnal conditions. This model, called the P-model, used automated weather station data as input. The opportunity arose to obtain a second model capable of predicting temperatures. This model, Blackadar's Boundary Layer Model, was a more rigorous treatment of the atmospheric boundary layer than the original SFFS model (Blackadar, 1979). The model has been used by Blackadar mostly for educational and demonstration purposes. This is an application of the model under a specific condition--cold nights in Florida.

The purpose of this study is to apply the Boundary Layer Model to the Florida nocturnal environment, compare its predictions and the P-model predictions with the observed cooling curve, and determine which model provides a more realistic prediction of the observed cooling curve.

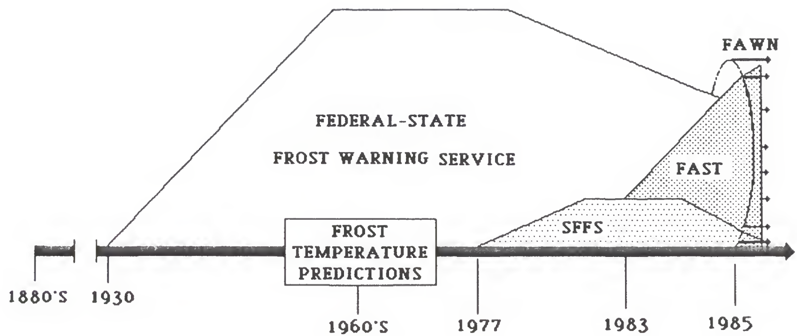

Figure 1. Time-line diagram of services that provide temperature predictions and other agricultural weather information to users in Florida. FAST and FAWN are explained in the Literature Review. Vertical axis represents relative importance.

LITERATURE REVIEW

This project was developed as part of the Satellite Frost Forecast System (SFFS). The forecasting aspect of SFFS dealt with the use of a temperature prediction model. Therefore, the review covers two areas: The Satellite Frost Forecast System, to provide a historical background of the temperature prediction effort in Florida; and atmospheric modeling, to show examples of other applied research in the area of prediction of atmospheric variables.

The Satellite Frost Forecast System

The Satellite Frost Forecast System was developed through contracts with the National Aeronautics and Space Administration (NASA), with the original goal of providing GOES (Geostationary Operational Environmental Satellite) thermal infrared images and results of a temperature prediction model to National Weather Service (NWS) forecasters. These images and predictions were to aid the forecasters in making predictions during frost nights. Several reports from the Climatology Laboratory at the University of Florida to NASA document the details of the system development from 1977 to 1983 (Martsolf, 1983a).

Bartholic and Sutherland (1978) described a data collection station network. Twelve stations located around the state of Florida collected hourly measurements of air temperature, wind speed, soil temperature, dew

point temperature, and net radiation. These measurements were made manually by volunteers. The measurements were used as input to a temperature prediction model, called the Physical model (or P-model) (Bartholic and Sutherland, 1978; Sutherland, 1980). The P-model was developed for SFFS and based on previous efforts by Georg (1971). The P-model simulated a soil surface energy balance. It provided 1.5-m air temperature predictions throughout a frost night for several locations across Florida. Sutherland (1980) reported that the model predicted within 3 C of the observed temperature in 98% of 141 runs and within 2 C in 81.6% of the runs during the winter of 1977-1978. The use of synoptic forecasts of radiation and wind speed as model input increased its accuracy. Further examples of P-model results were given by Martsolf and Gerber (1981). The P-model predictions were considered satisfactory, with mean errors of -0.4 C and -0.2 C for two given examples, but the standard deviations were high, indicating large variability in the hour-to-hour predictions:

The Geostationary Operational Environmental Satellite (GOES) East images were obtained on a near real-time basis to aid forecasters in frost temperature prediction (Barnett et al., 1980). The maps were originally obtained from the National Oceanic and Atmospheric Administration (NOAA) in Miami, Florida, through phone lines (Sutherland et al., 1979; Gaby, 1980). A Hewlett-Packard (HP) minicomputer located at the NWS forecasting office in Ruskin, Florida, called Miami hourly and downloaded data covering the state of Florida. The satellite data were transmitted through phone lines by analog signal, then digitized into map form by the HP computer. The data were sampled in order to present an undistorted image of Florida, but this process reduced the data and introduced some errors. However, the errors were insignificant for qualitative evaluation of the temperatures

over this large an area. The idea of providing these maps to agricultural users was proposed at this early date (Bartholic and Sutherland, 1978). One method proposed was to display the maps on a grower's home television screen through use of electronics similar to what was used in home television games. Personal computers were not yet readily available.

P-model predictions from ten sites were used as input to a second model, called the S-model (Bartholic and Sutherland, 1978). The S-model used an observed satellite map as a base, and extrapolated the temperature changes with time from the P-model across the base map to produce a forecasted map. This map was identical in appearance to the observed map, but showed predicted instead of observed temperatures in color-coded ranges.

The acquisition of digital satellite data from NOAA files at the National Meteorological Center (NMC) in Camp Springs, Maryland, began in 1979, replacing the digital-to-analog, analog-to-digital procedure (Martsolf, 1979a). The reduction of conversions improved the accuracy of the incoming data, although the maps appeared to have a decrease in resolution due to the removal of smoothing between conversions.

Martsolf (1980) described improvements in SFFS from its early years. The collection stations were automated during the Fall of 1979. The Ruskin computer would interrogate a microprocessor on each automated weather station to acquire wind speed and temperature measurements. The measurements were then automatically read by the P-model.

The system began to move into a second phase about this time, with the beginning of dissemination to agricultural users (Martsolf, 1980). An experimental microcomputer network was developed between two county extension offices and the SFFS computer in Gainesville, allowing the transfer of maps to the agricultural sector. APPLE II microcomputers

called into the SFFS HP computer through modems and phone lines to download the satellite maps. Methods for direct interface between agricultural users and SFFS were proposed.

Satellite data acquisition success and automated weather station access success were documented by Martsolf and Gerber (1981). The success rate of acquiring maps from NMC varied from 7% to 100% which was considered unsatisfactory. Most acquisition failures were due to unavailability of maps in the queue at NMC. A direct digital downlink to GOES at Gainesville was proposed. The direct dissemination system to agricultural users expanded to six county extension offices. All acquired the satellite data with APPLE II computers through phone lines (Martsolf, 1981).

The capability of SFFS map acquisition increased greatly after the installation of a direct digital downlink with GOES (Martsolf, 1982). The direct link upgraded the access rate of maps from every hour to every half hour and doubled the number of pixels per map. The addition of the Institute of Food and Agricultural Sciences (IFAS) VAX 750 computer as another node in the system was also described by Martsolf. The information was transmitted to the VAX on a regular basis through a 4800-baud dedicated line. The VAX allowed anyone associated with IFAS that had access to a microcomputer or terminal to obtain SFFS weather data. The number of agricultural extension offices in the network grew to 10. Martsolf mentions the possible use of a Control Data Corporation CYBER 730 to aid in acquisition and dissemination.

Jackson and Ferguson (1983) developed an experimental microcomputer network to disseminate SFFS information and other products to growers. The system, called LOIS (Lake-Orange Information System), used the county extension office APPLE II+ microcomputers as nodes to growers who had

their own microcomputers. Initially, eight growers would call the extension offices through modems and phone lines to download relevant information. Users could call in as often as they wished except during freeze nights when demand increased considerably.

The Satellite Frost Forecast System began acquiring text weather information from NWS through a dedicated phone line between Ruskin and the SFFS computer in Gainesville (Martsolf, 1983a). A listen-only link was made between the NWS HP computer in Ruskin and the Automated Field Operational System (AFOS), which is the NWS computer network through which weather information is passed. This link was initially established to obtain dew point temperatures from the State Weather Roundups to be used as an additional input to the P-model (Martsolf, 1983b). It was found that the dew points were still sufficiently high in the early evening of a frost night to cause the P-model to underpredict. The use of forecasted dewpoint minima was tried with more success. The NWS fruit frost forecasters requested that the system permit the delivery of their minimum temperature forecast from AFOS to SFFS users through this link. The establishment of the AFOS link also allowed other text information to be obtained via the same link. The text data included zone, agricultural weather and freeze forecasts, weather roundups, and radar summaries.

An experiment to use satellite data as input to the P-model was made by Heinemann and Martsolf (1984). The average of nine pixels from each automated weather station location was calculated and used as surface temperature. The success of the predictions was limited; the procedure worked for areas that were clear and dry, but the presence of clouds or moisture interfered with the correct measurements of surface temperatures, reducing the prediction accuracy.

Development of rainfall products began on the system (Martsolf et al., 1984; Heinemann et al., 1984). Manually digitized radar (MDR) data from seven radar stations covering the state of Florida were acquired through AFOS. The cold cloud top temperatures shown by the infrared satellite measurements usually indicated an area of rain; the low resolution MDR (32 km) verified the presence and intensity of rain. Overlay of the satellite data onto the MDR increased the rainfall resolution to 6 x 8 km areas.

Martsolf (1983b) gave a description of the possible successor to SFFS, Florida Agricultural Services and Technology, Inc. (FAST), which was designed to be a not-for-profit organization to disseminate weather and other products to users not associated with IFAS. The development of products such as the rainfall maps and acquisition of the text information made this effort feasible. They began using a CYBER 730 to act as a node to the public.

Florida Agricultural Services and Technology was in operation by the Spring of 1984 (Martsolf, et al. 1985). In the near future, the FAST CYBER is expected to become the hub of the weather information acquisition and dissemination system, which will be called FAWN (Florida Agricultural Weather Network).

Modeling

Modeling is a useful method of gaining a better understanding of real world processes. This review covers models that pertain to the atmospheric boundary layer processes, temperature prediction, and large scale atmospheric predictions.

Atmospheric prediction models can be divided into several categories. The atmospheric processes affecting global circulation actually begin at the microscale (less than 1 km) and extend through the synoptic scale (greater than 100 km). Kolsky (1972) estimated that a model that encompasses all aspects of atmospheric processes would need a scale ratio on the order of 10^{10}, which even with today's supercomputers would be unreasonable. Therefore, the physical models are divided into synoptic, mesoscale, and microscale regimes.

The first major large scale numerical weather forecasts were attempted by Richardson (1922). Primitive hydrodynamic equations formed the base of his model. Richardson proposed applying the model to an operational weather network, but there were two major problems with Richardson's approach. First, poor data for the initial conditions and inclusion of gravity and sound waves, referred to as 'noise' by Charney (1949), greatly amplified errors through the forecast period. Second, in that pre-computer era, the numerical process was quite cumbersome, so no further serious efforts were made for another twenty years (Petterssen, 1956).

The invention of computers made simulations of physical processes feasible and practical. Complex models have been developed that can be run in reasonable time periods with the increased speed and size of computers.

Charney (1949) was responsible for filtering out meteorological noise by reducing the complexity of the equations. He determined that the high-speed gravity and sound waves had no significant effect on the larger and slower moving atmospheric motions. The first operational weather prediction model was the result of this work, and was known as the barotropic model. The barotropic model was a dynamic model based on continuity

equations, but all pressure surfaces were parallel; density, temperature, and pressure coincided. Because of this, the barotropic model neglected thermal advection, so new weather systems could not be developed by the model.

The limitations in the barotropic model led to the development of the baroclinic model (Haltiner, 1971). The baroclinic model contained more than one level to determine thicknesses between pressure surfaces, and the wind flow could cross isobars. This enabled the model to account for temperature advection and the development of new weather systems.

Combinations of these models were used to produce operational weather forecasts. Two operational weather prediction models are used by the National Meteorological Center. A six-layer baroclinic model based on primitive hydrostatic, hydrodynamic, and thermodynamic equations was developed by Shuman and Hovermale (1968). The model gridding was 380 km over the Northern Hemisphere. This model significantly improved the large-scale weather predictions over previous efforts. A finer grid model (190 km) known as the Limited Fine Mesh (LFM) is used over the United States and adjacent coastal waters (Holton, 1979).

A more complex forecasting model became operational in Europe, called the ECMWF (European Centre for Medium Range Weather Forecasts) model (Tiedtke, 1983). The ECMWF model consists of 15 levels. The grid spacing is presently 170 km, which is being improved to 100 km with the acquisition of a Cray XMP-22 (Kerr, 1985b). The synoptic model also includes mesoscale and microscale processes such as radiation, condensation, cumulus convection, and turbulence.

The latest model developed by the NMC is the Regional Analysis Forecast System (RAFS) (Kerr, 1985a), which has 16 vertical layers, and uses nested

grid spacing. The Western Hemisphere above the equator has a grid spacing of 320 km. A large square of 160 km is embedded within the 320-km spacing, and a second embedded square of 80-km grid spacing covers North America. The RAFS model improved prediction of some important processes over the LFM. Two examples are prediction of winter rainfall, both in coverage and total amounts, and the January 1985 freeze in Florida.

The large scale prediction models generally predict events occurring over thousands of kilometers spatially and several hours to several days temporally. Therefore, the output from these models feature synoptic processes such as movement and development of pressure systems. Output that predicts some of the smaller scale phenomena tends to be suppressed because of the volume of data produced.

Mesoscale (1 km to 100 km) and microscale models emphasize the smaller scale processes. Temporally, the models usually do not predict beyond 24 hours. The numerical procedure time increments are in minutes or seconds. Proper integration of the smaller scale models into the synoptic scale models can increase the accuracy of the large-scale predictions, but the limiting factor is computer capability. The following paragraphs provide some examples of mesoscale and microscale models.

One of the earlier mesoscale models was developed by Pielke (1974). Pielke modeled the sea breeze to predict shower activity along the convergence regions of Florida coastal winds. It was based on a moisture continuity equation and the horizontal and vertical equations of motion similar to those used in the synoptic scale models, but Pielke's model required greater resolution than that used in the large scale models. Some of the boundary layer parameterizations used were developed by Blackadar and Tennekes (1968).

The SFFS P-model was based on a surface energy balance model developed by Georg (1971). The Georg model simulated the balance between soil heat flux, surface radiation loss, background radiation, and convective heat exchange in the air layer just above the surface. The model used inputs from four soil temperatures, a surface temperature, a 1.5 m air temperature, wind speeds at 9 and 18 m, net radiation, and dew point temperature. The model produced good minimum temperature predictions when compared to observed values; twenty-six of the 45 predicted minimums were within 1 C of the observed.

Deardorff (1977) suggested a method of estimating the soil moisture fraction (measured soil moisture/saturation value) based on a rate equation. Most models involving soil properties usually hold the soil moisture constant. This method gave the diurnal variation of soil moisture fraction over several days. It involved bulk soil moisture content, soil-surface evaporation rate, and precipitation rate.

A one-dimensional numerical model simulating surface temperature and heat flux was developed by Carlson and Boland (1978). This model used K-type parameterization, included radiative flux divergence (0.15 C h^{-1} at night), and neglected advection. The model describes a 1.5-meter deep substrate beneath the earth's surface, a 50-meter surface layer which includes a transition layer over a crop canopy or urban surface, and a mixed layer above. They concluded that the thermal inertia and the moisture availability were the two most important parameters in this model, but that these are difficult to measure for heterogeneous urban and rural terrain.

A forest microclimate was modeled by Waggoner et al. (1969). The forest canopy energy exchange was simulated, based on radiant, sensible,

and latent heat fluxes. The model was used to study effects of stomatal changes on evaporation within the forest canopy. This model used an electrical network analogy, representing the various fluxes as flow and resistances.

Some prediction models were based on statistical rather than physical considerations. Aron (1975) used regression equations to predict the number of hours that air temperature would remain below a given threshold, in order to calculate chilling units. The regressions were based on a 16-year sample of hourly temperature and humidity measurements recorded at first order collection stations in California. Linear regression of predicted versus observed hours below the threshold temperature of 45 F gave a correlation coefficient on the order of 0.98.

Petersen (1976) described a model that simulates atmospheric turbulence, through the use of generalized spectral analysis. This model was based on a statistical approach. The model simultaneously generated all three velocity components, and dealt with velocity variations on the order of seconds.

A model to predict hourly temperatures through a purely statistical method was developed by Hansen and Driscoll (1977). The parameters are based on an 11-year developmental sample. Hansen and Driscoll concluded that the model is most effective for predictions of long-term temperature events, such as durations of temperatures above or below a certain point, and temperature extremes.

Parton and Logan (1981) developed a model that predicted diurnal variation in air and soil temperatures. The model used mathematical functions to determine temperature based on maxima and minima. A truncated sine wave was used for daytime temperatures and an exponential function

was used for nighttime temperatures. The results produced a maximum absolute mean error of 2.64 C for a 10-cm air temperature.

Another statistical temperature prediction model was developed by Miller (1981). This model, known as GEM, predicted temperatures and other meteorological variables up to 12 hours in advance. The predictions were calculated through multiple linear regression of local meteorological observations. The GEM model calculated the probability that a temperature will fall within a certain range for each hour.

MODELS AND METHODS

The two models used in this study were the P-model, which was the original SFFS prediction model, and Blackadar's Boundary Layer Model (BLM). The models were used to predict a cooling curve of a nocturnal environment. Although the two models are of different scales (BLM is mesoscale, the P-model is microscale), the energy balance approach used in the P-model is similar to some of the low-level microscale processes simulated by the BLM. This and the willingness and cooperation of the BLM's author in allowing the BLM to be used for this study were the main reasons for the selection of this particular model. The BLM was obtained directly from Dr. Alfred Blackadar by computer-to-computer link over phone lines (Blackadar, 1983, personal communication). This section describes the important physics and equations of each model. Each model is divided into discernible modules, each module representing a physical process simulated by the model.

The Models

The P-model

The P-model simulates a soil surface energy balance (Sutherland, 1980) (Figure 2). The model is based on previous work by Georg (1971). The model can be divided into three modules, each representing the rate

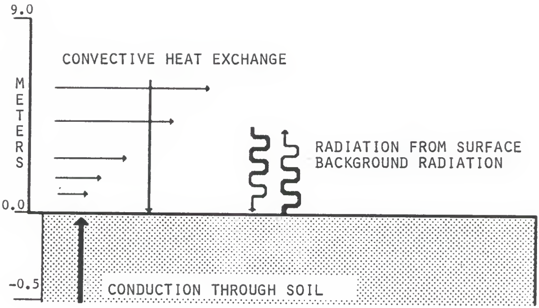

Figure 2. Physical processes involved in the P-model.

of temperature change with time, and each is governed by a differential equation:

the sub-surface layer,

$$C_s \frac{\partial T}{\partial t} = K_s \frac{\partial^2 T}{\partial z^2} , \tag{1}$$

the earth-air interface,

$$C_s \frac{dT}{dt} = H + S + R + B , \tag{2}$$

and the air layer,

$$C_a \frac{\partial T}{\partial t} = - \frac{H}{h} + \frac{1}{\alpha U_*} \frac{dU^*}{dt} \frac{H}{K(U_*, z)} , \tag{3}$$

where

C_s = soil specific heat (KJ Kg^{-1} C^{-1}),

T_s = soil temperature (C),

t = time (s),

z = depth or height (m),

H = air layer sensible heat flux (W m^{-2}),

S = soil heat flux (W m^{-2}),

R = surface radiative flux (W m^{-2}),

B = background radiative flux (W m^{-2}),

C_a = air volumetric specific heat (J K^{-1} m^{-3}),

h = parameter related to height of nocturnal boundary layer (m),

U_* = friction velocity (m s^{-1}),

K_h = convective heat transfer coefficient (W m^{-2} C^{-1}),

K_s = thermal conductivity (W m^{-1} C^{-1}).

Sutherland does not define α ; this is discussed in following paragraphs.

Equation 1 is the Fourier heat transfer equation for conduction of energy through a solid. Equation 1 is applied to the soil in the P-model; numerical approximations of the Fourier equation are used to determine the soil heat flux from a depth of constant temperature to the surface (Wierenga and de Wit, 1970).

Equation 2 is the surface energy balance, which drives the model. This form of the energy balance is non-steady state but would approach steady state as the temperature change with time term on the left-hand side approaches zero. The soil heat flux S is provided by equation 1. The air layer sensible heat flux found in equation 2 is the same value calculated from equation 3. The surface radiation R is calculated from the Stephan-Boltzmann law using the ground surface temperature T_s, and the background radiation B is calculated from initial measurements of net radiation.

The sensible heat flux H in equation 3 is calculated from

$$H = K(U_*, z)\frac{\Delta T}{\Delta z} \quad , \tag{4}$$

$$K(U_*, z) = K_a \exp(\beta U_* z) \quad , \tag{5}$$

and

$$U_* = kU_9 \ln(z/z_o) \quad , \tag{6}$$

where

U_9 = wind speed at 9 m (m s^{-1}),

z = height (m),

z_o = roughness length (m),

k = Von Karman Constant (0.4).

Beta and K_a are derived by setting the right-hand side of equation 5 equal to the linear form $K = kU_*z$.

There was controversy with regard to Sutherland's formulation of some model components. Shaw (1981) commented on four sections of the P-model. First, Shaw questioned the possibility of an infinitely thin surface having a mass, as characterized by C_s in equation 2. The units of C_s were also inconsistent; Shaw contends that the heat capacity per unit area for the surface should not have the same symbol (and therefore the same units) as the soil heat capacity per unit volume. Sutherland (1981) counters that equation 2 is in steady-state, therefore the left side becomes zero and the solution is trivial. Sutherland could have avoided this problem in two ways. The surface would have a volumetric heat capacity if a finite surface thickness of perhaps a few millimeters was used. The steady state assumption would still set the left side to zero, so the presence of a volumetric heat capacity would not change the outcome of the energy balance calculations. Also, by using a flux form of the left side of equation 2, the need for a heat capacity term would have been eliminated.

Second, a question arises from Sutherland's wind profile equation (right-hand side of equation 3), since the parameter α is not defined for this equation. Sutherland points out that this is a typographical error, and the term should be βU_*^2 instead of αU_*.

Third, a related question is the use of the exponential wind profile that had been derived for a plant canopy when no mention of a plant canopy was made. Sutherland justifies its use because it works better than the neutral form, but he would have been more convincing if he had mentioned that the P-model was being applied to a vegetated environment. Another problem with the development of the convective heat transfer coefficient equations is that Sutherland uses a linear wind profile form in equation

5 to determine the parameters used in the exponential wind profile (equation 3). The P-model is modele use only a one-level wind input and an assumed roughness height where the wind velocity should be zero. Two measured wind levels and the roughness height would provide a better value of the convective heat transfer coefficient.

A fourth and final point of contention is the use of the surface temperatures for determination of soil and sensible heat fluxes since the near-surface temperature profile would be highly non-linear. This is true within a few centimeters of the surface, but measurement of the temperature profile within a few centimeters of the surface is very difficult. More importantly, the error imposed from the assumption that the surface and the air just above the surface are at the same temperature would probably not be significant enough to cause a significant error in the flux calculations.

The Modified P-model

The original version of the P-model used automated weather station (AWS) data as input. Ten stations were located around the state of Florida. The SFFS computer would call the stations each hour to acquire the input measurements. Two major problems arose from the automated weather station data acquisition that reduced the data reliability (Martsolf, 1983a). First, high noise levels on the phone lines between the AWS and the main computer interfered with the received signal quality. Second, the AWS hardware sometimes failed. The hardware failure included the AWS microprocessor, modem, or measurement sensors. The AWS data acquisition success rate was approximately 70% during the last winter of full AWS

operation. The idea of using remotely-sensed temperatures from satellite as input to the P-model was proposed as an alternative to the automated weather station measurements (Heinemann and Martsolf, 1984).

The P-model was modified to accept GOES (Geostationary Operational Environmental Satellite) surface temperatures as input instead of AWS measurements. The model ran correctly only if the AWS inputs indicated the presence of a nocturnal inversion. Restrictions included in the previous P-model developed an inversion in the event that automated weather station data were missing or were insubstantial. A subroutine within the model read the surface temperature, and added 1.0 C for the 1.5 m temperature, 2.0 C for the 3 m temperature, and 3.0 C for the 9.0 m temperature, but only if the measured change in temperature with height was less than this. In the case of the Modified P-model, the model read the satellite surface temperature, then used these restrictions to produce an inversion profile based on the surface temperature.

The Boundary Layer Model

Blackadar's Boundary Layer Model (BLM) simulates the boundary layer processes occurring in the first 2000 meters of the atmosphere over a 24-hour period (Blackadar, 1976). Although the BLM is a mesoscale model, it rigorously models many of the microscale physical processes necessary for prediction of the low-level temperatures. The BLM is built upon theoretical and empirical relationships, and is based on equations for the mean velocity (u and v components), and the mean potential temperature at each of 30 layers (assuming vertical velocity is zero):

$$\frac{\partial U}{\partial t} + U\frac{\partial U}{\partial x} + V\frac{\partial U}{\partial y} + W\frac{\partial U}{\partial z} = - \frac{1}{\rho}\frac{\partial p}{\partial x} + fV + \frac{\partial}{\partial z} K_m\frac{\partial U}{\partial z} , \quad (7)$$

$$\frac{\partial V}{\partial t} + U\frac{\partial V}{\partial x} + V\frac{\partial V}{\partial y} + W\frac{\partial V}{\partial z} = - \frac{1}{\rho}\frac{\partial p}{\partial y} - fU + \frac{\partial}{\partial z} K_m \frac{\partial V}{\partial z} , \quad (8)$$

$$\frac{\partial \Theta}{\partial t} + U\frac{\partial \Theta}{\partial x} + V\frac{\partial \Theta}{\partial y} + W\frac{\partial \Theta}{\partial z} = -\frac{1}{C_p \rho}\frac{\partial R_n}{\partial z} + \frac{\partial}{\partial z} K_h \frac{\partial \Theta}{\partial z} , \quad (9)$$

where

U,V = east-west and north-south wind components (m s^{-1}),

t = time (s),

x,y,z = spatial coordinates (m),

f = coriolis parameter (s^{-1}),

K_m = turbulent exchange coefficient for momentum (m^2 s^{-1}),

ρ = air density (kg m^{-3}),

K_h = turbulent exchange coefficient for heat (m^2 s^{-1}),

C_p = air heat capacity (kJ C^{-1} m^{-3}),

Θ = potential temperature (K),

R_n = Net Radiation (W m^{-2}),

p = atmospheric pressure (n m^{-2}).

Equations 7 and 8 describe the momentum transfer processes. Equation 7 is the east-west component and equation 8 is the north-south component. The first term on the left side of each of these two equations is the change in wind speed with change in time. The second, third, and fourth terms on the left side of these two equations are the mass advection terms. The first term on the right side is the pressure gradient. The last term on the right side describes the vertical turbulent eddy momentum transfer.

Equation 9 describes the heat transfer processes. The first term on the left side of equation 9 is the rate of temperature change with time. The surface air layer temperature change with time is the desired output for this study. The second, third, and fourth terms on the left side are

the advection terms. The first term on the right side of equation 9 accounts for the radiative transfer. The last term on the right side describes the vertical turbulent eddy heat transfer.

The BLM can be divided into modules, each providing an essential process to the model. A diagram of the BLM modules is shown in Figure 3. The modules are integrated so that processes occuring in one may have direct effect on another. Blackadar (1979) provides a detailed discussion of the model.

The main purpose of the soil slab model is to provide a soil surface temperature, T_g, for calculation of radiative and sensible heat fluxes from the surface (Figure 4). Conduction through the soil is calculated from a solution of the Fourier heat transfer equation (equation 1), under the conditions that at an infinite depth the soil temperature approaches a constant temperature T_m and that the soil heat flux is continuous at the surface. The conductive flux through the soil is dependant on soil conductivity, thermal diffusivity, heat capacity, and water content.

T_g is calculated from

$$\frac{\partial T_g}{\partial t} = \frac{1}{C_g} (S + I\downarrow - \sigma T_g^4 - H_o) - k_m(T_g - T_m), \qquad (10)$$

where

S = solar insolation (W m^{-2}),

$I\downarrow$ = long wave atmospheric back radiation (W m^{-2}),

σ = Stephan-Boltzmann constant (W m^{-2} K^{-4}),

H_o = heat flux removed from surface by turbulence (W m^{-2}),

k_m = 1.18 ,

ω = angular velocity of earth's rotation (s^{-1}),

C_g = soil heat capacity (kJ C^{-1} m^{-3}).

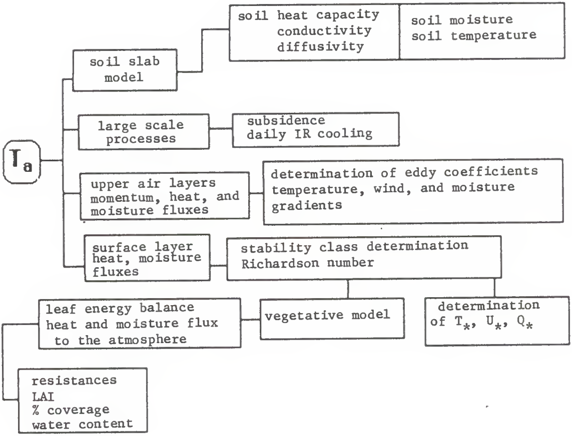

Figure 3. The Boundary Layer Model modules and important aspects of each. T_a is the surface air layer temperature.

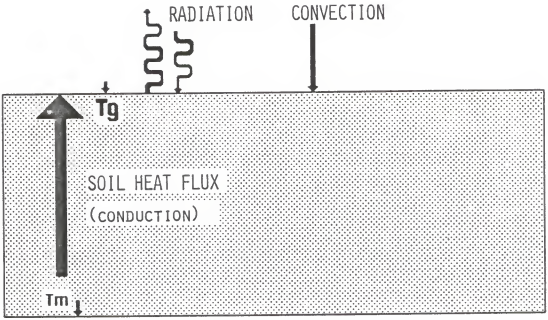

Figure 4. The BLM soil slab model. T_g and T_m are from equation 10.

The vegetative model accounts for water transport from the soil to the air by way of the plant, and is affected by root, stomatal, and leaf boundary layer aerodynamic resistances (Figure 5). Vegetative radiation and sensible heat fluxes are also calculated. Removal of water from the soil affects the soil heat flux by lowering the total soil heat capacity.

Daily radiation loss and large-scale subsidence are calculated. The radiation loss would occur through the fall and early winter, until the radiation balance of the northern hemisphere reverses and net heating begins. The subsidence term is added as a cooling mechanism. After the passage of a cold front, air is sinking as the high pressure builds in behind it. The sinking air would experience adiabatic warming, but the net effect of the subsiding air on the lower levels of the boundary layer would be cooling. These are simply additive terms, so a constant value is provided for each process.

Turbulent exchange accounts for the heat, moisture, and momentum transfer between the upper air layers (Figure 6). Turbulent transfer is described by K-type parameterization. The turbulent heat transfer coefficient (K_h) and the coefficient of momentum transfer (K_m) are assumed equal. The K values are calculated from the equation

$$K_m = K_h = 1.1 \frac{Rc - Ri}{Rc} l^2 s \quad \text{if } Ri \geq Rc, \qquad (11)$$
$$= 0.0 \quad \text{if } Ri \leq Rc,$$

where

Ri = Richardson number,

Rc = 0.25 (critical Richardson number),

l = parameter that characterizes the size of turbulent eddy (m),

s = wind shear ($m\ s^{-1}/m$).

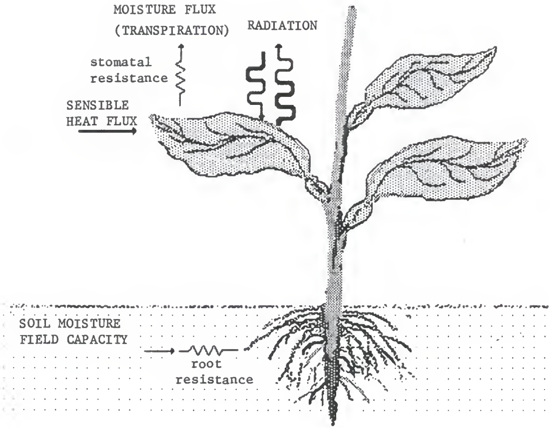

Figure 5. The BLM vegetation model.

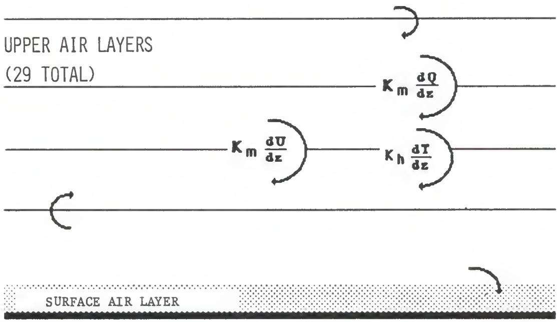

Figure 6. Physical representation of the upper air layers, showing turbulent heat, momentum, and moisture exchange. K_m and K_h are from equation 11; terms using T, U, and Q are the heat, wind, and moisture gradients, respectively.

The Richardson number is the ratio of bouyant to mechanical forces, and is used as an indicator of atmospheric stability. It includes wind speed, mixing length, and temperature gradient (Rosenberg, 1974; Monteith, 1980). Generally, the Richardson number distinguishes between stability and instability, and dominance of mechanical or bouyant turbulence within the unstable regime. The sign of the Richardson number is determined by the temperature gradient; positive indicates inversion conditions and negative indicates lapse conditions. Large negative values characterize strong instability due to predominantly bouyant forces, small positive values (less than 0.25 in this model) characterize dominance by mechanical turbulence, large positive values characterize strong stability and suppressed turbulence. The atmosphere in the boundary layer is usually under a stable turbulent regime during clear calm nocturnal conditions, with Ri just less than 0.25.

The heat transfer between the surface air layer and the first upper air layer above is turbulent (Figure 7). However, heat transfer in the surface air layer is complicated by other transfer processes such as sensible heat resulting from soil heat flux, radiation loss from the surface, moisture from soil and vegetation, and radiation and sensible heat from vegetation.

The model uses an assumed height of 1.0 meter above which temperature change is dominated by turbulence and below which is dominated by radiative flux divergence and turbulent flux convergence. The surface air layer sensible heat flux is calculated from determinations of T_* and u_*, under normal stable turbulent conditions occurring at night:

$$T_* = \frac{T_1 - T_a}{\ln(z_1/z_o) - \Psi_h} \qquad (12)$$

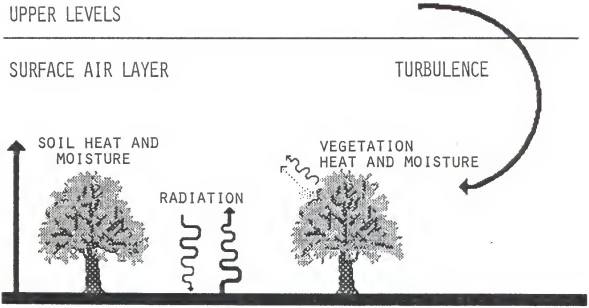

Figure 7. Physical representation of processes occurring within the surface air layer.

$$u_* = \frac{kW_1}{\ln(z_1/z_o) - \Psi_m} , \qquad (13)$$

$$\Psi_h = \Psi_m = 5z_1/L , \qquad (14)$$

where

T_1 = temperature in first upper air layer (C),

k = von Karman constant (0.4),

W_1 = wind velocity in first upper air layer (m s^{-1}),

z_o = roughness length (m),

z_1 = height of surface air layer (m).

L is the Monin length, which is a function of the heat and momentum fluxes. As with the Richardson number, it is a parameter that indicates stability by measuring the ratio of energy produced by buoyant forces and energy dissipated through mechanical forces (Monteith, 1980).

The BLM was adapted to the nocturnal environment (Heinemann et al., 1985). The one-dimensional version used in this study neglected the mass advection terms found on the left-hand-side of equations 7 and 8, and the heat advection term found in equation 9. The model contáins a free convection section that was not considered in this project, since under frost conditions free convection is very unlikely to occur. Free convection occurs when strong surface heating creates positive buoyant forces in the surface air layer, forcing large parcels of air to ascend into the upper layers. Under radiative frost conditions, stratification of the lower boundary layer and the development of the nocturnal inversion cause the buoyancy forces to become negative, hence an increase in the lower level stability (Monteith, 1980), but turbulence from mechanical forces is still prevalent.

Model Inputs

Each model requires a set of initial conditions provided by an input file. The P-model and modified P-model use three sets of conditions observed hourly as their prediction base. The BLM uses one set of conditions as input.

P-model Inputs

The inputs required to drive the P-model are shown in Figure 8. Soil heat flux was determined from the differential in the initial soil temperatures. Outgoing radiation was calculated from the measured surface temperature through the Stephan-Boltzmann equation, and background radiation was measured by net radiometer. The air temperatures provide a profile of the lower section of the inversion layer. The convective heat exchange was calculated from the initial wind speed and air temperature profile.

Modified P-model Inputs

The satellite data used in this study were obtained from GOES West meteorological satellite for the winter of 1984-85 (after the failure of GOES East in July 1984). The Geostationary Operational Environmental Satellite is positioned in geosynchronous orbit 38,000 km above the equator over the western hemisphere (Anonymous, 1980). The satellite is centered over the equator and longitude 100 W, and views the entire United States. The infrared (IR) scanner on GOES receives outgoing radiation emitted from the earth's surface (and any emitting mass between the surface and the

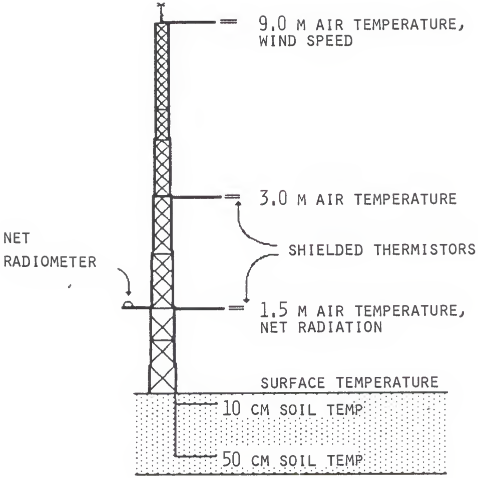

Figure 8. Required inputs for the P-model.

satellite), then calibrates the radiation to temperature through the Stephan-Boltzmann Law. The best pixel resolution for GOES is 3.6 km, but due to distortion from the earth's curvature, a GOES West pixel represents a 4.0 x 8.6 km area over Florida.

Good agreement between satellite-sensed temperatures and ground measurements has been observed for clear radiative night conditions. Martsolf and Gerber (1981) noted ground measurements within 1 C of satellite-sensed temperatures. Chen et al. (1983) compared ground measurements and satellite observations from clear nights during winters of 1978 through 1981. They arrived at a mean correlation coefficient of 0.87 and an average standard deviation from regression of 1.57 C.

BLM Inputs

The BLM required a sounding of the atmospheric boundary layer as input, including measurements of temperature, wind velocity components, geostrophic wind components, and mixing ratio at 100-meter increments up to 3000 meters. An example of a BLM input file is shown in Table 1.

The air temperatures were converted to potential temperatures (Iribarne and Godson, 1973):

$$\theta = T\ (1000/P_o)^x, \qquad (15)$$

where

θ = potential temperature (K),

T = temperature at a given pressure level (K),

P_o = atmospheric pressure (mb),

Table 1. Sample BLM input file. Values at top are explained in Table 2.

GAINESVILLE SOUNDING

TA= 10.00	UA = 4.24	VA = 0.00	QA = .0102
UGA = 4.24	VGA = 0.00	GLATD = 29.5	DECLD =-20.0
Z0 = 1.5000	CAPG = 107193.560	TM = 11.00	IDOWN = 319.0
TX = 40.	TN = 0.	GOTIME = 420.00	TRANSM = .95
TG = 11.00	RHOGX = 100.00	RHOWLT = 50.00	RHOM = 75.00
RHOG = 100.00	CSD = 2928800.	CSW = 4190000.	FN = 3.0
SIGMAF = .75			

POTENTIAL TEMPERATURES T(I) (C)

8.858	9.048	9.105	9.300	9.527	9.825	10.044	10.320	11.205
13.797	14.473	15.185	15.957	16.768	18.342	20.028	21.636	23.184
24.621	25.307	26.091	26.808	27.655	28.407	29.175	30.051	30.887

WIND COMPONENTS U(I) ($m\ s^{-1}$)

3.821	4.702	5.270	5.838	6.407	6.975	7.543	8.112	8.680
9.816	10.385	10.953	11.521	12.117	12.859	13.598	14.337	15.076
16.553	17.292	18.031	18.769	19.508	20.247	20.986	21.724	22.463

WIND COMPONENTS V(I) ($m\ s^{-1}$)

0.000	0.000	0.000	0.000	0.000	0.000	0.000	0.000	0.000
0.000	0.000	0.000	0.000	0.000	0.000	0.000	0.000	0.000
0.000	0.000	0.000	0.000	0.000	0.000	0.000	0.000	0.000

MIXING RATIOS Q(I)X1000 (kg water vapor per kg air)

2.108	2.003	1.978	1.640	1.339	1.133	1.028	.999	.843
.589	.584	.580	.575	.602	.997	1.671	2.738	4.140
3.332	2.982	2.668	2.385	2.131	1.903	1.699	1.515	1.351

GEOSTROPHIC COMPS. UG(I) ($m\ s^{-1}$)

3.821	4.702	5.270	5.838	6.407	6.975	7.543	8.112	8.680
9.816	10.385	10.953	11.521	12.117	12.859	13.598	14.337	15.076
16.553	17.292	18.031	18.769	19.508	20.247	20.986	21.724	22.463

GEOSTROPHIC COMPS. VG(I) ($m\ s^{-1}$)

0.000	0.000	0.000	0.000	0.000	0.000	0.000	0.000	0.000
0.000	0.000	0.000	0.000	0.000	0.000	0.000	0.000	0.000

x = .286, or R/C_p,

R = ideal gas constant (J kg^{-1} K^{-1}),

C_p = specific heat (kJ kg^{-2} C^{-1}).

The potential temperature is the temperature of a parcel of air if its ambient volume was compressed or expanded to a pressure of 1000 mb by a dry adiabatic process. This is done as a normalization of the temperature. One reason for this was to make testing of the model easier. For example, the potential temperature can be set to a single value for a neutrally stable boundary layer profile.

The mixing ratio is the fraction of mass water vapor per unit mass dry air. It was calculated from the dry bulb and dew point temperatures using the following relationships (Iribarne and Godson, 1973; Merva, 1975):

$$\log U = -.000425\ T\ T_d/(T-T_d), \tag{16}$$

$$\ln e_s = -2937.4/T - 4.9283 \log T + 23.5518, \tag{17}$$

$$e = e_s U, \tag{18}$$

$$w = 0.622\ e/p, \tag{19}$$

where

T = dry bulb temperature (K),

T_d = dew point temperature (K),

U = relative humidity,

e = vapor pressure at ambient temperature (kpa),

e_s = saturation vapor pressure (kpa),

w = mixing ratio (kg water vapor/kg dry air),

p = atmospheric pressure (kpa).

The geostrophic wind is the flow that would be produced solely by the balance between the pressure gradient force and the coriolis effect, in the absence of friction (Sutton, 1953):

$$V_g = \frac{1}{2\rho\omega\sin\phi} \nabla_H p \quad , \tag{20}$$

and,

$$\nabla_H p = \frac{\partial p}{\partial x} + \frac{\partial p}{\partial y} \quad , \tag{21}$$

where

ω = angular velocity of earth's rotation (s^{-1}),

ϕ = geographic latitude (degrees north),

ρ = air density (kg m^{-3}),

$2\omega\sin\phi$ = coriolis parameter (s^{-1}),

p = air pressure (n m^{-2}),

t = time (s),

x,y = horizontal distances (m).

The measured wind near the surface deviates from the the geostrophic flow due the surface frictional effects. The measured wind approximates the geostrophic wind within and above the higher levels of the boundary layer. McIntosh (1972) places the transition level at about 600 meters.

The geostrophic flow was calculated from the measured wind by use of the pressure gradient force (Clarke et al., 1971). The pressure gradient was determined from the sounding measurements through a numerical approximation of the Laplacian:

$$\nabla_o^2 p \approx \frac{p_1 + p_2 + p_3 + p_4 - 4p_o}{b}, \tag{22}$$

where

p = pressure of surrounding locations (mb),

p_o = pressure at central location (mb),

b = distance from central station to surrounding stations (m).

There were additional inputs to the BLM. Several of these depended on location, time of year, and soil conditions. Appropriate values for Florida locations were used (Table 1), and are explained in Table 2. Some assumptions were made in lieu of actual measurements. The high atmospheric transmissivity is for a clear dry night. The field capacity and wilt limit are for sandy soil found in Florida agricultural regions. The soil moisture and slab soil moisture are assumed; the effects of estimation errors are shown in the sensitivity analysis section.

Procedure

The P-model and the BLM each required input data from different outside sources. This section describes the input data sources, acquisition of the data, and the process to produce the temperature predictions.

Ground Measurements

Model output was verified with 1.5 m air temperature measurements. These were recorded at Gainesville and Ruskin by different means. A station similar to the automated weather station shown in Figure 8 was set up for the winter of 1984 at the University of Florida's Horticultural Unit. Measurements were logged on a Campbell Scientific CR5 Digital

Table 2. Additional BLM inputs.

Parameter	Value	Source
Geographical Latitude	29.5 (degrees North)	
Solar Declination	-20.0 (degrees)	
roughness parameter	1.5 (m) (grove environment)	1
vegetated fraction of surface	0.75 (grove environment)	assumed
ground albedo	0.18	2
vegetative albedo	0.2	2
atmospheric transmissivity	0.95 (clear night conditions)	assumed
heat capacity (dry soil)	2928800 J m^{-3} C^{-1}	3
soil moisture--field capacity	100.0 (kg m^{-3}) H_2O	4
wilt limit	50.0 (kg m^{-3}) H_2O	4
subsoil	75.0 (kg m^{-3}) H_2O	assumed
slab soil moisture	100.0 (kg m^{-3}) H_2O	assumed
leaf area index	3.0	assumed

[1]Rosenberg (1974)
[2]Van Wijk (1963)
[3]Armson (1977)
[4]Brady (1974)

Recorder. Temperatures were measured by copper-constantan thermocouples. The thermocouples were calibrated in a well-stirred ice bath and the bath temperature was recorded over several minutes by the CR5. The thermocouples averaged 0.6 $\pm$ 0.1 C over the time period. The thermocouples were also compared to a glass thermometer over a temperature range of -8.0 to +8.0 C in a well stirred salt solution (Figure 9). The P-model had been running operationally without net radiation measurements from the automated weather stations over the last four years, so no net radiometer was set up for this study. Measurements were made in the field at the levels indicated in Figure 8. Measurements were taken at 10-minute intervals.

Attempts were made to have a similar station operating at the Weather Service Office (WSO) in Ruskin, Florida, during the Winter of 1984-85, but the station was never upgraded to an operational mode. A thermograph located at the Ruskin WSO on a grass surface about 30 meters from any man-made structure, placed 1.5 meters above the ground, was used. The meteorologists at the Ruskin office suggest that this area was representative of an agricultural environment. The thermograph was checked for calibration weekly, and had an associated measurement error of $\pm$ 1.0 C. Temperature values were read from the thermographs at 30-minute intervals.

The quick response time of thermocouples and the greater sampling frequency of the CR5 provided much more detailed information about the temperature changes at the Gainesville site than at the Ruskin site. The thermograph tends to smooth out the fluctuations, as shown in cooling curves found in appendices B and C.

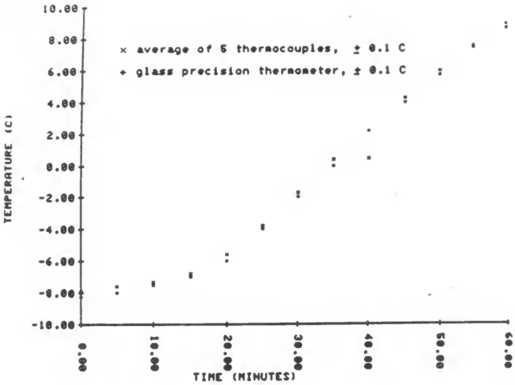

Figure 9. Calibration of CR5 with thermocouples.

Satellite

Satellite temperatures were used as initial surface temperature for the modified P-model. Temperatures of nine pixels were averaged to determine the surface temperature. This was done for both the Gainesville and the Ruskin sites.

The thermal IR data were acquired by the Gainesville HP every half hour (Martsolf, 1982). The satellite scans the entire hemisphere and transmits the raw binary data to Wallop's Island, Virginia, where gridding is added. The stretched data are retransmitted, and the binary data are received through the Gainesville antenna. The data are reduced into a primary sector by a Schlumberger EMR 822 sectorizor, and a Florida sector consisting of an array of 180 x 100 pixels is produced through software.

Slight drift in the satellite caused misalignment between maps. The program that averages the nine pixels may not be using the same pixels from one map to the next if the maps are not registered. Therefore, two alignment routines were developed to search for an outstanding map feature. The first routine used the map grid bits to find the outline of Lake Okeechobee. The grid outline of Lake Okeechobee was compared to the grid outline from a base map. The difference in east-west and north-south pixel locations between the base map and the map under consideration determined the offsets. A second routine was written that searches the actual IR data for Lake Okeechobee. The lake temperatures are usually warmer than the surrounding land areas during a frost night. The program searched for and highlighted the strongest temperature gradients, producing an outline of the lake. The outline was then compared to a base map outline and the best fit was calculated. East-west and north-south pixel

offsets were determined and added to the latest map to align it with the first map of the night. The first method was satisfactory only if the gridding was placed correctly onto the map, but was necessary in case there were clouds over Lake Okeechobee early in the evening.

The average of nine pixels surrounding each automated weather station location was calculated to provide a substitute for the surface temperature. Atmospheric corrections were not necessary because the atmosphere absorbs very little outgoing radiation on clear winter nights (Sutherland et al., 1979). Each pixel provides the average surface temperature of the 34.0 square kilometer area, and nine were averaged to smooth anomalous pixel temperatures.

The satellite provided surface temperature and a value of net radiation which was calculated from the surface temperature through the Stephan-Boltzmann law. Since the satellite measured only outgoing radiation, the calculated surface term ignored the back radiation from the sky, and therefore overestimated surface cooling for the rest of the night. Surface emissivity is usually in the range of 0.90 to 0.98 (Sellers, 1965), and the effective clear sky emissivity is between 0.5 and 0.7 (Monteith, 1980). The sky emissivity is directly related to the water vapor content to the lower atmosphere, and increases with increasing temperature and water vapor. An emissivity of 0.66 was used in the equation to account for the effects of back radiation.

Atmospheric Soundings

The National Weather Service Automated Field Operational System (AFOS) provided input to the BLM. Upper air soundings from Centreville, Alabama,

Waycross, Georgia, Apalachicola, Ruskin, Cape Canaveral, West Palm Beach, and Key West, Florida provided atmospheric measurements through and beyond the boundary layer at 00:00 and 12:00 CUT daily.

The TTAA atmospheric sounding report (Table 3) provided dry bulb and dew point temperature, height of the pressure surface, wind speed, and wind direction at mandatory pressure levels. The mandatory levels were surface, 1000 mb, 850 mb, 700 mb, 500 mb, 400 mb, and 200 mb. The TTBB sounding report provided pressure, dry bulb temperature, and wet bulb temperature at significant levels (Table 3).

The TTAA sounding reported at least three measurements that are within the boundary layer: surface, 1000 mb, and 850 mb levels. The 700 mb level is usually located around 3000 meters, just beyond the boundary layer. Several measurements from the TTBB report often fell within the first 3000 meters of the atmosphere, so it provided additional inputs. The 100-meter interval inputs required for the boundary layer model could be interpolated from these sounding measurements, since measurements from the first 3000 meters were used. A linear regression was first run on height versus pressure. This was necessary to determine the pressure at each 100-meter interval so that each potential temperature could be calculated. The correlation coefficients of 10 pressure-vs.-height regressions from soundings were averaged. The results gave an average r of .999 $\pm$ .001, indicating strong linearity between the pressure and height (Little and Hills, 1978).

The dry bulb temperature, dew point temperature, and wind speed were extracted from the sounding through the use of piecewise linear interpolation (Burden et al., 1978). The TTBB report indicates changes of linearity in dry bulb or dew point vs. height, so this interpolating procedure should

Table 3. Example of an upper air sounding from AFOS.

```
MIAMANTBW
 WOUS00 KTBW 101200
 72210 TTAA  60121 72210 99017 22205 09002 00161 25243 16504
 85579 18256 30503 70211 06846 06007 50591 07980 08012 40760
 20980 04508 30967 35359 34512 25091 455// 33510 20236 551//
 34520 15416 651// 04046 10660 677// 06521 88124 703// 06535
 77999 51515 10164 00001 10194 26504 03504=

 MIASGLTBW
  WOUS00 KTBW 161200
  72210 TTBB  6612/ 72210 00017 22012 11000 24413 22904 19250
  33850 15838 44756 10460 55700 07450 66690 07058 77679 05840
  88653 04680 99518 06163 11500 08944 22494 09902 33453 12922
  44433 15156 55418 16350 66410 17560 77400 18756 88388 19759
  99376 21558 11363 22966 22300 33580 33274 38964 44190 589//
```

provide good representation of the actual interval values (Cahir et al., 1978). The complete input for the BLM was produced through the following sequence:

a. Read TTAA, TTBB reports, collect pressure versus height, dry bulb and dew point temperatures, and wind speed;
b. Sort the TTAA and TTBB results in height-increasing order;
c. Perform linear regression on pressure vs. height, equation calculated;
d. Perform piecewise linear interpolation for temperature vs. height, temperatures interpolated at 100-m intervals starting at 100 m;
e. Perform piecewise linear interpolation for dew point temperature;
f. Perform piecewise linear interpolation for wind speed;
g. Calculate potential temperature from c and d;
h. Calculate mixing ratio from e;
i. Calculate geostrophic wind speed from pressure gradients.

A diagram of source data acquisition and transfer is shown in Figure 10. The sounding information is transferred from the AFOS Data General NOVA computer to an HP 21MX-M computer at the Ruskin National Weather Service Office. The data are moved from Ruskin to the SFFS HP 21MX-E via a DS-1000 link over a dedicated phone line. The sounding data are processed into BLM input files on the SFFS computer. The input files are then sent to the Florida Agricultural Service and Technology CYBER 730. The P-model was run on the HP 21MX-E, the BLM on the CYBER 730. Both were run interactively from user sessions. Details of the procedure to run the models and programs used to process the input files are found in Appendix E.

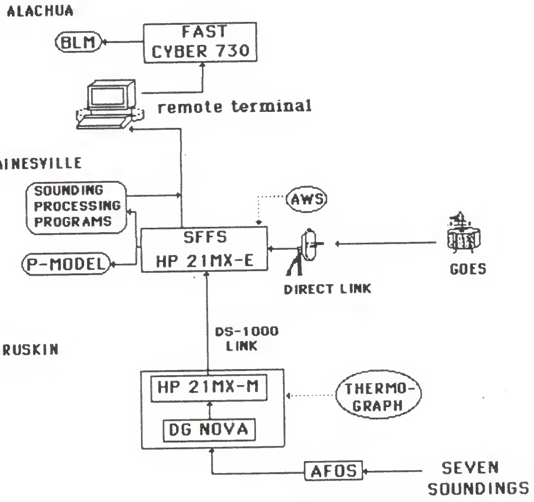

Figure 10. Diagram of the acquisition, transfer, and processing of data for model predictions.

RESULTS

The nights observed for this study are grouped into three categories. The first is the radiative nights, during which the dominant cooling mechanism in the surface air layer was radiative heat loss to the sky. The second is advective nights, when cold air flow into the area was the dominant cooling mechanism. The third consists of episodes that didn't fit into either catagory. These episodes involved situations where the microclimate was influenced by larger scale atmospheric occurrences.

Two sites are analyzed to test the BLM and P-model predictions against observed temperature. Eleven nights are observed for Ruskin (RUS) and twelve nights are observed for Gainesville (GNV) (Table 4). The Boundary Layer Model and Modified P-model were run on both the Gainesville and Ruskin sites. The original P-model was run on the Gainesville site only, since the measurement tower was not put into operation by the WSO staff at Ruskin during the Winter of 1984-85.

Linear regression was run on predicted versus observed temperatures. Linear regression is a standard approach to evaluating model performance, and can show details of the performance, with limitations. Ideally, the predicted versus observed curve should have an r value of 1.0, indicating a straight line, and a slope of 1.0, indicating the difference between the observed and predicted temperatures did not change at each time period.

Willmott (1984) reports that the correlation coefficient r and explained variance r^2 alone may not be indicative of actual model performance

Table 4. List of nights observed for this study.

site	radiative	advective	anomalous
GNV	Jan. 6, 1985	Jan. 5, 1985	Jan. 13, 1985
	Jan. 16, 1985	Jan. 21, 1985	Jan. 22, 1985
	Jan. 20, 1985	Jan. 26, 1985	Jan. 23, 1985
	Jan. 24, 1985		
	Jan. 27, 1985		
	Feb. 10, 1985		
	Feb. 17, 1985		
RUS	Dec. 8, 1984	Dec. 7, 1984	Jan. 23, 1985
	Dec. 9, 1984	Jan. 21, 1985	
	Jan. 6, 1985	Jan. 26, 1985	
	Jan. 16, 1985		
	Jan. 24, 1985		
	Jan. 27, 1985		
	Feb. 16, 1985		

under certain circumstances. For example, the predicted versus observed curve may give an r value of 1.0, indicating a straight line, but the slope may deviate considerably from 1.0 and the intercept may be different from zero. In this case the model performance could be quite poor. Willmott suggested other methods of evaluating model performance. Root mean square error (RMSE) and Mean Absolute Error (MAE) are two comparison techniques used in this project.

The RMSE and MAE represent average magnitude differences between the observed and predicted values. This is a very useful method of presenting the error associated with the predictions. The RMSE tends to be greater than the MAE because the differences are squared, so any large errors will amplify the average difference.

T-tests were run on the difference between predicted and observed values ($\Delta T = T_p - T_o$) to determine if ΔT is significantly different from zero at each hourly time interval. The t-tests were run at a 95% confidence level.

Model results are summarized in Table 5. The graphs of predicted versus observed temperatures for the BLM, P-model, and Modified P-model for all radiative nights at the Gainesville site are shown in Figures 11, 12, and 13, respectively. The results of the t-tests for the BLM, P-model, and Modified P-model are shown in Figures 14, 15, and 16, respectively. The graphs of predicted versus observed temperatures and results of t-tests for all radiative nights at the Ruskin site are shown in Figures 17-19. The predicted versus observed temperatures for the BLM and P-model during advective nights for the Gainesville and Ruskin sites are shown in Figures 20-22.

Table 5. Summary of model results from radiative nights. The values shown are the average and standard deviations of 95% confidence intervals from t-tests run on the hypothesis that the difference between predicted and observed temperatures is not significantly different from zero. The averages are for all hours of radiation and advection nights from each site.

site	model	95% confidence interval (C)
GNV	BLM	3.4 ± 1.2
	P-model	5.8 ± 1.0
	Mod. P-model	5.7 ± 0.9
RUS	BLM	2.7 ± 0.6
	Mod. P-model	18.8 ± 2.4
	**Mod. P-model	9.2 ± 1.5

**cloudy nights removed

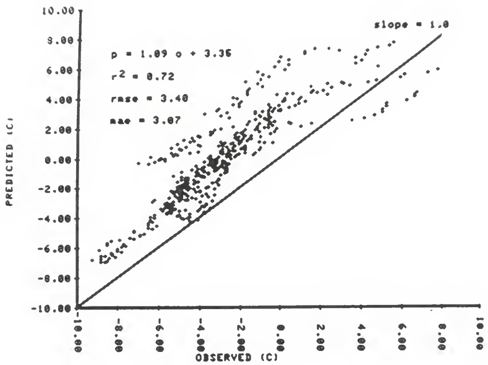

Figure 11. BLM predicted versus observed temperatures for all radiation nights, Gainesville location. Solid line indicates perfect fit.

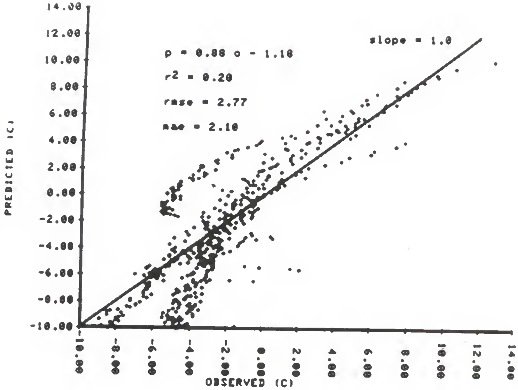

Figure 12. P-model predicted versus observed temperatures for all radiation nights, Gainesville location. Solid line indicates perfect fit.

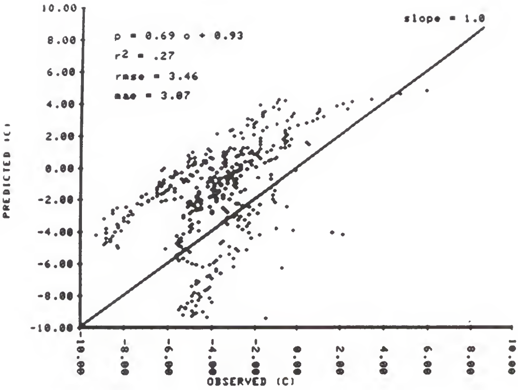

Figure 13. Modified P-model predicted versus observed temperatures for all radiation nights, Gainesville location. Solid line indicates perfect fit.

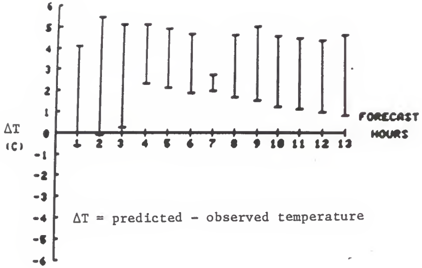

Figure 14. Results of t-tests on difference between BLM predicted and observed temperatures being significantly different from zero, showing 95% confidence intervals, Gainesville location.

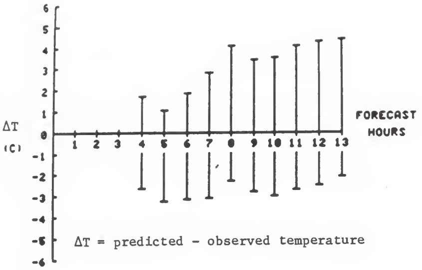

Figure 15. Results of t-tests on difference between P-model predicted and observed temperatures being significantly different from zero, showing 95% confidence intervals, Gainesville location.

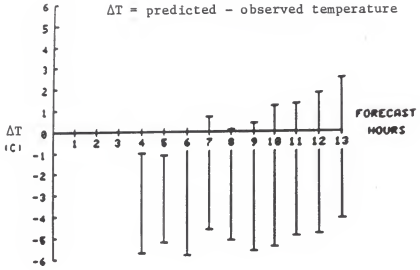

Figure 16. Results of t-tests on difference between Modified P-model predicted and observed temperatures being significantly different from zero, showing 95% confidence intervals, Gainesville location.

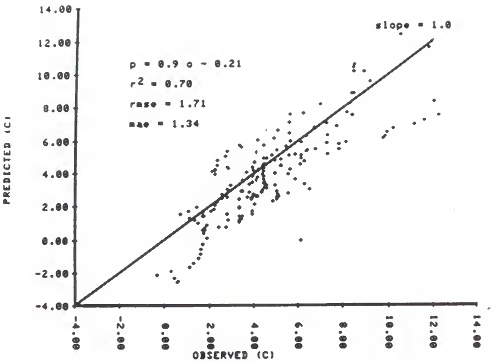

Figure 17. BLM predicted versus observed temperatures for all radiation nights, Ruskin location. Solid line indicates perfect fit.

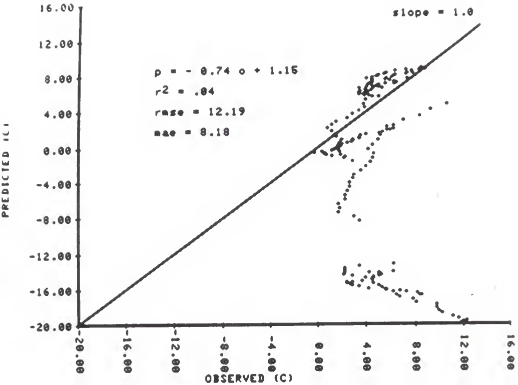

Figure 18. Modified P-model predicted versus observed temperatures for all radiation nights, Ruskin location.

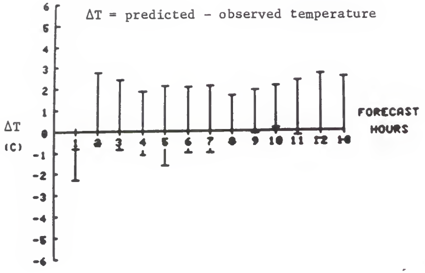

Figure 19. Results of t-tests on difference between BLM predicted and observed temperatures being significantly different from zero, showing 95% confidence intervals, Ruskin location.

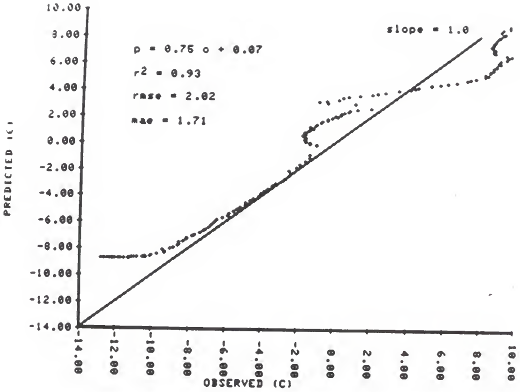

Figure 20. BLM predicted versus observed temperatures for all advection nights, Gainesville location.

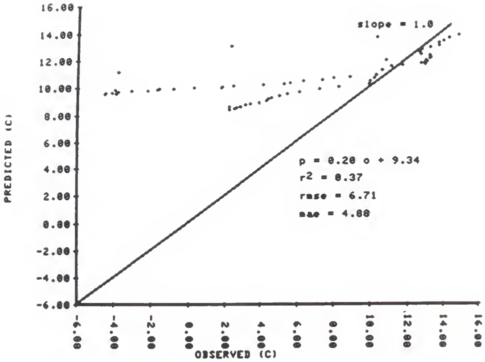

Figure 21. BLM predicted versus observed temperatures for all advection nights, Ruskin location.

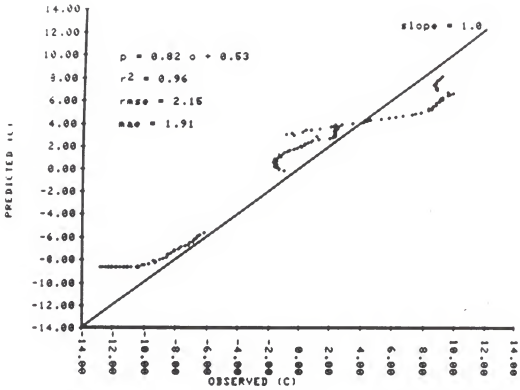

Figure 22. P-model predicted versus observed temperatures for all advection nights, Gainesville location.

DISCUSSION

The observed cooling curve followed a decaying exponential curve, typical for a radiative frost night, in six of the twelve nights studied at the Gainesville location and seven of the eleven nights studied at the Ruskin site. Of the remaining nights, three of the Gainesville nights and three Ruskin nights were advective, and three Gainesville nights and one Ruskin night showed unusual meteorological circumstances that fall into an anomalous category. Discussion of the individual nights and cooling curves from the individual nights are in Appendices B and C.

Radiative Nights

The typical radiative night cooling curve is produced from strong radiative heat loss from the ground and vegetative surfaces, and from the air in the layer near the ground surface. A divergence of heat occurs at the ground surface when the radiative heat loss is greater than the conduction of heat through the soil to the soil surface. The radiative heat flux decreases as the surface cools. Blackadar (1979) suggested another contributing factor to the decaying exponential curve. The wind shear between the upper layers and the surface air layer is small in the early evening because the upper level winds have just begun to accelerate. As the upper winds increase, so does the wind shear, which in turn increases mixing at the lower levels.

Linear regressions were run starting with the fourth forecast hour when comparing the P-model to the BLM. The reason for this is that the first three hours of the observed values form the base for the P-model predictions, and therefore the P-model curve is the same as the observed for those hours. The predictions then begin to deviate from the observed after the third hour.

Gainesville

The y intercept of the linear regression curve indicates that the BLM predicted the cooling curve warmer than the observed (Figure 11, page 53). This is discussed in the sensitivity analysis section. However, based on the results of the t-tests, the variance between predicted and observed temperatures was considerably less for the BLM than for the P-model throughout the night. The BLM curves were very similar in fit to the observed curves under ordinary radiative conditions as shown by a slope of 1.09 and r^2 of .72, although displaced upwards by an average of 3.35 C. The difference between the observed and predicted is significantly different from 0.0 at most hours for the BLM (Figure 14, page 56), because of the 3.35 C displacement. The 95% confidence interval resulting from the t-tests averages $\pm$ 1.7 C over the night. The difference between predicted and observed temperatures for the P-model varies much more, predicting too warm in some cases, and too cold in others. The slope of the regressed temperatures is 0.88, (Figure 12, page 54), but the graph indicates a large variation in difference between the predicted and observed temperatures. The 95% confidence intervals average $\pm$ 2.9 C over the night for the P-model (Figure 15, page 57). The Modified P-model results were

similar to the P-model results (Figure 13, page 55) with confidence intervals averaging $\pm$ 2.9 C (Figure 16, page 58).

Ruskin

The BLM-predicted cooling was very close to the observed cooling for radiation nights at the Ruskin sounding site. The slope was 0.9, the intercept value -.2 C, and r^2 was 0.7 (Figure 17, page 59). The modified P-model produced large errors in its predictions at the Ruskin site, due to the presence of clouds during the prediction base hours (Figure 18, page 60). The satellite receives radiation from the cold cloud tops, and as the clouds clear the satellite-measured temperatures begin to increase. The increase in base temperature forced the P-model to predict warming instead of cooling. This occurred on two of the seven radiative nights at Ruskin. Excluding those two nights, the modified P-model still had large variation in difference between predicted and observed temperatures (95% confidence intervals of $\pm$ 4.6 C). The t-tests showed that the BLM-predicted temperatures for the Ruskin site were closer to the observed temperatures than for any other case (Figure 19, page 61). There was no significant difference between the predicted minus observed temperature difference and zero for 11 of the 13 time periods, and the 95% confidence interval value averaged $\pm$ 1.4 C.

These results show that the BLM predicted more precisely than the P-model for the radiative nights at both sites. This is due to the BLM modeling three important processes in more depth than the P-model: The surface radiation flux, the turbulent heat transfer, and presence of vegetation. First, the initial radiation terms of the P-model are either

assumed or calculated from the measured ground surface temperature. An exponential regression is then performed using the three-hour base radiation measurements. The assumption that the radiation flux will decay in an exponential manner is good, but using assumed values or calculating radiation flux from surface temperatures (which are inherently difficult to measure accurately with thermocouples), will tend to lessen the accuracy of the radiation values. The BLM, on the other hand, calculates the radiation term from a ground surface temperature that has been determined from calculations of soil heat flux and radiation flux divergence. The new radiation terms are calculated at each time step (two minutes).

Another process that is handled better by the BLM is the turbulent convective heat transfer. The P-model considers only the first 9 m of the boundary layer, where the wind profile decays exponentially from the 9 m velocity to zero at z_o. Neither vertical heat nor momentum transfer is accounted for by the P-model. Only a convective heat transfer coefficient is calculated (see Models and Methods chapter). The BLM takes into account the heat and momentum transfer from the air layers above the surface air layer, and calculates a new turbulent eddy transfer coefficient at every time increment.

Finally, the BLM includes a vegetation model; the P-model does not. The vegetative canopy acts as a radiation absorber and emitter. The vegetation section also accounts for ground soil and plant moisture which can add to the evaporative effects as well as instability in the surface air layer, although these are small at night.

Advective Nights

Cold air was rapidly moving into the prediction area with the passage of a cold front on certain nights. Since the soundings used for BLM input were taken at a single point in time, the impending arrival of the advected cold air mass was not always taken into consideration by the model. The magnitude of the BLM predicted and observed temperature difference was not large for the Gainesville site (Figure 20, page 62), but the model underpredicted the cooling. The difference increased as the nights progressed. The difference for Ruskin was much greater (Figure 21, page 63) as indicated by a y intercept of 9.2 C. Most of this error was from the night of January 21.

The errors in the P-model predictions were slightly smaller than the BLM for Gainesville advective nights. The temperature trend could have been detected by the P-model if the advection was occurring during the three-hour base period (Figure 22, page 64), making the predictions closer to the observed.

Anomalous Nights

In certain situations meso- and synoptic-scale processes were occurring that the models could not anticipate. These processes tended to moderate the cooling. The BLM predicted the worst case given an initial set of conditions in these situations, so the moderation prevented the actual temperatures from dropping below the predicted temperatures.

Gainesville BLM Predictions Compared to Observed Satellite Data

The Gainesville predictions were compared to the satellite temperatures since the satellite covers a larger area and therefore is spatially averaged. Satellite temperatures and BLM predictions versus time are shown in Figures 23-29. The BLM did not predict the satellite temperatures very accurately. The only night that the BLM predictions were similar to the satellite was on the 24th of January (Figure 27). The reason for this may be that the near-surface temperature can vary to a great extent horizontally during a frost night, depending on surface features and topography (Bartholic and Martsolf, 1979). Chen et al. (1983) showed that the temperatures across Florida counties can vary by several degrees Celsius.

Sensitivity Tests

Sensitivity tests were performed on the BLM to determine the cause of the Gainesville predictions being too high. The temperature predictions from the night of February 16-17 (048) were tested for sensitivity to various inputs.

The sensitivity analysis used the following equations:

absolute:

$$S(y_1, p) = \frac{\partial y}{\partial p} \simeq \frac{\{y_t, p+\frac{\Delta p}{2} - y_t, p-\frac{\Delta p}{2}\}}{\Delta p} , \qquad (23)$$

relative:

$$S(y_1, p) = \frac{\partial y}{\partial p} \quad \frac{\{y_t, p+\frac{\Delta p}{2} - y_t, p-\frac{\Delta p}{2}\}}{\Delta p} \quad \frac{p}{y} ,$$

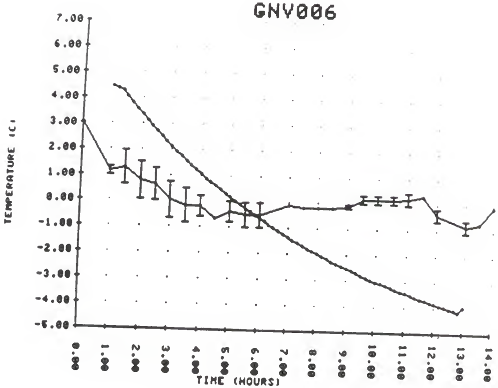

Figure 23. Average and standard deviations of nine satellite pixels and BLM temperature predictions versus time, Gainesville location, Jan. 6, 1985.

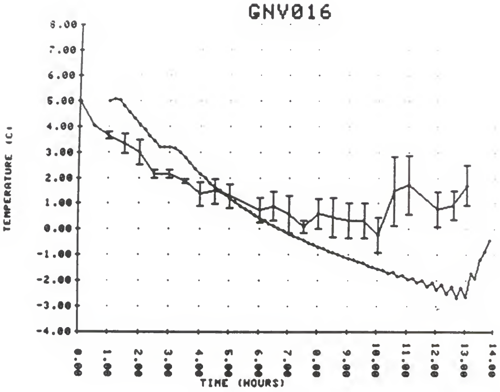

Figure 24. Average and standard deviations of nine satellite pixels and BLM temperature predictions versus time, Gainesville location, Jan. 16, 1985.

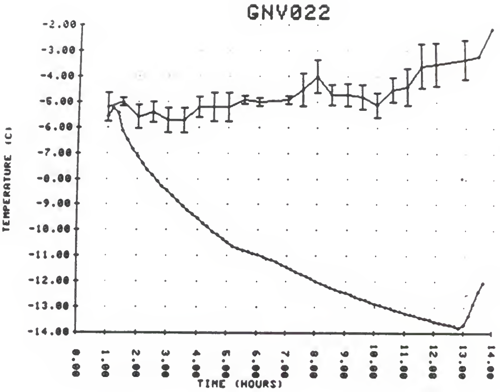

Figure 25. Average and standard deviations of nine satellite pixels and BLM temperature predictions versus time, Gainesville location, Jan. 22, 1985.

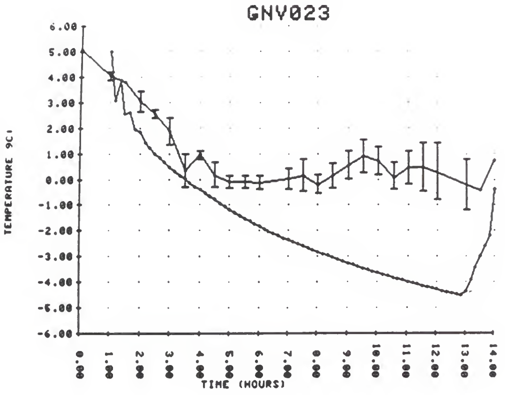

Figure 26. Average and standard deviations of nine satellite pixels and BLM temperature predictions versus time, Gainesville location, Jan. 23, 1985.

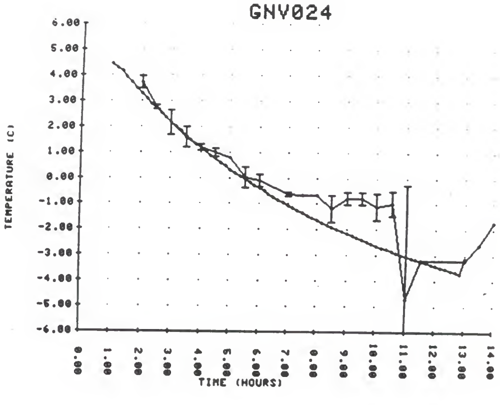

Figure 27. Average and standard deviations of nine satellite pixels and BLM temperature predictions versus time, Gainesville location, Jan. 24, 1985.

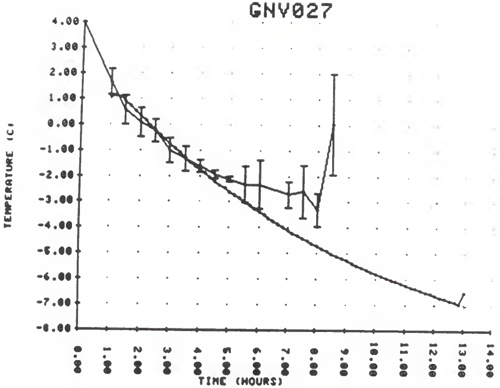

Figure 28. Average and standard deviations of nine satellite pixels and BLM temperature predictions versus time, Gainesville location, Jan. 27, 1985.

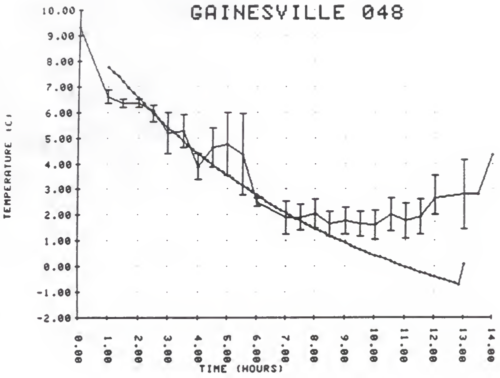

Figure 29. Average and standard deviations of nine satellite pixels and BLM temperature predictions versus time, Gainesville location, Feb. 17, 1985.

where

y = the output variable to be analyzed,

p = the input variable or parameter to be analyzed.

Equation 23 indicates the percentage change in output variable y given a percentage change in input parameter p. The surface air layer temperature is the output variable studied here. The percentage of change in the inputs was based on the magnitude of error that was associated with the input measurements or variability of an assumed parameter. For example, the error associated with the satellite temperature measurements was on the order of $\pm$ 1.0 C, so the effect of a 1% change in the input surface temperature was used.

The results of sensitivity tests are shown in Tables 6 and 7. Two forecast hours, the fourth and the twelth, are selected to show if the effects of the change in initial input is increasing or decreasing the change in output as the night progresses.

The results show that the surface air temperature is most sensitive to the initial soil properties and temperatures, and the initial surface air layer temperature. The soil properties affect the soil heat flux which in turn affects the soil surface temperature T_g. The outgoing radiation is determined from T_g. Since radiation is the dominant process in the first meter of the surface air layer, these inputs would have the greatest effect on the air surface temperature. Later in the night the variables affecting the turbulent heat exchange become important, as shown by the increase in sensitivity to z_1 and z_o, but the soil properties still dominate. Note the strong effects of the initial temperatures; only a 1% change in T_a, T_g, and T_m brings about a .1 to .6% change in predicted T_a.

Table 6. Inputs and parameters tested in sensitivity analysis.

parameter	symbol	input value
sfc air temp	(Ta)	280.9 K
sfc air wind speed	(Ua)	4.77 m s^{-1}
sfc air geostrophic wind speed	(Uga)	4.77 m s^{-1}
roughness length	(zo)	1.0 m
slab heat capacity	(capg)	107194.0 J m^{-3} C^{-1}
base Temp	(Tm)	281.9 K
atmospheric transmissivity	(transm)	.95
ground sfc. temp	(Tg)	281.9 K
soil field capacity	(rhogx)	100.0 kg m^{-3}
soil wilt limit	(rhowlt)	50.0 kg m^{-3}
subsoil water content	(rhom)	75.0 kg m^{-3}
slab water content	(rhog)	50.0 kg m^{-3}
dry soil heat capacity	(csd)	2.0x10e+6 J m^{-3} C^{-1}
water heat capacity	(csw)	4.19x10e+6 J m^{-3} C^{-1}
leaf area index	(LAI)	3.0
vegetative coverage	(sigmaf)	0.75
sfc air mixing ratio	(qa)	.0076 kg/kg
daily IR cooling	(rcool)	.833x10e-3 C $hour^{-1}$
subsidence	(wdown)	1.0 cm $hour^{-1}$
mixing depth	(z1)	60.0 m
soil thermal conductivity	(lamdag)	.66614 W m^{-1} C^{-1}
turbulent heat trans. coef.	(K)	.5 m^2 s^{-1}

Table 7. Results of sensitivity tests. Δp is the change in the input parameter given in equations 22 and 23.

	% change input	relative sensitivity %change Ta 4.00	relative sensitivity %change Ta 12.00	Ta at hour 4.00 +Δp	Ta at hour 4.00 -Δp	Ta at hour 12.00 +Δp	Ta at hour 12.00 -Δp
Ta	1.0	.173	.066	4.66	4.18	-.31	-.49
Ua	100.0	0.00	0.00	4.42	4.42	-.40	-.40
Uga	100.0	0.00	0.00	4.42	4.42	-.40	-.40
zo	20.0	.079	.088	4.81	5.03	-.01	.23
capg	10.0	0.00	0.00	4.42	4.42	-.40	-.40
Tm	1.0	.299	.641	4.82	3.99	.47	-1.28
transm	10.0	0.00	0.00	4.42	4.42	-.40	-.40
Tg	1.0	.270	.095	4.79	4.04	-.27	-.53
rhogx	20.0	.054	.264	4.45	4.38	-.23	-.59
rhowlt	20.0	0.00	0.00	4.42	4.42	-.40	-.40
rhom	20.0	0.00	0.00	4.42	4.42	-.40	-.40
rhog	100.0	.170	.312	4.46	3.99	.31	-.54
csd	100.0	.259	.799	4.70	3.98	.42	-1.76
csw	10.0	.072	.015	4.43	4.42	-.39	-.41
lai	100.0	-.123	-.132	4.35	4.69	-.47	-.11
sigmaf	20.0	-.068	-.070	4.34	4.53	-.48	-.29
qa	100.0	.274	.990	4.79	4.03	-.27	-.54
z1	100.0	.022	.579	4.27	4.21	.01	-1.57
lamdag	100.0	.316	.981	4.72	3.93	.48	-1.93
rcool**	100.0	-.162	-.338	3.97	4.42	-1.32	-.40
wdown**	100.0	0.00	.022	4.65	4.65	.14	.08
K	100.0	.040	.253	4.47	4.36	-.12	-.81

**These two parameters were set to 0.00 in the original model run.

The geostrophic wind has an indirect effect on the temperature predictions, but is very important in the development of the predicted wind profile. Since $f(V_g-V)$ is an additive term (equations 4 and 5), the presence of geostrophic wind increases the predicted wind velocity in the lower levels, causing the predicted low-level nocturnal jet to develop. The measured wind tends to become more geostrophic with height, so the $f(V_g-V)$ term becomes smaller.

The geostrophic wind must be calculated from good pressure gradient data. The addition of geostrophic wind to the BLM infile often caused a fluctuation in the predicted temperature similar in appearance to the fluctuations observed in the actual environment. However, the variation in the predictions was due to programmatic numerical instability rather than modeled meteorological processes. Apparently, the spatial density of the NWS sounding station network was not sufficient for calculating accurate pressure gradients, therefore the geostrophic determinations were insufficient.

The idea of obtaining calculated geostrophic wind from the synoptic models was suggested near the end of the data collection period. The National Weather Service passes a file containing results of LFM analysis and predictions through AFOS. This file (FRH63) includes the geostrophic wind for the lowest 50 mb, from the analysis time through forecasts up to 48 hours in 6-hour forecast increments.

The sensitivity tests do not reveal any particular input variable being responsible for the high Gainesville predictions. This led to the conclusion that the consistently high BLM predictions for the Gainesville site were due to the interpolation of the input sounding. The Gainesville sounding was produced from interpolation between the Ruskin and Waycross

sounding sites. The original plan was to interpolate between these two plus two additional soundings, Apalachicola and Cape Canaveral. The Cape Canaveral site does not follow the standard NWS sounding schedule so soundings were usually unavailable at 0000 CUT; this eliminated the use of four soundings. Spatially, Gainesville is located almost midway between Waycross and Ruskin. However, Waycross and Gainesville are inland sites, whereas Ruskin is located within 20 km of the Tampa Bay. The interpolated input temperature may be biased upward toward the Ruskin profile, when in fact the boundary layer temperature profile for Gainesville may be better represented by the Waycross sounding.

One of the biggest drawbacks of using the BLM on an operational basis is the problem of inputs. The model does very well at the sounding site, but the sounding network is not dense enough to cover inland areas of Florida. Interpolation does not seem to be the best method of obtaining data between sounding stations. The possibility exists that the VAS (VISSR atmospheric sounder) may provide sufficient information from satellites to develop BLM inputs from satellite data (Jedlovec, 1985). This would enable the model to predict for any location within the satellite view, without the need to interpolate between radiosonde launch sites.

The VAS radiometer views 12 channels to discern vertical moisture and temperature profiles through the atmosphere. The spatial resolution is similar to the GOES IR (7.0 km), as opposed to the low density sounding station network (100-200 km over land and practically absent over the ocean). Also, the potential exists for temporal increases in the profiles, perhaps as often as every half hour. This could enable the BLM to self-correct as time progresses into the night.

The VAS data are being researched to determine the VAS accuracy with respect to the radiosonde data. VAS data are difficult to obtain on an operational basis, but in the future this information could become quite valuable as model input.

SUMMARY AND CONCLUSIONS

Two atmospheric models were analyzed and compared to determine which would more accurately predict the cooling of a vegetated environment under nocturnal conditions. The two models were the P-model, which was developed on the Satellite Frost Forecast System, and a Boundary Layer Model (BLM) developed by Alfred Blackadar.

Atmospheric soundings were used as input to the BLM. These were obtained from National Weather Service AFOS, through a DS-1000 link between Gainesville and the WSO in Ruskin, Florida. Satellite data and automated weather station measurements were used for P-model input. The satellite data were obtained from GOES West through a direct digital downlink.

Model-produced predictions were analyzed for 12 nights at the Gainesville site and 11 at the Ruskin site. The predicted versus observed temperatures were compared using linear regression, t-test, RMSE, and MAE. A sensitivity analysis was performed on the Gainesville site for the night of the February 16-17, 1985.

The Boundary Layer Model predicted the cooling curve more precisely than the P-model and Modified P-model during radiative nights in the vegetated environment. For Gainesville, the overall regressions of observed versus predicted temperatures from the fourth forecast hour through the remainder of the night were:

BLM	predicted = 1.09*observed + 3.35	r^2 = .72,
P-model	predicted = 0.88*observed - 1.18	r^2 = .28,
modified P-model	predicted = 0.69*observed + 0.93	r^2 = .27.

The Ruskin regressions were:

BLM predicted = 0.90*observed - 0.21 $r^2 = .70$,

modified P-model predicted = -0.74*observed - 1.15 $r^2 = .30$.

The BLM-predicted cooling curve fit the observed curve closely, but the BLM consistently predicted about 3 C too warm for the Gainesville site. The results of t-tests showed that the difference between observed and predicted temperature was not significantly different from zero for the BLM at the Ruskin site and the P-model at the Gainesville site, but significantly different from zero for the BLM at the Gainesville site due to a 3.35 C displacement. However, the variation in the hourly BLM predictions was about half that of the P-model during radiation nights for both sites. The 95% confidence intervals for the BLM at the Gainesville site averaged 3.4 C, for the P-model 5.8 C. The sensitivity analysis showed that the displacement was most likely due to the interpolated input files rather than any particular input parameter.

The greatest errors in the overall BLM predictions were due to advection. The advective terms in equation 9 are not included in the model since the model is simulating only one point in the horizontal. Incorporating the BLM into a three-dimensional regional or synoptic scale model would improve its performance during advective events. This could possibly be done with the soundings presently acquired through AFOS, but VAS may prove to be much more valuable due to the higher resolution of data.

The performance of the Boundary Layer Model shows improvement over the P-model. The model in its present form is recommended for prediction of radiation night situations. Presently, however, the inputs are not sufficient for model predictions for every desired location in the state,

due to the low sounding network density. The Gainesville sounding interpolation resulted in a consistent bias. The interpolation procedure could be used for other sites after the bias is determined and corrections are included in the prediction. The fact that all sounding sites in Florida are coastal is a potential problem. The land-sea interface produces mesoscale processes not associated with inland sites, such as nocturnal land breezes. VAS may prove valuable for the increase of input data, both in frequency and in resolution.

The Modified P-model had an advantage over the original P-model and the BLM because it could use inputs from any location in Florida. However, the Modified P-model did not make accurate site-specific predictions. Use of a single measurement as input to the Modified P-model made the model very susceptible to anomalous data and therefore less reliable than the original P-model and the BLM. The presence of clouds and moisture masked outgoing surface radiation so the temperature measured by the satellite was not representative of the actual surface temperature. Atmospheric corrections may reduce the error caused by masking.

The Boundary Layer Model was run in real-time on some of the frost nights during the Winter of 1984-85, but not as an operational program. The BLM could be run in an operational environment as an aid to forecasters making frost night predictions, in the same way that the P-model was originally envisioned. The predicted cooling curves could also be sent directly to users through the Florida Agricultural Weather Network. The predictions could be transferred as files, utilizing the graphic capabilities of user's microcomputers to display the predicted temperature versus time for their area.

Models that simulate specific agricultural practices, such as orchard heating, sprinkler irrigation, and fog production, can be incorporated into the Boundary Layer Model to study the effects of these practices on the upper layers of the boundary layer. The BLM lends itself well to this since it has the separate surface air layer, into which these other models could be fitted. Some examples of models that could possibly be used are sprinkler models (Perry et al., 1982; Gerber and Harrison, 1964), and heater models (Welles, Norman, and Martsolf, 1979, 1981).

APPENDIX A
DISCUSSION OF INDIVIDUAL NIGHTS

Error in the difference between BLM-predicted and observed temperatures was consistent for the radiative frost nights, but not for the advective nor anomalous nights. The following is a discussion of processes that were occurring and possible reasons why the model did not do as well on these particular nights.

The three advective nights at Gainesville were January 5, 21, and 26 (Figures 30a, b, and c). The predicted curve follows the observed curve rather closely until the seventh predicted hour for the January 26 case. At this point the winds shifted from southwest to northwest and increased in speed; the increased turbulence mixed the stratified atmosphere causing a temporary warming trend. After the tenth forecast hour the cold advection became evident and the temperature dropped quickly, well below the predicted value.

The advection on January 21 brought one of the worst freezes in the last 100 years in Florida (Figure 30b). The advection had already begun when the Waycross sounding was made. The predicted cooling was similar to the observed for the early part of the evening at Gainesville. However, the model assumed that the outgoing radiation flux would decrease as the surface cooled, decreasing the slope of the cooling curve later in the event. The observed curve shows a steady drop in temperature through the night as the cold air quickly moved over the area. The air mass appeared

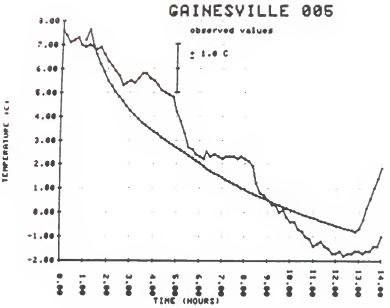

a

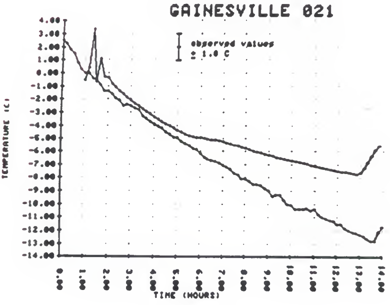

b

Figure 30. Cooling curves from three advective nights, Gainesville location. a) Jan. 5, 1985; b) Jan. 21, 1985; c) Jan. 26, 1985.

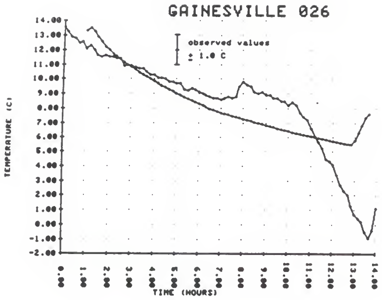

c

Figure 30--continued

to be isothermal with height, unlike a radiative frost event, as shown by the fairly smooth observed curve. Strong winds accompanied this cold air mass, creating strong turbulence, but due to the isothermal conditions little turbulent exchange of heat occurred.

The presence of an upper air disturbance over the Gulf of Mexico creates the unusual temperature pattern for the night of January 13 at Gainesville (Figure 31a). Clouds intermittently passed over the site, altering the net radiation. Also, the wind periodically increased, most notably beginning at the fifth and eighth forecast hours. The resulting increase in mixing raised the 1.5 m air temperature during the episode of higher wind. The model has no way of accounting for synoptic scale influences such as this upper air disturbance.

The night of January 22 was predicted (by forecasters) to be as cold as the previous night, and the BLM anticipated that with its prediction (Figure 31b). The observed temperature decreased rapidly in the early evening. As the temperature began to level off, the wind increased and continued through the entire evening. Apparently a layer of moisture also moved into the area cutting down on the radiative heat loss.

The air temperature decreased quite rapidly early on the night of January 23 (Figure 31c), much more quickly than the model predicted. However, the cooling was sharply cut off with an increase in the wind and mixing at the fifth prediction hour. The predicted minimum and the observed temperature were within 0.5 C and 30 minutes of each other at the end of the frost event.

For seven of the eleven nights studied at the Ruskin site, the observed curve followed the typical decaying exponential temperature drop of a radiative frost night. However, unlike the Gainesville site which tends

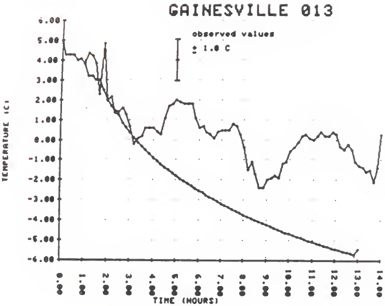

a

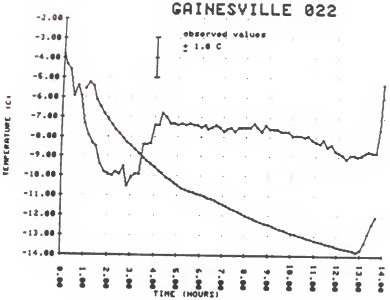

b

Figure 31. Cooling curves from anomalous nights, Gainesville location. a) Jan. 13, 1985; b) Jan. 22, 1985; c) Jan. 23, 1985.

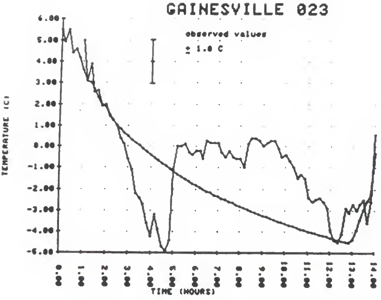

c

Figure 31--continued

to be a cold pocket on frost nights, the Ruskin site is located near the Tampa Bay. The influence of this large body of water can be seen in the observed curves of the graphs. The prevailing winds carried some moisture off the bay over the site in some cases, partially masking the outgoing radiation. The site is in close enough proximity to the bay to be influenced by the nocturnal land breeze that develops because of the land-sea temperature differential. This breeze could have been responsible for an increase in mixing of the stratified layers. The radiation and the land breeze were probably responsible for the environment not cooling quite to the degree that the BLM predicted. This occurred on the nights of December 8, 1984, January 23, 1985, and February 16, 1985 (Figures 32a, b, and c, respectively). The night of January 23 is a good example of possible bay influence. The BLM predicted strong radiative heat loss in the early hours, then a rapid decrease in heat loss after the second forecast hour. The actual cooling was moderated in the early hours, but then increased after the seventh forecast hour (Figure 32b). The predicted minimum was only about 1 C less than the actual minimum.

The BLM predicted the cooling quite accurately for the nights of December 9, 1984, January 24, 1985, and January 27, 1985 (Figures 33a, b, and c, respectively). It is interesting to note how close the predicted and observed curves fit, particularly on January 24. In this case the model predicted the strong radiative heat loss early in the evening that is quite evident on the observed curve. The inflection point, where the strong cooling decreases considerably, differed by less than one hour between the two curves.

Three of the ten nights at the Ruskin were affected by cold advection, December 7, 1984, January 21, 1985, and January 26, 1985 (Figures 34a, b,

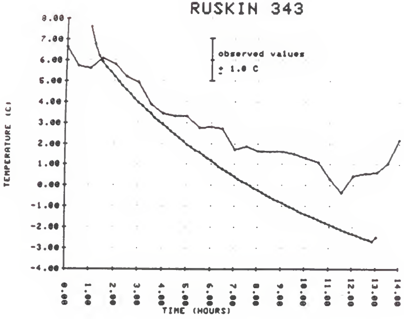

a

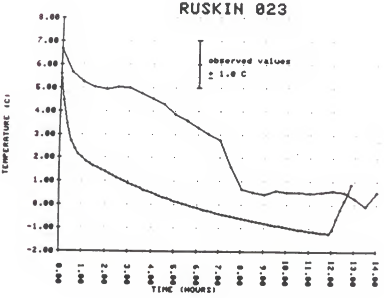

b

Figure 32. Cooling curves from anomalous nights, Ruskin location. a) Dec. 8, 1984; b) Jan. 23, 1985; c) Feb. 16, 1985.

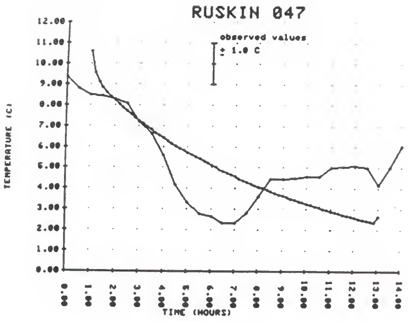

c

Figure 32--continued

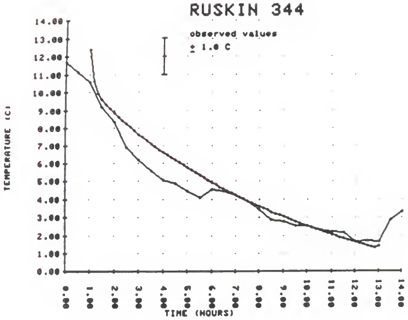

a

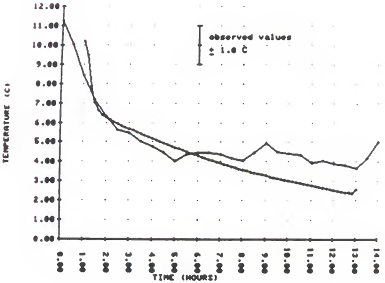

b

Figure 33. Cooling curves from radiation nights, Ruskin location. a) Dec. 9, 1984; b) Jan. 24, 1985; c) Jan. 27, 1985.

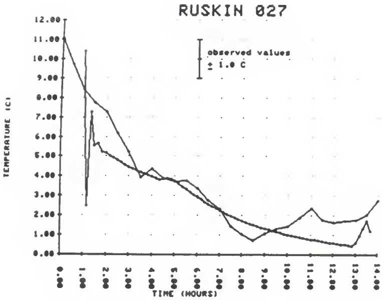

c

Figure 33--continued

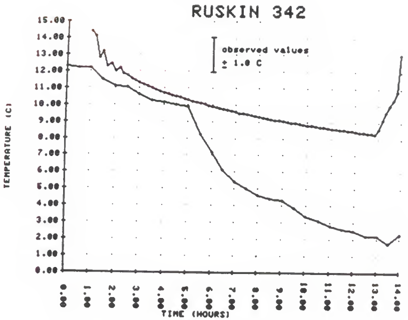

a

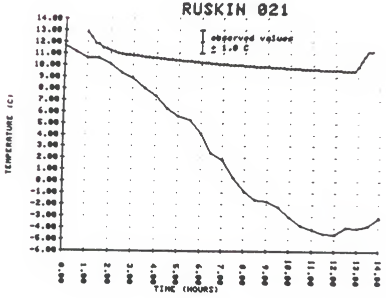

b

Figure 34. Cooling curves from advection nights, Ruskin location. a) Dec. 7, 1984; b) Jan. 21, 1985; c) Jan. 26, 1985.

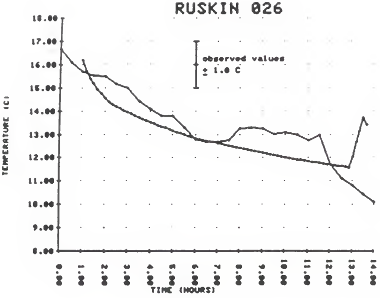

c

Figure 34--continued

and c). On December 7, the predicted curve was similar to the observed curve until the fifth prediction hour, then the cold air mass began moving in and the temperatures dropped rapidly. On January 21 the colder air arrived just after the sounding was made. This proved to be the worst BLM forecast, because the unaffected air mass over Ruskin at the sounding time was rather humid, and the surface was warm. The BLM anticipated a very slow drop in temperatures through the night, when in actuality the advected air dropped the temperatures quickly. The prediction for January 26 was quite close to the observed up until the eleventh forecast hour when the advection began to occur.

APPENDIX B

ADDITIONAL GRAPHS OF COOLING CURVES

FOR INDIVIDUAL NIGHTS

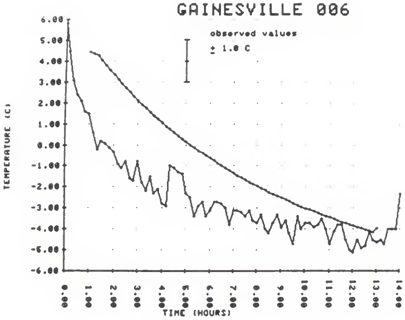
GAINESVILLE 006
observed values
± 1.0 C
TEMPERATURE (C)
TIME (HOURS)

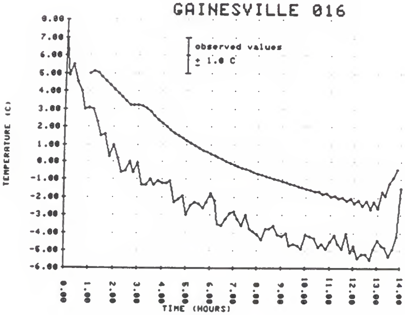
GAINESVILLE 016
observed values
± 1.0 C
TEMPERATURE (C)
TIME (HOURS)

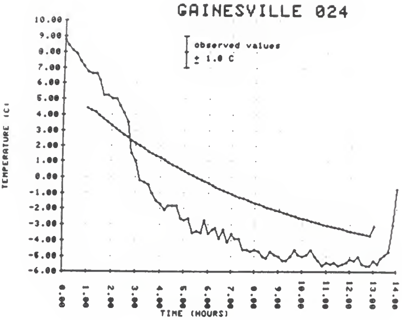
GAINESVILLE 024
observed values
± 1.0 C
TEMPERATURE (C)
TIME (HOURS)

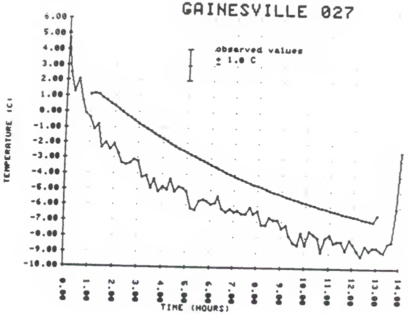
GAINESVILLE 027
observed values
± 1.0 C
TEMPERATURE (C)
TIME (HOURS)

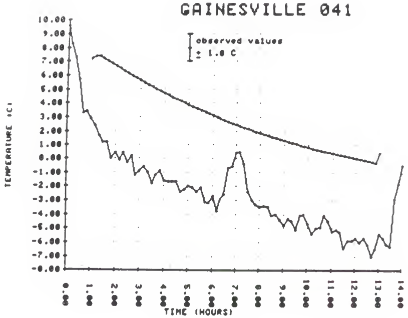
GAINESVILLE 041
observed values
± 1.0 C
TEMPERATURE (C)
TIME (HOURS)
10.00
9.00
8.00
7.00
6.00
5.00
4.00
3.00
2.00
1.00
0.00
-1.00
-2.00
-3.00
-4.00
-5.00
-6.00
-7.00
-8.00
0.00
1.00
2.00
3.00
4.00
5.00
6.00
7.00
8.00
9.00
10.00
11.00
12.00
13.00
14.00

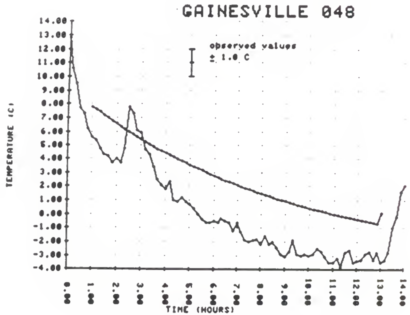
GAINESVILLE 048
observed values
± 1.0 C
TEMPERATURE (C)
TIME (HOURS)
14.00
13.00
12.00
11.00
10.00
9.00
8.00
7.00
6.00
5.00
4.00
3.00
2.00
1.00
0.00
-1.00
-2.00
-3.00
-4.00
0.00
1.00
2.00
3.00
4.00
5.00
6.00
7.00
8.00
9.00
10.00
11.00
12.00
13.00
14.00

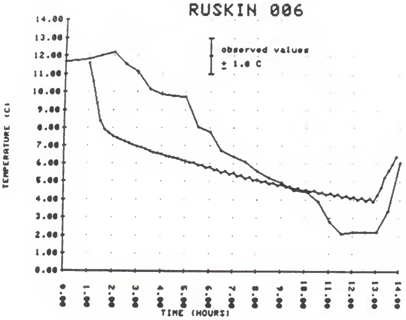
RUSKIN 006
observed values
± 1.0 C
TEMPERATURE (C)
14.00
13.00
12.00
11.00
10.00
9.00
8.00
7.00
6.00
5.00
4.00
3.00
2.00
1.00
0.00
0.00
1.00
2.00
3.00
4.00
5.00
6.00
7.00
8.00
9.00
10.00
11.00
12.00
13.00
14.00
TIME (HOURS)

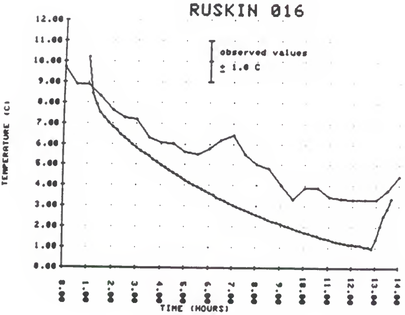
RUSKIN 016
observed values
± 1.0 C
TEMPERATURE (C)
12.00
11.00
10.00
9.00
8.00
7.00
6.00
5.00
4.00
3.00
2.00
1.00
0.00
0.00
1.00
2.00
3.00
4.00
5.00
6.00
7.00
8.00
9.00
10.00
11.00
12.00
13.00
14.00
TIME (HOURS)

APPENDIX C

LISTING OF PROGRAMS AND PROCEDURE TO PRODUCE TEMPERATURE PREDICTIONS FROM THE MODELS

1. The P-model

Equipment used: HP 21MX-E
HP terminal
Programs used: AKD
PMODG (version of P-model used in this study)

The P-model input files must be in a special non-ASCII form to be read by the model software. The measurements can be placed in an ASCII file in the following format:

```
year,julian day
station
time,Tsur,Ts10,Ts50,Ta1.5,Ta3,Ta9,v,dir,Rn
```

where Tsur = soil surface temperature (F),
Ts10 = 10 cm soil depth temperature,
Ts50 = 50 cm soil depth temperature,
Ta1.5 = 1.5 m air temperature,
Ta3 = 3.0 m air temperature,
Ta9 = 9.0 m air temperature,
v = wind speed (mph),
dir = wind direction
Rn = net radiation (Cal cm^{-2} s^{-1}).

example:

```
013,1985
GNV
 1,46.4,57.6,53.6,40.3,41.0,41.5,7.6,0,1.0
 2,45.1,57.6,52.7,38.8,39.4,39.9,5.7,0,1.0
 3,43.3,57.6,52.0,35.6,37.0,37.9,5.7,0,1.0
```

Running program AKD will convert this ASCII file to the P-model input file. The file name usually takes the form KYYDDD, where yy is the year and ddd the julian day (e.g. K85013). When the P-model is run interactively,

the user will be interrogated for the input file name. At the present time AKD must have data from all 10 stations. However, the desired station is the only one that needs real data, and the user will be interrogated for the number of that station.

2. The Modified P-model

Equipment used:	HP 21 MX-E HP terminal
Programs used:	GOES, SCTRZ EDGE LOCAT (or LOC) SAT2B AKD PMODG

The programs GOES and SCTRZ are scheduled by the SFFS scheduler to produce the Florida sector. EDGE and LOCAT (or LOC) are programs used for registration of the satellite maps. EDGE enhances the strongest temperature gradients so the outline of Lake Okeechobee stands out. LOCAT compares the Lake outline with a base map to determine the offsets. LOC matches the Florida sector grid outline with a base map, to be used if Lake Okeechobee is covered with clouds. All three programs are run interactively and will ask for the map names.

SAT2B reads the satellite temperatures and produces an ASCII file for AKD to process into P-model input files. The user must create a file with the map names and x and y offsets for SAT2B to read. SAT2B will ask for the file name. The procedure from this point on is the same as in 1.

3. The Boundary Layer Model

Equipment used:	HP 21 MX-E HP terminal CYBER 730 or VAX 750 VIKING, VT, or HP terminal
Programs used:	DSORT

UPAIR
IN2
EMUL8
PBL (latest version of BLM on CYBER) or
  BLACK3 (latest version of BLM on VAX)

Upper air soundings are acquired from Ruskin WSO through the DS-1000 link by program DSORT. They may need minor editing, and their format should be identical to the example in Table 3. All seven soundings should be obtained. Program UPAIR reads the upper air soundings, strips off the necessary values, sorts the values, and places them into files. Program IN2 then reads those files, interpolates the data, and produces BLM input files for each station, including the additional inputs found in Table 2. These programs are run on the HP 21 MX-E. The files need to be transferred to the CYBER or the VAX where the executable BLM program is located. This can easily be done with the HP program EMUL8, through file transfer. Once the input files are transferred, the best approach is to use a VIKING terminal for the CYBER or a VT terminal for the VAX to run the BLM. The BLM is interactive, and will interrogate the user for the desired input file.

APPENDIX D

BLM AND P-MODEL INPUT FILES

BLM input files

```
RUSKIN SOUNDING  342,1984

TA= 14.40          UA =  5.30          VA =  5.30          QA =   .0077
UOA =   5.30       VOA =   0.00        GLATD =  29.0       DECLD =-20.0
ZO =  1.5000       CAPG = 107193.560   TM = 23.20          IDOWN =  319.0
TX =  40.          TN =    0.          GOTIME =   420.00   TRANSM =  .95
TG = 15.40         RHOGX = 100.00      RHOWLT =  50.00     RHOM =  75.00
RHOG = 100.00      CSD =  1000000.     CSW = 3190000.      FN = 3.0
SIGMAF =  .75

POTENTIAL TEMPERATURES T(I)
  14.134  14.855  14.488  14.208  13.849  13.495  13.144  12.799  12.840  19.091
  20.045  20.874  22.467  23.990  25.531  26.416  27.035  27.566  28.110  28.667
  29.237  29.930  30.529  31.143  31.772  32.534  33.196  33.875  34.572  35.410

WIND COMPONENTS U(I)
   6.498   7.581   8.283   8.985   9.687  10.389  11.091  11.793  12.495  13.197
  13.899  14.601  15.303  16.005  16.707  17.191  17.552  17.914  18.275  18.636
  18.997  19.358  19.720  20.081  20.442  20.803  21.165  21.526  21.887  22.248

WIND COMPONENTS              V(I)
   0.000   0.000   0.000   0.000   0.000   0.000   0.000   0.000   0.000   0.000
   0.000   0.000   0.000   0.000   0.000   0.000   0.000   0.000   0.000   0.000
   0.000   0.000   0.000   0.000   0.000   0.000   0.000   0.000   0.000   0.000

MIXING RATIOS Q(I)X1000
   7.701   8.466   8.144   7.833   7.533   7.244   6.965   6.695   2.779   2.729
   3.891   5.885   3.790   2.365   1.442   1.229   1.277   1.328   1.381   1.435
   1.493   1.552   1.614   1.678   1.745   1.815   1.888   1.964   2.043   2.125

GEOSTROPHIC COMPS. UG(I)
   6.498   7.581   8.283   8.985   9.687  10.389  11.091  11.793  12.495  13.197
  13.899  14.601  15.303  16.005  16.707  17.191  17.552  17.914  18.275  18.636
  18.997  19.358  19.720  20.081  20.442  20.803  21.165  21.526  21.887  22.248

GEOSTROPHIC COMPS. VG(I)
   0.000   0.000   0.000   0.000   0.000   0.000   0.000   0.000   0.000   0.000
   0.000   0.000   0.000   0.000   0.000   0.000   0.000   0.000   0.000   0.000
   0.000   0.000   0.000   0.000   0.000   0.000   0.000   0.000   0.000   0.000
```

RUSKIN SOUNDING 006,1985

```
TA= 11.60          UA =  3.18           VA =  3.18          QA =    .0057
UOA =   3.18       VOA =    0.00        OLATD =  29.0       DECLD =-20.0
ZO =  1.5000       CAPG = 107193.560    TM = 15.40          IDOWN =  319.0
TX =  40.          TM =   0.            GOTIME =    420.00  TRANSM =  .95
TG = 12.60         RHOGX = 100.00       RHOWLT =  50.00     RHOM =  75.00
RHOG = 100.00      CSD =  2000000.      CSW = 4190000.      FN = 3.0
SIGMAF =  .75
```

POTENTIAL TEMPERATURES T(I)

10.276	10.208	10.343	10.404	10.471	10.630	10.712	10.800	10.984	11.088
11.290	11.453	14.536	18.087	19.720	20.291	20.893	21.408	21.936	22.581
23.136	23.812	24.396	24.995	25.721	26.352	26.998	27.779	28.461	29.160

WIND COMPONENTS U(I)

4.703	5.830	5.830	5.830	5.830	5.830	5.830	5.830	5.830	5.830
5.830	5.830	5.830	5.830	5.830	5.799	5.765	5.732	5.698	5.664
5.631	5.597	5.564	5.530	5.496	5.463	5.429	5.396	5.362	5.329

WIND COMPONENTS V(I)

0.000	0.000	0.000	0.000	0.000	0.000	0.000	0.000	0.000	0.000
0.000	0.000	0.000	0.000	0.000	0.000	0.000	0.000	0.000	0.000
0.000	0.000	0.000	0.000	0.000	0.000	0.000	0.000	0.000	0.000

MIXING RATIOS Q(I)X1000

5.677	5.410	5.358	5.308	5.259	5.210	5.162	5.115	5.069	5.023
4.979	4.618	1.769	1.890	1.816	1.679	1.546	1.424	1.310	1.204
1.106	1.015	.931	.853	.781	.715	.653	.597	.545	.497

GEOSTROPHIC COMPS. UG(I)

4.703	5.830	5.830	5.830	5.830	5.830	5.830	5.830	5.830	5.830
5.830	5.830	5.830	5.830	5.830	5.799	5.765	5.732	5.698	5.664
5.631	5.597	5.564	5.530	5.496	5.463	5.429	5.396	5.362	5.329

GEOSTROPHIC COMPS. VG(I)

0.000	0.000	0.000	0.000	0.000	0.000	0.000	0.000	0.000	0.000
0.000	0.000	0.000	0.000	0.000	0.000	0.000	0.000	0.000	0.000
0.000	0.000	0.000	0.000	0.000	0.000	0.000	0.000	0.000	0.000

RUSKIN SOUNDING 016,1985

```
TA= 10.20          UA =  3.18           VA =  3.18          QA =    .0043
UGA =   3.18       VOA =    0.00        OLATD =  29.0       DECLD =-20.0
ZO =  1.5000       CAPG = 107193.560    TM = 11.20          IDOWN =  319.0
TX =  40.          TM =   0.            GOTIME =    420.00  TRANSM =  .95
TG = 10.20         RHOGX = 100.00       RHOWLT =  50.00     RHOM =  75.00
RHOG = 100.00      CSD =  2000000.      CSW = 4190000.      FN = 3.0
SIGMAF =  .95
```

POTENTIAL TEMPERATURES T(I)

9.487	9.959	10.197	10.980	11.997	13.112	14.072	14.879	15.787	16.619
17.463	18.320	19.285	20.169	21.068	22.894	24.619	26.365	27.865	28.415
28.978	29.665	30.258	30.865	31.488	32.242	32.898	33.571	34.383	35.093

WIND COMPONENTS U(I)

4.391	5.448	6.038	6.629	7.220	7.810	8.401	8.991	9.582	10.173
10.763	11.354	11.945	12.535	13.126	13.668	14.197	14.726	15.255	15.784
16.313	16.842	17.371	17.900	18.429	18.958	19.487	20.016	20.545	21.074

WIND COMPONENTS V(I)

0.000	0.000	0.000	0.000	0.000	0.000	0.000	0.000	0.000	0.000
0.000	0.000	0.000	0.000	0.000	0.000	0.000	0.000	0.000	0.000
0.000	0.000	0.000	0.000	0.000	0.000	0.000	0.000	0.000	0.000

MIXING RATIOS Q(I)X1000

4.297	4.030	4.072	2.927	1.825	1.111	.790	.794	.797	.801
.805	.808	.812	.816	.820	1.333	2.347	4.018	5.508	4.747
4.081	3.499	2.993	2.553	2.171	1.841	1.557	1.313	1.103	.924

GEOSTROPHIC COMPS. UG(I)

4.391	5.448	6.038	6.629	7.220	7.810	8.401	8.991	9.582	10.173
10.763	11.354	11.945	12.535	13.126	13.668	14.197	14.726	15.255	15.784
16.313	16.842	17.371	17.900	18.429	18.958	19.487	20.016	20.545	21.074

GEOSTROPHIC COMPS. VG(I)

0.000	0.000	0.000	0.000	0.000	0.000	0.000	0.000	0.000	0.000
0.000	0.000	0.000	0.000	0.000	0.000	0.000	0.000	0.000	0.000
0.000	0.000	0.000	0.000	0.000	0.000	0.000	0.000	0.000	0.000

```
RUSKIN SOUNDING  021,1985

TA= 12.80          UA =  2.65          VA =  2.65          QA =   .0080
UGA =   2.65       VOA =   0.00        OLATD =  29.0       DECLD =-20.0
ZO =  1.5000       CAPG = 107193.560   TM = 22.00          IDOWN =  319.0
TX =  40.          TM =   0.           GOTIME =    420.00  TRANSM =  .95
TG = 13.80         RHOGX = 100.00      RHOWLT =  50.00     RHOM =  75.00
RHOG = 100.00      CSD =  2000000.     CSW = 4190000.      FN = 3.0
SIGMAF =  .75

POTENTIAL TEMPERATURES T(I)
  12.494  12.179  12.083  12.759  13.360  14.056  14.675  15.677  17.141  18.712
  19.596  19.764  20.034  20.217  21.075  21.877  22.791  23.120  23.382  23.821
  24.166  24.629  24.995  25.483  25.985  26.387  26.916  27.343  27.901  28.476

WIND COMPONENTS U(I)
   5.415   6.530   7.353   8.176   8.999   9.823  10.646  11.469  12.292  13.116
  13.939  14.762  15.585  16.408  17.060  17.362  17.664  17.966  18.268  18.570
  18.872  19.174  19.476  19.778  20.081  20.383  20.685  20.987  21.289  21.591

WIND COMPONENTS           V(I)
   0.000   0.000   0.000   0.000   0.000   0.000   0.000   0.000   0.000   0.000
   0.000   0.000   0.000   0.000   0.000   0.000   0.000   0.000   0.000   0.000
   0.000   0.000   0.000   0.000   0.000   0.000   0.000   0.000   0.000   0.000

MIXING RATIOS Q(I)X1000
   8.001   7.818   7.650   7.496   7.346   7.198   7.053   7.172   7.821   8.522
   8.691   8.355   8.030   7.718   5.495   5.183   4.885   5.302   5.322   4.876
   4.464   4.082   3.731   3.406   3.106   2.830   2.576   2.343   2.129   1.932

GEOSTROPHIC COMPS. UG(I)
   5.415   6.530   7.353   8.176   8.999   9.823  10.646  11.469  12.292  13.116
  13.939  14.762  15.585  16.408  17.060  17.362  17.664  17.966  18.268  18.570
  18.872  19.174  19.476  19.778  20.081  20.383  20.685  20.987  21.289  21.591

GEOSTROPHIC COMPS. VG(I)
   0.000   0.000   0.000   0.000   0.000   0.000   0.000   0.080   0.000   0.000
   0.000   0.000   0.000   0.000   0.000   0.000   0.000   0.000   0.000   0.000
   0.000   0.000   0.000   0.000   0.000   0.000   0.000   0.000   0.000   0.000
```

```
RUSKIN SOUNDING  023,1985

TA=  5.60          UA =  3.18          VA =  3.18          QA =   .0036
UGA =   3.18       VOA =   0.00        OLATD =  29.0       DECLD =-20.0
ZO =  1.5000       CAPG = 107193.560   TM = 10.40          IDOWN =  319.0
TX =  40.          TM =   0.           GOTIME =    420.00  TRANSM =  .95
TG =  6.60         RHOGX = 100.00      RHOWLT =  50.00     RHOM =  75.00
RHOG = 100.00      CSD =  2000000.     CSW = 4190000.      FN = 3.0
SIGMAF =  .75

POTENTIAL TEMPERATURES T(I)
   4.019   3.940   4.055   4.105   4.243   4.390   4.495   4.888   5.406   7.928
   9.214  10.606  11.923  13.351  14.703  16.005  17.293  18.500  19.826  20.528
  21.230  21.842  22.583  23.462  24.469  25.384  26.433  27.386  28.479  29.596

WIND COMPONENTS U(I)
   4.972   6.765   7.153   7.437   7.720   8.003   8.286   8.569   8.853   9.136
   9.419   9.702   9.985  10.269  10.552  10.909  11.281  11.653  12.025  12.397
  12.769  13.141  13.513  13.885  14.257  14.629  15.001  15.373  15.745  16.117

WIND COMPONENTS           V(I)
   0.000   0.000   0.000   0.000   0.000   0.000   0.000   0.000   0.000   0.000
   0.000   0.000   0.000   0.000   0.000   0.000   0.000   0.000   0.000   0.000
   0.000   0.000   0.000   0.000   0.000   0.000   0.000   0.000   0.000   0.000

MIXING RATIOS Q(I)X1000
   3.560   3.258   3.302   3.374   3.448   3.524   3.514   3.038   2.465   1.365
   1.364   1.364   1.363   1.362   1.361   1.679   2.151   2.742   3.477   3.282
   2.901   2.560   2.259   2.141   2.029   1.922   1.821   1.724   1.631   1.543

GEOSTROPHIC COMPS. UG(I)
   4.972   6.765   7.153   7.437   7.720   8.003   8.286   8.569   8.853   9.136
   9.419   9.702   9.985  10.269  10.552  10.909  11.281  11.653  12.025  12.397
  12.769  13.141  13.513  13.885  14.257  14.629  15.001  15.373  15.745  16.117

GEOSTROPHIC COMPS. VG(I)
   0.000   0.000   0.000   0.000   0.000   0.000   0.000   0.000   0.000   0.000
   0.000   0.000   0.000   0.000   0.000   0.000   0.000   0.000   0.000   0.000
   0.000   0.000   0.000   0.000   0.000   0.000   0.000   0.000   0.000   0.000
```

```
RUSKIN SOUNDINO  024,1985

TA= 10.20          UA =  3.18          VA =  3.18         QA =     .0044
UOA =    3.18      VOA =    0.00       GLATD =  29.0      DECLD =-20.0
ZO =  1.5000       CAPG = 107193.560   TM = 14.40         IDOWN =  319.0
TX =  40.          TN =    0.          GOTIME =    420.00 TRANSM =  .95
TG = 11.20         RHOGX = 100.00      RHOWLT =  50.00    RHOM =  75.00
RHOG = 100.00      CSD =  2000000.     CSW = 4190000.     FN = 3.0
SIGMAF =  .75

POTENTIAL TEMPERATURES T(I)
   9.264   9.569   9.708   9.937  10.091  10.337  10.507  11.184  11.960  12.552
  13.066  13.682  14.219  14.861  15.421  16.115  16.935  18.249  20.339  22.345
  24.399  25.532  26.331  27.037  27.872  28.611  29.485  30.261  31.055  31.991

WIND COMPONENTS U(I)
   3.479   3.920   4.835   5.749   6.664   7.578   8.493   9.407  10.322  11.236
  12.151  13.065  13.980  14.894  15.809  16.263  16.665  17.068  17.471  17.874
  18.276  18.679  19.082  19.485  19.888  20.290  20.693  21.096  21.499  21.902

WIND COMPONENTS                V(I)
   0.000   0.000   0.000   0.000   0.000   0.000   0.000   0.000   0.000   0.000
   0.000   0.000   0.000   0.000   0.000   0.000   0.000   0.000   0.000   0.000
   0.000   0.000   0.000   0.000   0.000   0.000   0.000   0.000   0.000   0.000

MIXING RATIOS Q(I)X1000
   4.405   4.212   4.278   4.346   4.415   4.486   4.558   5.050   5.572   5.188
   4.829   4.491   4.174   3.877   3.600   3.941   4.390   4.071   3.049   2.406
   3.831   4.229   3.841   3.485   3.158   2.860   2.586   2.336   2.108   1.900

GEOSTROPHIC COMPS. UG(I)
   3.479   3.920   4.835   5.749   6.664   7.578   8.493   9.407  10.322  11.236
  12.151  13.065  13.980  14.894  15.809  16.263  16.665  17.068  17.471  17.874
  18.276  18.679  19.082  19.485  19.888  20.290  20.693  21.096  21.499  21.902

GEOSTROPHIC COMPS. VG(I)
   0.000   0.000   0.000   0.000   0.000   0.000   0.000   0.000   0.000   0.000
   0.000   0.000   0.000   0.000   0.000   0.000   0.000   0.000   0.000   0.000
   0.000   0.000   0.000   0.000   0.000   0.000   0.000   0.000   0.000   0.000
```

```
RUSKIN SOUNDING  026,1985

TA= 16.20          UA =  3.18          VA =  3.18         QA =     .0102
UOA =    3.18      VOA =    0.00       OLATD =  29.0      DECLD =-20.0
ZO =  1.5000       CAPG = 107193.560   TM = 23.20         IDOWN =  319.0
TX =  40.          TN =    0.          GOTIME =    420.00 TRANSM =  .95
TG = 17.20         RHOGX = 100.00      RHOWLT =  50.00    RHOM =  75.00
RHOG = 100.00      CSD =  2000000.     CSW = 4190000.     FN = 3.0
SIGMAF =  .75

POTENTIAL TEMPERATURES T(I)
  15.549  15.719  16.034  16.272  16.602  16.941  17.289  17.646  17.921  18.769
  19.827  21.265  22.249  23.096  23.689  24.295  24.914  25.443  26.087  26.744
  27.415  27.513  27.681  27.861  28.198  28.626  29.183  29.754  30.342  30.947

WIND COMPONENTS U(I)
   4.983   6.467   7.669   8.871  10.073  11.275  12.477  13.678  14.880  16.082
  17.284  18.486  19.688  20.890  22.092  22.346  22.445  22.545  22.644  22.744
  22.843  22.943  23.042  23.142  23.241  23.341  23.440  23.540  23.639  23.739

WIND COMPONENTS                V(I)
   0.000   0.000   0.000   0.000   0.000   0.000   0.000   0.000   0.000   0.000
   0.000   0.000   0.000   0.000   0.000   0.000   0.000   0.000   0.000   0.000
   0.000   0.000   0.000   0.000   0.000   0.000   0.000   0.000   0.000   0.000

MIXING RATIOS Q(I)X1000
  10.215  10.206   9.982   9.764   9.549   9.339   9.134   8.933   8.737   7.679
   5.884   3.462   5.490   7.127   7.579   7.791   7.966   8.147   8.331   8.520
   8.715   8.192   7.629   7.102   6.633   6.226   5.840   5.475   5.131   4.807

GEOSTROPHIC COMPS. UG(I)
   4.983   6.467   7.669   8.871  10.073  11.275  12.477  13.678  14.880  16.082
  17.284  18.486  19.688  20.890  22.092  22.346  22.445  22.545  22.644  22.744
  22.843  22.943  23.042  23.142  23.241  23.341  23.440  23.540  23.639  23.739

GEOSTROPHIC COMPS. VG(I)
   0.000   0.000   0.000   0.000   0.000   0.000   0.000   0.000   0.000   0.000
   0.000   0.000   0.000   0.000   0.000   0.000   0.000   0.000   0.000   0.000
   0.000   0.000   0.000   0.000   0.000   0.000   0.000   0.000   0.000   0.000
```

RUSKIN SOUNDING 027,1985

TA= 10.40	UA = 3.18	VA = 3.18	QA = .0021
UOA = 3.18	VOA = 0.00	OLATD = 29.0	DECLD =-20.0
ZO = 1.5000	CAPG = 107193.560	TM = 12.00	IDOWN = 319.0
TX = 40.	TN = 0.	GOTIME = 420.00	TRANSM = .95
TG = 11.40	RHOGX = 100.00	RHOWLT = 50.00	RHOM = 75.00
RHOG = 100.00	CSD = 2000000.	CSW = 4190000.	FN = 3.0
SIGMAF = .75			

POTENTIAL TEMPERATURES T(I)

9.896	10.330	10.283	10.238	10.284	10.252	10.311	10.293	10.368	10.909
12.029	15.182	18.362	19.803	20.374	21.140	21.881	22.816	24.351	25.905
27.588	29.185	30.766	31.183	31.728	32.173	32.752	33.229	33.722	34.355

WIND COMPONENTS U(I)

3.952	4.724	4.919	5.078	5.237	5.396	5.554	5.713	5.872	6.031
6.190	6.348	6.507	6.666	6.825	7.027	7.259	7.491	7.722	7.954
8.186	8.418	8.650	8.882	9.114	9.346	9.577	9.809	10.041	10.273

WIND COMPONENTS V(I)

0.000	0.000	0.000	0.000	0.000	0.000	0.000	0.000	0.000	0.000
0.000	0.000	0.000	0.000	0.000	0.000	0.000	0.000	0.000	0.000
0.000	0.000	0.000	0.000	0.000	0.000	0.000	0.000	0.000	0.000

MIXING RATIOS Q(I)X1000

2.090	1.963	1.911	1.863	1.817	1.772	1.728	1.685	1.642	1.510
1.318	2.309	3.930	2.630	1.127	.775	.768	.796	1.216	1.829
2.709	3.960	5.320	4.259	3.390	2.684	2.112	1.651	1.283	.990

GEOSTROPHIC COMPS. UG(I)

3.952	4.724	4.919	5 078	5.237	5.396	5.554	5.713	5.872	6.031
6.190	6.348	6.507	6.666	6.825	7.027	7.259	7.491	7.722	7.954
8.186	8.418	8.650	8.882	9.114	9.346	9.577	9.809	10.041	10.273

GEOSTROPHIC COMPS. VG(I)

0.000	0.000	0.000	0.000	0.000	0.000	0.000	0.000	0.000	0.000
0.000	0.000	0.000	0.000	0.000	0.000	0.000	0.000	0.000	0.000
0.000	0.000	0.000	0.000	0.000	0.000	0.000	0.000	0.000	0.000

RUSKIN SOUNDING 047,1985

TA= 10.60	UA = 2.65	VA = 0.00	QA = .0038
UOA = 2.65	VOA = 0.00	OLATD = 29.0	DECLD =-20.0
ZO = 1.5000	CAPG = 107193.560	TM = 12.60	IDOWN = 319.0
TX = 40.	TN = 0.	GOTIME = 420.00	TRANSM = .95
TG = 11.60	RHOGX = 100.00	RHOWLT = 50.00	RHOM = 75.00
RHOG = 100.00	CSD = 2000000.	CSW = 4190000.	FN = 3.0
SIGMAF = .75			

POTENTIAL TEMPERATURES T(I)

11.326	11.646	11.749	11.858	11.972	12.092	12.218	12.377	12.568	12.855
13.059	13.271	13.490	12.904	12.279	12.540	12.810	13.087	13.373	13.668
14.074	14.388	14.712	17.203	19.926	22.677	25.454	28.259	31.093	33.956

WIND COMPONENTS U(I)

2.988	3.523	4.321	5.118	5.916	6.713	7.511	8.309	9.106	9.904
10.701	11.499	12.296	13.094	13.858	14.412	14.967	15.521	16.076	16.631
17.185	17.740	18.295	18.849	19.404	19.958	20.513	21.068	21.622	22.177

WIND COMPONENTS V(I)

0.000	0.000	0.000	0.000	0.000	0.000	0.000	0.000	0.000	0.000
0.000	0.000	0.000	0.000	0.000	0.000	0.000	0.000	0.000	0.000
0.000	0.000	0.000	0.000	0.000	0.000	0.000	0.000	0.000	0.000

MIXING RATIOS Q(I)X1000

3.772	3.009	2.297	1.739	1.306	.973	.718	.608	.583	.559
.535	.513	.491	1.023	2.145	2.279	2.421	2.571	2.730	2.899
3.078	3.268	3.468	3.754	4.068	4.405	4.766	5.152	5.566	6.009

GEOSTROPHIC COMPS. UG(I)

2.988	3.523	4.321	5.118	5.916	6.713	7.511	8.309	9.106	9.904
10.701	11.499	12.296	13.094	13.858	14.412	14.967	15.521	16.076	16.631
17.185	17.740	18.295	18.849	19.404	19.958	20.513	21.068	21.622	22.177

GEOSTROPHIC COMPS. VG(I)

0.000	0.000	0.000	0.000	0.000	0.000	0.000	0.000	0.000	0.000
0.000	0.000	0.000	0.000	0.000	0.000	0.000	0.000	0.000	0.000
0.000	0.000	0.000	0.000	0.000	0.000	0.000	0.000	0.000	0.000

OAINESVILLE SOUNDINO 005,1985

TA= 7.22	UA = 11.13	VA = 11.13	QA = .0082
UGA = 11.13	VGA = 0.00	GLATD = 29.0	DECLD =-20.0
ZO = 1.5000	CAPG = 107193.560	TM = 8.22	IDOWN = 319.0
TX = 40.	TN = 0.	GOTIME = 420.00	TRANSM = .95
TG = 8.22	RHOGX = 100.00	RHOWLT = 50.00	RHOM = 75.00
RHOG = 100.00	CSD = 2000000.	CSW = 4190000.	FN = 3.0
SIGMAF = .75			

POTENTIAL TEMPERATURES T(I)

9.588	9.491	9.343	9.156	8.973	8.793	8.659	8.487	8.433	8.410
8.393	8.557	8.774	8.998	9.259	11.025	13.325	14.136	14.958	15.791
16.635	17.331	21.436	23.013	23.764	24.472	25.191	26.130	27.184	28.253

WIND COMPONENTS U(I)

7.077	8.096	8.987	9.878	10.769	11.660	12.551	13.442	14.333	15.224
16.115	17.006	17.897	18.788	19.370	20.051	20.732	21.414	22.095	22.777
23.458	24.140	24.821	25.503	26.184	26.866	27.547	28.229	28.910	29.592

WIND COMPONENTS V(I)

0.000	0.000	0.000	0.000	0.000	0.000	0.000	0.000	0.000	0.000
0.000	0.000	0.000	0.000	0.000	0.000	0.000	0.000	0.000	0.000
0.000	0.000	0.000	0.000	0.000	0.000	0.000	0.000	0.000	0.000

MIXING RATIOS Q(I)X1000

4.539	4.580	4.558	4.536	4.515	4.494	4.473	4.452	4.370	4.275
4.182	4.074	3.965	3.858	3.760	3.481	3.479	3.546	3.623	3.712
3.813	3.720	2.178	1.509	1.337	1.190	1.064	1.095	1.207	1.335

GEOSTROPHIC COMPS. UG(I)

7.077	8.096	8.987	9.878	10.769	11.660	12.551	13.442	14.333	15.224
16.115	17.006	17.897	18.788	19.370	20.051	20.732	21.414	22.095	22.777
23.458	24.140	24.821	25.503	26.184	26.866	27.547	28.229	28.910	29.592

OEOSTROPHIC COMPS. VG(I)

0.000	0.000	0.000	0.000	0.000	0.000	0.000	0.000	0.000	0.000
0.000	0.000	0.000	0.000	0.000	0.000	0.000	0.000	0.000	0.000
0.000	0.000	0.000	0.000	0.000	0.000	0.000	0.000	0.000	0.000

OAINESVILLE SOUNDING 006,1985

TA= 4.44	UA = 5.83	VA = 5.83	QA = .0077
UOA = 5.83	VOA = 0.00	OLATD = 29.0	DECLD =-20.0
ZO = 1.5000	CAPG = 107193.560	TM = 5.44	IDOWN = 319.0
TX = 40.	TN = 0.	GOTIME = 420.00	TRANSM = .95
TG = 5.44	RHOGX = 100.00	RHOWLT = 50.00	RHOM = 75.00
RHOG = 100.00	CSD = 2000000.	CSW = 4190000.	FN = 3.0
SIGMAF = .75			

POTENTIAL TEMPERATURES T(I)

7.958	8.191	8.272	8.358	8.411	8.513	8.621	8.695	8.863	10.883
11.706	12.133	13.979	16.114	17.295	18.216	19.096	19.830	20.630	21.446
22.277	23.108	23.894	24.752	25.628	26.523	27.379	28.235	28.768	29.256

WIND COMPONENTS U(I)

4.315	5.355	5.516	5.677	5.838	5.999	6.160	6.321	6.482	6.644
6.805	6.966	7.127	7.288	7.399	7.265	7.130	6.995	6.859	6.724
6.589	6.454	6.319	6.184	6.049	5.914	5.779	5.644	5.509	5.373

WIND COMPONENTS V(I)

0.000	0.000	0.000	0.000	0.000	0.000	0.000	0.000	0.000	0.000
0.000	0.000	0.000	0.000	0.000	0.000	0.000	0.000	0.000	0.000
0.000	0.000	0.000	0.000	0.000	0.000	0.000	0.000	0.000	0.000

MIXING RATIOS Q(I)X1000

3.917	3.822	3.811	3.800	3.790	3.781	3.772	3.765	3.758	3.890
3.711	3.311	1.702	1.610	1.530	1.937	2.430	1.818	1.381	1.069
.848	.829	.898	1.004	1.157	1.368	1.650	1.746	.986	.582

OEOSTROPHIC COMPS. UG(I)

4.315	5.355	5.516	5.677	5.838	5.999	6.160	6.321	6.482	6.644
6.805	6.966	7.127	7.288	7.399	7.265	7.130	6.995	6.859	6.724
6.589	6.454	6.319	6.184	6.049	5.914	5.779	5.644	5.509	5.373

OEOSTROPHIC COMPS. VG(I)

0.000	0.000	0.000	0.000	0.000	0.000	0.000	0.000	0.000	0.000
0.000	0.000	0.000	0.000	0.000	0.000	0.000	0.000	0.000	0.000
0.000	0.000	0.000	0.000	0.000	0.000	0.000	0.000	0.000	0.000

GAINESVILLE SOUNDING 013,1985

TA= 3.89	UA = 7.95	VA = 7.95	QA = .0119
UGA = 11.02	VGA = 0.00	GLATD = 29.0	DECLD =-20.0
ZO = 1.5000	CAPG = 107193.560	TM = 4.89	IDOWN = 319.0
TX = 40.	TN = 0.	GOTIME = 420.00	TRANSM = .95
TG = 4.89	RHOGX = 100.00	RHOWLT = 50.00	RHOM = 75.00
RHOG = 100.00	CSD = 2000000.	CSW = 4190000.	FN = 3.0
SIGMAF = .95			

POTENTIAL TEMPERATURES T(I)

2.226	2.572	2.858	3.194	3.457	3.811	4.090	4.770	6.238	7.941
9.055	10.506	12.542	14.380	15.775	16.752	17.722	18.710	19.713	20.735
21.773	22.830	23.906	25.002	25.834	26.679	27.602	28.427	29.491	30.746

WIND COMPONENTS U(I)

6.032	7.995	8.563	9.130	9.698	10.266	10.833	11.401	11.969	12.536
13.104	13.672	14.239	14.807	15.411	16.091	16.751	17.412	18.072	18.732
19.393	20.053	20.713	21.374	22.034	22.694	23.355	24.015	24.675	25.336

WIND COMPONENTS V(I)

0.000	0.000	0.000	0.000	0.000	0.000	0.000	0.000	0.000	0.000
0.000	0.000	0.000	0.000	0.000	0.000	0.000	0.000	0.000	0.000
0.000	0.000	0.000	0.000	0.000	0.000	0.000	0.000	0.000	0.000

MIXING RATIOS Q(I)X1000

2.529	2.439	2.366	2.298	2.234	2.174	2.119	1.682	1.107	.998
1.205	1.385	1.797	1.664	.968	.855	.825	.797	.771	.746
.723	.701	.681	.662	.751	.871	1.029	1.231	1.588	2.160

GEOSTROPHIC COMPS. UG(I)

4.180	4.882	5.585	6.286	6.989	7.690	8.393	9.094	9.797	10.499
11.201	11.903	12.605	13.307	14.009	14.711	15.413	16.115	16.817	17.519
18.221	18.923	19.625	20.327	21.029	21.731	22.433	23.135	23.837	24.539

GEOSTROPHIC COMPS. VG(I)

0.000	0.000	0.000	0.000	0.000	0.000	0.000	0.000	0.000	0.000
0.000	0.000	0.000	0.000	0.000	0.000	0.000	0.000	0.000	0.000
0.000	0.000	0.000	0.000	0.000	0.000	0.000	0.000	0.000	0.000

GAINESVILLE SOUNDING 016,1985

TA= 5.00	UA = 4.24	VA = 4.24	QA = .0103
UGA = 22.05	VGA = 0.00	OLATD = 29.0	DECLD =-20.0
ZO = 1.5000	CAPG = 107193.560	TM = 6.00	IDOWN = 319.0
TX = 40.	TN = 0.	GOTIME = 420.00	TRANSM = .95
TG = 6.00	RHOGX = 100.00	RHOWLT = 50.00	RHOM = 75.00
RHOG = 100.00	CSD = 2000000.	CSW = 4190000.	FN = 3.0
SIGMAF = .95			

POTENTIAL TEMPERATURES T(I)

9.055	9.339	9.434	9.846	10.337	10.922	11.391	11.787	12.727	14.227
15.020	15.756	16.552	17.361	18.201	19.928	21.565	23.221	24.809	25.431
26.067	26.826	27.493	28.231	28.929	29.702	30.492	31.243	32.133	32.921

WIND COMPONENTS U(I)

4.011	4.950	5.526	6.102	6.678	7.253	7.829	8.405	8.981	9.556
10.132	10.708	11.284	11.859	12.454	13.129	13.798	14.467	15.135	15.804
16.473	17.142	17.811	18.480	19.148	19.817	20.486	21.155	21.824	22.493

WIND COMPONENTS V(I)

0.000	0.000	0.000	0.000	0.000	0.000	0.000	0.000	0.000	0.000
0.000	0.000	0.000	0.000	0.000	0.000	0.000	0.000	0.000	0.000
0.000	0.000	0.000	0.000	0.000	0.000	0.000	0.000	0.000	0.000

MIXING RATIOS Q(I)X1000

2.837	2.678	2.675	2.080	1.508	1.130	.949	.931	.829	.667
.661	.659	.657	.656	.675	1.112	1.906	3.187	4.592	4.054
3.576	3.150	2.773	2.438	2.143	1.882	1.651	1.448	1.269	1.111

GEOSTROPHIC COMPS. UG(I)

12.949	13.270	13.590	13.910	14.230	14.550	14.871	15.190	15.511	15.831
16.152	16.472	16.791	17.112	17.432	17.752	18.072	18.393	18.713	19.033
19.353	19.673	19.994	20.314	20.634	20.954	21.274	21.595	21.914	22.235

GEOSTROPHIC COMPS. VG(I)

0.000	0.000	0.000	0.000	0.000	0.000	0.000	0.000	0.000	0.000
0.000	0.000	0.000	0.000	0.000	0.000	0.000	0.000	0.000	0.000
0.000	0.000	0.000	0.000	0.000	0.000	0.000	0.000	0.000	0.000

GAINESVILLE SOUNDING 021,1985

TA= -.56	UA = 2.12	VA = 2.12	QA = .0112
UGA = 2.12	VGA = 0.00	GLATD = 29.0	DECLD =-20.0
ZO = 1.5000	CAPG = 107193.560	TM = .44	IDOWN = 319.0
TX = 40.	TN = 0.	GOTIME = 420.00	TRANSM = .95
TG = .44	RHOGX = 100.00	RHOWLT = 50.00	RHOM = 75.00
RHOG = 100.00	CSD = 2000000.	CSW = 4190000.	FN = 3.0
SIGMAF = .75			

POTENTIAL TEMPERATURES T(I)

3.138	3.023	2.987	3.340	3.658	4.025	4.357	4.883	5.644	6.639
7.420	9.264	11.055	12.717	14.195	15.574	17.018	18.179	19.316	20.551
19.287	21.272	21.733	22.261	22.801	23.297	23.862	24.383	24.976	25.583

WIND COMPONENTS U(I)

6.599	7.761	8.676	9.591	10.506	11.421	12.335	13.250	14.165	15.080
15.994	16.909	17.824	18.739	19.447	19.963	20.479	20.994	21.510	22.026
22.542	23.058	23.573	24.089	24.605	25.121	25.636	26.152	26.668	27.184

WIND COMPONENTS V(I)

0.000	0.000	0.000	0.000	0.000	0.000	0.000	0.000	0.000	0.000
0.000	0.000	0.000	0.000	0.000	0.000	0.000	0.000	0.000	0.000
0.000	0.000	0.000	0.000	0.000	0.000	0.000	0.000	0.000	0.000

MIXING RATIOS Q(I)X1000

4.446	4.337	4.257	4.184	4.113	4.043	3.975	4.038	4.367	4.671
4.685	4.316	4.116	3.986	2.942	2.893	2.904	3.345	3.690	3.942
3.377	3.992	3.815	3.652	3.502	3.365	3.238	3.122	3.015	2.917

GEOSTROPHIC COMPS. UG(I)

6.599	7.761	8.676	9.591	10.506	11.421	12.335	13.250	14.165	15.080
15.994	16.909	17.824	18.739	19.447	19.963	20.479	20.994	21.510	22.026
22.542	23.058	23.573	24.089	24.605	25.121	25.636	26.152	26.668	27.184

GEOSTROPHIC COMPS. VG(I)

0.000	0.000	0.000	0.000	0.000	0.000	0.000	0.000	0.000	0.000
0.000	0.000	0.000	0.000	0.000	0.000	0.000	0.000	0.000	0.000
0.000	0.000	0.000	0.000	0.000	0.000	0.000	0.000	0.000	0.000

GAINESVILLE SOUNDING 022,1985

TA= -5.56	UA = 10.07	VA = 10.07	QA = .0053
UGA = 10.07	VGA = 0.00	GLATD = 29.0	DECLD =-20.0
ZO = 1.5000	CAPG = 107193.560	TM = -4.56	IDOWN = 319.0
TX = 40.	TN = 0.	GOTIME = 420.00	TRANSM = .95
TG = -4.56	RHOGX = 100.00	RHOWLT = 50.00	RHOM = 75.00
RHOG = 100.00	CSD = 2000000.	CSW = 4190000.	FN = 3.0
SIGMAF = .75			

POTENTIAL TEMPERATURES T(I)

-4.031	-3.899	-3.800	-3.748	-3.652	-3.550	-3.441	-3.284	-3.202	-3.122
-3.144	6.975	7.371	6.519	8.092	9.403	10.730	12.076	13.438	14.817
16.215	17.580	19.015	20.469	21.944	23.440	24.902	26.500	28.063	28.773

WIND COMPONENTS U(I)

5.909	7.048	7.791	8.501	9.211	9.921	10.631	11.341	12.051	12.761
13.471	14.180	14.890	15.600	16.227	16.722	17.216	17.710	18.204	18.698
19.193	19.687	20.181	20.675	21.169	21.664	22.158	22.652	23.146	23.641

WIND COMPONENTS V(I)

0.000	0.000	0.000	0.000	0.000	0.000	0.000	0.000	0.000	0.000
0.000	0.000	0.000	0.000	0.000	0.000	0.000	0.000	0.000	0.000
0.000	0.000	0.000	0.000	0.000	0.000	0.000	0.000	0.000	0.000

MIXING RATIOS Q(I)X1000

1.916	1.744	1.694	1.674	1.654	1.635	1.616	1.598	1.579	1.326
.825	2.724	1.996	1.270	1.115	1.180	1.250	1.326	1.408	1.497
1.593	1.698	1.811	1.933	2.066	2.209	2.364	2.532	2.714	2.379

GEOSTROPHIC COMPS. UG(I)

5.909	7.048	7.791	8.501	9.211	9.921	10.631	11.341	12.051	12.761
13.471	14.180	14.890	15.600	16.227	16.722	17.216	17.710	18.204	18.698
19.193	19.687	20.181	20.675	21.169	21.664	22.158	22.652	23.146	23.641

GEOSTROPHIC COMPS. VG(I)

0.000	0.000	0.000	0.000	0.000	0.000	0.000	0.000	0.000	0.000
0.000	0.000	0.000	0.000	0.000	0.000	0.000	0.000	0.000	0.000
0.000	0.000	0.000	0.000	0.000	0.000	0.000	0.000	0.000	0.000

```
GAINESVILLE SOUNDING  023,1985

TA=  5.00         UA =  5.83          VA =  5.83          QA =   .0058
UGA =   5.83      VGA =   0.00        GLATD =  29.0       DECLD =-20.0
ZO =  1.5000      CAPG = 107193.560   TM =  6.00          IDOWN =  319.0
TX =  40.         TN =   0.           GOTIME =   420.00   TRANSM =  .95
TG =  6.00        RHOGI = 100.00      RHOWLT =  50.00     RHOM =  75.00
RHOG = 100.00     CSD =  2000000.     CSW = 4190000.      FN = 3.0
SIGMAF =  .75

POTENTIAL TEMPERATURES T(I)
   4.424   4.563   4.660   4.770   4.886   5.051   5.158   5.455   5.820   7.147
   7.904   8.675   9.992  11.697  13.185  14.265  15.394  16.441  17.605  18.467
  19.287  20.122  20.978  21.967  22.974  24.002  25.050  25.813  26.582  27.311

WIND COMPONENTS U(I)
   5.094   6.650   7.211   7.718   8.226   8.734   9.241   9.749  10.257  10.764
  11.272  11.780  12.287  12.795  13.280  13.716  14.159  14.602  15.046  15.489
  15.932  16.376  16.819  17.262  17.705  18.149  18.592  19.035  19.479  19.922

WIND COMPONENTS           V(I)
   0.000   0.000   0.000   0.000   0.000   0.000   0.000   0.000   0.000   0.000
   0.000   0.000   0.000   0.000   0.000   0.000   0.000   0.000   0.000   0.000
   0.000   0.000   0.000   0.000   0.000   0.000   0.000   0.000   0.000   0.000

MIXING RATIOS Q(I)X1000
   2.465   2.320   2.325   2.345   2.365   2.387   2.367   2.114   1.813   1.249
   1.234   1.220   1.103    .961    .859   1.018   1.255   1.551   1.919   1.822
   1.632   1.462   1.312   1.254   1.199   1.146   1.096   1.136   1.253   1.456

GEOSTROPHIC COMPS. UG(I)
   5.094   6.650   7.211   7.718   8.226   8.734   9.241   9.749  10.257  10.764
  11.272  11.780  12.287  12.795  13.280  13.716  14.159  14.602  15.046  15.489
  15.932  16.376  16.819  17.262  17.705  18.149  18.592  19.035  19.479  19.922

GEOSTROPHIC COMPS. VG(I)
   0.000   0.000   0.000   0.000   0.000   0.000   0.000   0.000   0.000   0.000
   0.000   0.000   0.000   0.000   0.000   0.000   0.000   0.000   0.000   0.000
   0.000   0.000   0.000   0.000   0.000   0.000   0.000   0.000   0.000   0.000
```

```
GAINESVILLE SOUNDING  024,1985

TA=  4.44         UA =  1.59          VA =  1.59          QA =   .0066
UGA =   1.59      VGA =   0.00        GLATD =  29.0       DECLD =-20.0
ZO =  1.5000      CAPG = 107193.560   TM =  5.44          IDOWN =  319.0
TX =  40.         TN =   0.           GOTIME =   420.00   TRANSM =  .95
TG =  5.44        RHOGI = 100.00      RHOWLT =  50.00     RHOM =  75.00
RHOG = 100.00     CSD =  2000000.     CSW = 4190000.      FN = 3.0
SIGMAF =  .75

POTENTIAL TEMPERATURES T(I)
   8.124   8.490   8.611   8.820   8.955   9.182   9.332   9.782  10.244  10.661
  11.000  11.439  11.797  12.260  12.734  13.512  14.312  15.416  16.866  18.513
  20.164  22.467  24.699  24.984  25.655  26.343  27.049  27.772  28.455  29.279

WIND COMPONENTS U(I)
   4.444   5.309   6.151   6.992   7.834   8.676   9.517  10.359  11.200  12.042
  12.884  13.725  14.567  15.408  16.218  16.737  17.230  17.722  18.215  18.708
  19.201  19.693  20.186  20.679  21.172  21.665  22.157  22.650  23.143  23.636

WIND COMPONENTS           V(I)
   0.000   0.000   0.000   0.000   0.000   0.000   0.000   0.000   0.000   0.000
   0.000   0.000   0.000   0.000   0.000   0.000   0.000   0.000   0.000   0.000
   0.000   0.000   0.000   0.000   0.000   0.000   0.000   0.000   0.000   0.000

MIXING RATIOS Q(I)X1000
   2.858   2.746   2.753   2.762   2.773   2.786   2.800   3.024   3.265   3.054
   2.855   2.668   2.492   2.327   2.177   2.346   2.569   2.409   1.896   2.006
   3.710   4.290   4.369   3.153   2.880   2.629   2.397   2.184   1.988   1.808

GEOSTROPHIC COMPS. UG(I)
   4.444   5.309   6.151   6.992   7.834   8.676   9.517  10.359  11.200  12.042
  12.884  13.725  14.567  15.408  16.218  16.737  17.230  17.722  18.215  18.708
  19.201  19.693  20.186  20.679  21.172  21.665  22.157  22.650  23.143  23.636

GEOSTROPHIC COMPS. VG(I)
   0.000   0.000   0.000   0.000   0.000   0.000   0.000   0.000   0.000   0.000
   0.000   0.000   0.000   0.000   0.000   0.000   0.000   0.000   0.000   0.000
   0.000   0.000   0.000   0.000   0.000   0.000   0.000   0.000   0.000   0.000
```

OAINESVILLE SOUNDINO 026,1985

TA= 13.33	UA = 3.71	VA = 3.71	QA = .0124
UGA = 3.71	VGA = 0.00	GLATD = 29.0	DECLD =-20.0
ZO = 1.5000	CAPG = 107193.560	TM = 14.33	IDOWN = 319.0
TX = 40.	TN = 0.	GOTIME = 420.00	TRANSM = .95
TG = 14.33	RHOGX = 100.00	RHOWLT = 50.00	RHOM = 75.00
RHOG = 100.00	CSD = 2000000.	CSW = 4190000.	FN = 3.0
SIGMAF = .75			

POTENTIAL TEMPERATURES T(I)

15.254	15.311	15.486	15.583	15.728	15.924	16.084	16.295	16.424	16.842
17.415	18.135	18.596	19.032	19.553	20.268	21.046	21.736	22.612	23.603
24.610	25.391	26.142	26.511	27.020	27.527	28.103	28.694	29.196	29.105

WIND COMPONENTS U(I)

5.936	7.231	8.385	9.539	10.693	11.847	13.001	14.155	15.308	16.462
17.616	18.770	19.924	21.078	22.175	22.757	23.263	23.768	24.273	24.778
25.283	25.789	26.294	26.799	27.304	27.809	28.314	28.820	29.325	29.830

WIND COMPONENTS V(I)

0.000	0.000	0.000	0.000	0.000	0.000	0.000	0.000	0.000	0.000
0.000	0.000	0.000	0.000	0.000	0.000	0.000	0.000	0.000	0.000
0.000	0.000	0.000	0.000	0.000	0.000	0.000	0.000	0.000	0.000

MIXING RATIOS Q(I)X1000

6.992	6.982	6.863	6.748	6.634	6.523	6.415	6.309	6.205	5.671
4.768	3.552	4.390	5.019	5.162	5.253	5.325	5.401	5.439	5.405
5.386	5.018	4.654	4.574	4.560	4.619	4.740	4.547	4.113	3.975

GEOSTROPHIC COMPS. UO(I)

5.936	7.231	8.385	9.539	10.693	11.847	13.001	14.155	15.308	16.462
17.616	18.770	19.924	21.078	22.175	22.757	23.263	23.768	24.273	24.778
25.283	25.789	26.294	26.799	27.304	27.809	28.314	28.820	29.325	29.830

OEOSTROPHIC COMPS. VO(I)

0.000	0.000	0.000	0.000	0.000	0.000	0.000	0.000	0.000	0.000
0.000	0.000	0.000	0.000	0.000	0.000	0.000	0.000	0.000	0.000
0.000	0.000	0.000	0.000	0.000	0.000	0.000	0.000	0.000	0.000

OAINESVILLE SOUNDING 027,1985

TA= 1.11	UA = 7.42	VA = 7.42	QA = .0055
UGA = 7.42	VGA = 0.00	GLATD = 29.0	DECLD =-20.0
ZO = 1.5000	CAPG = 107193.560	TM = 2.11	IDOWN = 319.0
TX = 40.	TN = 0.	GOTIME = 420.00	TRANSM = .95
TG = 2.11	RHOGX = 100.00	RHOWLT = 50.00	RHOM = 75.00
RHOG = 100.00	CSD = 2000000.	CSW = 4190000.	FN = 3.0
SIGMAF = .75			

POTENTIAL TEMPERATURES T(I)

7.790	8.105	8.070	8.076	8.088	8.107	8.133	8.167	8.208	8.529
9.522	12.132	14.721	16.498	17.805	19.098	20.259	21.526	23.154	24.752
26.019	27.148	28.331	28.886	29.569	30.155	30.874	31.494	32.191	32.907

WIND COMPONENTS U(I)

3.558	4.201	4.581	4.943	5.306	5.669	6.031	6.394	6.756	7.119
7.482	7.844	8.207	8.570	8.932	9.290	9.658	10.025	10.393	10.761
11.128	11.496	11.864	12.231	12.599	12.967	13.334	13.702	14.070	14.437

WIND COMPONENTS V(I)

0.000	0.000	0.000	0.000	0.000	0.000	0.000	0.000	0.000	0.000
0.000	0.000	0.000	0.000	0.000	0.000	0.000	0.000	0.000	0.000
0.000	0.000	0.000	0.000	0.000	0.000	0.000	0.000	0.000	0.000

MIXING RATIOS Q(I)X1000

1.434	1.259	1.211	1.172	1.134	1.097	1.062	1.028	.995	.918
.824	1.338	2.169	1.541	.815	.659	.672	.704	.933	1.260
1.695	2.313	2.986	2.449	2.008	1.648	1.355	1.119	.928	.776

GEOSTROPHIC COMPS. UO(I)

3.558	4.201	4.581	4.943	5.306	5.669	6.031	6.394	6.756	7.119
7.482	7.844	8.207	8.570	8.932	9.290	9.658	10.025	10.393	10.761
11.128	11.496	11.864	12.231	12.599	12.967	13.334	13.702	14.070	14.437

OEOSTROPHIC COMPS. VO(I)

0.000	0.000	0.000	0.000	0.000	0.000	0.000	0.080	0.000	0.000
0.000	0.000	0.000	0.000	0.000	0.000	0.000	0.000	0.000	0.000
0.000	0.000	0.000	0.000	0.000	0.000	0.000	0.000	0.000	0.000

```
GAINESVILLE SOUNDING  041,1985

TA=  7.22          UA =  5.30          VA =  5.30          QA =    .0085
UGA =    5.30      VGA =    0.00       GLATD =  29.0       OECLD =-20.0
ZO =  1.5000       CAPG = 107193.560   TM =  8.22          IDOWN =  319.0
TX =  40.          TN =    0.          GOTIME =    420.00  TRANSM =  .95
TG =  8.22         RHOGX = 100.00      RHOWLT =  50.00     RHOM =  75.00
RHOG = 100.00      CSO =  2000000.     CSW = 4190000.      FN = 3.0
SIGMAF =  .75

POTENTIAL TEMPERATURES T(I)
  13.698  14.094  14.103  14.121  14.146  14.134  14.129  14.219  14.228  14.244
  14.542  14.912  15.246  15.637  15.752  16.094  16.704  17.278  17.918  18.649
  19.396  20.106  20.831  21.625  22.437  23.211  24.058  25.408  27.593  29.149

WIND COMPONENTS U(I)
   1.585   2.106   2.227   2.346   2.466   2.586   2.705   2.825   2.945   3.065
   3.184   3.304   3.424   3.544   3.663   3.966   4.425   4.884   5.342   5.801
   6.260   6.719   7.178   7.637   8.096   8.554   9.013   9.472   9.931  10.390

WIND COMPONENTS           V(I)
   0.000   0.000   0.000   0.000   0.000   0.000   0.000   0.000   0.000   0.000
   0.000   0.000   0.000   0.000   0.000   0.000   0.000   0.000   0.000   0.000
   0.000   0.000   0.000   0.000   0.000   0.000   0.000   0.000   0.000   0.000

MIXING RATIOS Q(I)X1000
   2.614   2.433   2.427   2.415   2.404   2.394   2.386   2.378   2.372   2.367
   2.346   2.322   2.301   2.284   1.814   1.339    .992    .756    .709    .743
    .790    .853    .935   1.038   1.164   1.318   1.504   1.063    .624   1.898

GEOSTROPHIC COMPS. UG(I)
   1.585   2.106   2.227   2.346   2.466   2.586   2.705   2.825   2.945   3.065
   3.184   3.304   3.424   3.544   3.663   3.966   4.425   4.884   5.342   5.801
   6.260   6.719   7.178   7.637   8.096   8.554   9.013   9.472   9.931  10.390

GEOSTROPHIC COMPS. VG(I)
   0.000   0.000   0.000   0.000   0.000   0.000   0.000   0.000   0.000   0.000
   0.000   0.000   0.000   0.000   0.000   0.000   0.000   0.000   0.000   0.000
   0.000   0.000   0.000   0.000   0.000   0.000   0.000   0.000   0.000   0.000
```

```
GAINESVILLE SOUNDING  048,1985

TA=  7.78          UA =  4.77          VA =  0.00          QA =    .0076
UGA =    4.77      VGA =    0.00       GLATD =  29.0       DECLD =-20.0
ZO =  1.5000       CAPG = 107193.560   TM =  8.78          IDOWN =  319.0
TX =  40.          TN =    0.          GOTIME =    420.00  TRANSM =  .95
TG =  8.78         RHOGX = 100.00      RHOWLT =  50.00     RHOM =  75.00
RHOG = 100.00      CSD =  2000000.     CSW = 4190000.      FN = 3.0
SIGMAF =  .75

POTENTIAL TEMPERATURES T(I)
  12.233  12.451  12.452  12.501  12.557  12.577  12.691  12.726  12.812  12.906
  13.009  13.119  13.171  13.268  13.519  15.550  16.996  18.463  19.765  20.761
  21.879  22.909  24.098  25.368  26.602  27.973  28.799  29.682  30.464  31.328

WIND COMPONENTS U(I)
   3.037   2.949   3.108   3.266   3.424   3.582   3.740   3.898   4.056   4.215
   4.373   4.531   4.689   4.847   5.013   5.290   5.543   5.797   6.050   6.303
   6.557   6.810   7.064   7.317   7.571   7.824   8.077   8.331   8.584   8.838

WIND COMPONENTS           V(I)
   0.000   0.000   0.000   0.000   0.000   0.000   0.000   0.000   0.000   0.000
   0.000   0.000   0.000   0.000   0.000   0.000   0.000   0.000   0.000   0.000
   0.000   0.000   0.000   0.000   0.000   0.000   0.000   0.000   0.000   0.000

MIXING RATIOS Q(I)X1000
   2.033   2.148   2.148   2.148   2.148   2.149   2.150   2.151   2.152   2.154
   2.155   2.157   2.212   2.417   2.374   2.046   2.057   2.070   1.895   1.549
   1.284   1.087   1.194   1.566   2.066   2.735   2.594   2.333   2.122   1.954

GEOSTROPHIC COMPS. UG(I)
   3.037   2.949   3.108   3.266   3.424   3.582   3.740   3.898   4.056   4.215
   4.373   4.531   4.689   4.847   5.013   5.290   5.543   5.797   6.050   6.303
   6.557   6.810   7.064   7.317   7.571   7.824   8.077   8.331   8.584   8.838

GEOSTROPHIC COMPS. VG(I)
   0.000   0.000   0.000   0.000   0.000   0.000   0.000   0.000   0.000   0.000
   0.000   0.000   0.000   0.000   0.000   0.000   0.000   0.000   0.000   0.000
   0.000   0.000   0.000   0.000   0.000   0.000   0.000   0.000   0.000   0.000
```

P-model input files

```
ONV
005,1985
 1,51.1,60.6,65.6,45.7,46.0,46.2,6.0,0,1.0
 2,50.5,59.4,65.1,44.4,45.0,45.0,4.0,0,1.0
 3,49.1,58.5,64.9,43.3,43.9,44.1,3.2,0.1.0

ONV
006,1985
 1,49.3,56.1,60.8,42.4,44.4,45.7,3.0,0,1.0
 2,46.4,54.9,60.6,34.7,35.8,36.7,1.0,0,1.0
 3,44.2,53.6,60.6,31.5,34.0,34.5,0.0,0,1.0

ONV
013,1985
 1,46.4,53.6,57.6,40.8,41.0,41.5,4.0,0,1.0
 2,45.1,52.7,57.6,38.8,39.4,39.9,3.0,0,1.0
 3,43.3,52.8,57.6,35.6,37.0,37.9,3.0,0,1.0

ONV
016,1985
 1,50.0,56.8,55.9,45.1,47.5,49.1,0.0,0,1.0
 2,45.7,55.4,56.1,37.6,40.6,40.8,0.0,0,1.0
 3,43.5,54.1,55.9,33.8,37.4,38.1,0.0,0,1.0

GNV
021,1985
 1,43.3,50.9,55.4,36.5,36.5,36.5,18.0,0,1.0
 2,40.8,49.6,55.2,32.0,32.0,32.0,24.1,0,1.0
 3,38.7,48.4,55.2,29.5,29.5,29.5,22.5,0,1.0

ONV
022,1985
 1,35.1,42.8,51.1,25.2,25.9,26.1,8.3,0,1.0
 2,33.4,41.9,51.3,18.9,21.9,23.5,0.0,0.1.0
 3,32.6,40.1,41.1,14.2,15.6,19.2,0.0,0,1.0

ONV
023,1985
 1,42.8,45.9,48.6,41.9,42.6,43.5,7.8,0,1.0
 2,39.7,45.1,48.7,38.5,39.4,39.7,8.8,0,1.0
 3,37.4,44.1,48.9,35.6,36.5,36.9,12.0,0,1.0

ONV
024,1985
 1,47.3,50.0,49.1,47.8,48.7,49.5,9.0,0,1.0
 2,43.7,49.1,49.3,44.1,45.3,45.9,8.5,0,1.0
 3,41.0,47.7,49.3,41.0,42.4,43.3,4.0,0,1.0


GNV
026,1985
  1,54.5,56.8,52.5,56.5,57.0,57.6,10.0,0,1.0
  2,51.6,55.6,52.7,53.8,54.5,54.9,9.0,0,1.0
  3,50.5,54.3,52.9,52.7,53.4,54.0,12.0,0,1.0

ONV
027,1985
 1,48.2,53.4,52.5,41.2,43.0,44.2,0.0,0,1.0
 2,43.0,51.8,52.7,31.3,34.5,35.4,0.0,0,1.0
 3,39.9,50.2,52.9,28.2,30.7,30.7,0.0,0,1.0

ONV
041,1985
 1,51.8,56.8,56.7,49.3,49.6,50.7,11.4,0,1.0
 2,46.8,55.4,56.7,37.2,40.6,41.4,0.0,0,1.0
 3,43.5,53.6,56.8,32.7,33.3,34.9,0.0,0,1.0

ONV
048,1985
 1,54.1,57.5,52.9,51.1,52.0,53.2,0.0,0,1.0
 2,48.6,56.5,53.1,42.1,45.3,46.9,0.0,0,1.0
 3,45.3,54.9,53.1,39.2,41.2,43.0,0,0,0,1.0
```

Modified P-model input files

```
343,1984
TAL
 1,25.0,0,0,0,0,0,0,0,0,.64
 2,28.7,0,0,0,0,0,0,0,0,.67
 3,26.4,0,0,0,0,0,0,0,0,.65
JAC
 1,13.6,0,0,0,0,0,0,0,0,.55
 2,27.9,0,0,0,0,0,0,0,0,.67
 3,26.9,0,0,0,0,0,0,0,0,.66
ONV
 1,23.5,0,0,0,0,0,0,0,0,.63
 2,29.1,0,0,0,0,0,0,0,0,.68
 3,27.9,0,0,0,0,0,0,0,0,.67
TAV
 1,26.0,0,0,0,0,0,0,0,0,.65
 2,30.7,0,0,0,0,0,0,0,0,.69
 3,30.4,0,0,0,0,0,0,0,0,.69
RUS
 1,37.0,0,0,0,0,0,0,0,0,.75
 2,37.2,0,0,0,0,0,0,0,0,.75
 3,40.2,0,0,0,0,0,0,0,0,.78
ARC
 1,35.0,0,0,0,0,0,0,0,0,.73
 2,32.3,0,0,0,0,0,0,0,0,.71
 3,31.6,0,0,0,0,0,0,0,0,.70
WES
 1,39.5,0,0,0,0,0,0,0,0,.78
 2,45.8,0,0,0,0,0,0,0,0,.84
 3,45.0,0,0,0,0,0,0,0,0,.83
BEL
 1,41.8,0,0,0,0,0,0,0,0,.80
 2,44.6,0,0,0,0,0,0,0,0,.83
 3,47.0,0,0,0,0,0,0,0,0,.85
IMM
 1,44.5,0,0,0,0,0,0,0,0,.83
 2,40.9,0,0,0,0,0,0,0,0,.79
 3,40.0,0,0,0,0,0,0,0,0,.78
HOM
 1,47.6,0,0,0,0,0,0,0,0,.86
 2,47.2,0,0,0,0,0,0,0,0,.86
 3,48.4,0,0,0,0,0,0,0,0,.87
```

```
0u6,1985
TAL
 1,37.8,0,0,0,0,0,0,0,0,.76
 2,34.6,0,0,0,0,0,0,0,0,.73
 3,33.1,0,0,0,0,0,0,0,0,.71
JAC
 1,38.3,0,0,0,0,0,0,0,0,.76
 2,36.0,0,0,0,0,0,0,0,0,.74
 3,33.8,0,0,0,0,0,0,0,0,.72
OAI
 1,37.4,0,0,0,0,0,0,0,0,.76
 2,35.0,0,0,0,0,0,0,0,0,.73
 3,33.4,0,0,0,0,0,0,0,0,.72
TAV
 1,-23.,0,0,0,0,0,0,0,0,.32
 2,-21.,0,0,0,0,0,0,0,0,.33
 3,39.1,0,0,0,0,0,0,0,0,.77
RUS
 1,-8.0,0,0,0,0,0,0,0,0,.40
 2,9.40,0,0,0,0,0,0,0,0,.52
 3,25.1,0,0,0,0,0,0,0,0,.64
ARC
 1,-13.,0,0,0,0,0,0,0,0,.37
 2,-.20,0,0,0,0,0,0,0,0,.45
 3,2.90,0,0,0,0,0,0,0,0,.47
WES
 1,47.6,0,0,0,0,0,0,0,0,.86
 2,48.6,0,0,0,0,0,0,0,0,.87
 3,47.3,0,0,0,0,0,0,0,0,.86
BEL
 1,44.0,0,0,0,0,0,0,0,0,.93
 2,45.9,0,0,0,0,0,0,0,0,.84
 3,52.6,0,0,0,0,0,0,0,0,.91
IMM
 1,50.0,0,0,0,0,0,0,0,0,.89
 2,48.5,0,0,0,0,0,0,0,0,.87
 3,46.9,0,0,0,0,0,0,0,0,.85
HOM
 1,42.1,0,0,0,0,0,0,0,0,.80
 2,47.4,0,0,0,0,0,0,0,0,.86
 3,40.1,0,0,0,0,0,0,0,0,.78
```

```
026,1985
TAL
 1,51.6,0,0,0,0,0,0,0,0,.90
 2,51.3,0,0,0,0,0,0,0,0,.90
 3,49.9,0,0,0,0,0,0,0,0,.88
JAC
 1,55.3,0,0,0,0,0,0,0,0,.95
 2,52.7,0,0,0,0,0,0,0,0,.92
 3,52.0,0,0,0,0,0,0,0,0,.91
OAI
 1,54.7,0,0,0,0,0,0,0,0,.94
 2,51.0,0,0,0,0,0,0,0,0,.90
 3,51.4,0,0,0,0,0,0,0,0,.90
TAV
 1,55.8,0,0,0,0,0,0,0,0,.95
 2,52.0,0,0,0,0,0,0,0,0,.91
 3,51.9,0,0,0,0,0,0,0,0,.91
RUS
 1,55.5,0,0,0,0,0,0,0,0,.95
 2,58.8,0,0,0,0,0,0,0,0,.99
 3,58.5,0,0,0,0,0,0,0,0,.98
ARC
 1,55.2,0,0,0,0,0,0,0,0,.94
 2,56.2,0,0,0,0,0,0,0,0,.96
 3,56.0,0,0,0,0,0,0,0,0,.95
WES
 1,41.1,0,0,0,0,0,0,0,0,.79
 2,41.1,0,0,0,0,0,0,0,0,.79
 3,38.4,0,0,0,0,0,0,0,0,.77
BEL
 1,42.1,0,0,0,0,0,0,0,0,.80
 2,41.8,0,0,0,0,0,0,0,0,.80
 3,40.0,0,0,0,0,0,0,0,0,.78
IMM
 1,42.0,0,0,0,0,0,0,0,0,.80
 2,41.9,0,0,0,0,0,0,0,0,.80
 3,40.4,0,0,0,0,0,0,0,0,.79
HOM
 1,43.5,0,0,0,0,0,0,0,0,.82
 2,46.7,0,0,0,0,0,0,0,0,.85
 3,43.5,0,0,0,0,0,0,0,0,.82
```

```
027,1985
TAL
 1,39.8,0,0,0,0,0,0,0,0,.78
 2,34.3,0,0,0,0,0,0,0,0,.73
 3,31.3,0,0,0,0,0,0,0,0,.70
JAC
 1,38.0,0,0,0,0,0,0,0,0,.76
 2,33.7,0,0,0,0,0,0,0,0,.72
 3,31.4,0,0,0,0,0,0,0,0,.70
OAI
 1,38.6,0,0,0,0,0,0,0,0,.77
 2,35.0,0,0,0,0,0,0,0,0,.73
 3,32.1,0,0,0,0,0,0,0,0,.71
TAV
 1,41.1,0,0,0,0,0,0,0,0,.79
 2,39.8,0,0,0,0,0,0,0,0,.78
 3,34.0,0,0,0,0,0,0,0,0,.72
RUS
 1,50.9,0,0,0,0,0,0,0,0,.90
 2,47.5,0,0,0,0,0,0,0,0,.86
 3,45.1,0,0,0,0,0,0,0,0,.83
ARC
 1,44.6,0,0,0,0,0,0,0,0,.83
 2,40.3,0,0,0,0,0,0,0,0,.78
 3,37.9,0,0,0,0,0,0,0,0,.76
WES
 1,48.7,0,0,0,0,0,0,0,0,.87
 2,49.0,0,0,0,0,0,0,0,0,.87
 3,48.0,0,0,0,0,0,0,0,0,.86
BEL
 1,52.8,0,0,0,0,0,0,0,0,.92
 2,53.3,0,0,0,0,0,0,0,0,.92
 3,48.9,0,0,0,0,0,0,0,0,.87
IMM
 1,52.2,0,0,0,0,0,0,0,0,.91
 2,49.3,0,0,0,0,0,0,0,0,.88
 3,46.4,0,0,0,0,0,0,0,0,.85
HOM
 1,55.2,0,0,0,0,0,0,0,0,.94
 2,53.7,0,0,0,0,0,0,0,0,.93
 3,51.6,0,0,0,0,0,0,0,0,.90
```

```
041,1985
TAL
 1,45.3,0,0,0,0,0,0,0,0,.84
 2,40.4,0,0,0,0,0,0,0,0,.79
 3,37.5,0,0,0,0,0,0,0,0,.76
JAC
 1,44.1,0,0,0,0,0,0,0,0,.82
 2,38.1,0,0,0,0,0,0,0,0,.76
 3,36.6,0,0,0,0,0,0,0,0,.75
OAI
 1,45.6,0,0,0,0,0,0,0,0,.84
 2,41.2,0,0,0,0,0,0,0,0,.79
 3,40.6,0,0,0,0,0,0,0,0,.79
TAV
 1,49.4,0,0,0,0,0,0,0,0,.88
 2,48.2,0,0,0,0,0,0,0,0,.87
 3,47.8,0,0,0,0,0,0,0,0,.86
RUS
 1,55.5,0,0,0,0,0,0,0,0,.95
 2,51.0,0,0,0,0,0,0,0,0,.90
 3,49.6,0,0,0,0,0,0,0,0,.88
ARC
 1,53.9,0,0,0,0,0,0,0,0,.93
 2,47.9,0,0,0,0,0,0,0,0,.86
 3,46.9,0,0,0,0,0,0,0,0,.85
WES
 1,56.0,0,0,0,0,0,0,0,0,.95
 2,50.4,0,0,0,0,0,0,0,0,.89
 3,49.6,0,0,0,0,0,0,0,0,.88
BEL
 1,56.1,0,0,0,0,0,0,0,0,.95
 2,53.7,0,0,0,0,0,0,0,0,.93
 3,49.6,0,0,0,0,0,0,0,0,.88
IMM
 1,57.8,0,0,0,0,0,0,0,0,.97
 2,54.1,0,0,0,0,0,0,0,0,.93
 3,51.2,0,0,0,0,0,0,0,0,.90
HOM
 1,58.2,0,0,0,0,0,0,0,0,.98
 2,54.4,0,0,0,0,0,0,0,0,.94
 3,52.6,0,0,0,0,0,0,0,0,.91
```

```
047,1985
TAL
 1,43.4,0,0,0,0,0,0,0,0,.82
 2,39.9,0,0,0,0,0,0,0,0,.78
 3,37.1,0,0,0,0,0,0,0,0,.75
JAC
 1,44.7,0,0,0,0,0,0,0,0,.83
 2,39.8,0,0,0,0,0,0,0,0,.78
 3,36.5,0,0,0,0,0,0,0,0,.75
OAI
 1,46.1,0,0,0,0,0,0,0,0,.84
 2,40.1,0,0,0,0,0,0,0,0,.78
 3,37.1,0,0,0,0,0,0,0,0,.75
TAV
 1,43.3,0,0,0,0,0,0,0,0,.81
 2,41.8,0,0,0,0,0,0,0,0,.80
 3,41.4,0,0,0,0,0,0,0,0,.80
RUS
 1,2.40,0,0,0,0,0,0,0,0,.47
 2,2.50,0,0,0,0,0,0,0,0,.47
 3,15.3,0,0,0,0,0,0,0,0,.56
ARC
 1,22.4,0,0,0,0,0,0,0,0,.62
 2,-.30,0,0,0,0,0,0,0,0,.45
 3,15.3,0,0,0,0,0,0,0,0,.56
WES
 1,11.1,0,0,0,0,0,0,0,0,.53
 2,8.20,0,0,0,0,0,0,0,0,.51
 3,8.80,0,0,0,0,0,0,0,0,.51
BEL
 1,12.7,0,0,0,0,0,0,0,0,.54
 2,8.70,0,0,0,0,0,0,0,0,.51
 3,12.4,0,0,0,0,0,0,0,0,.54
IMM
 1,15.1,0,0,0,0,0,0,0,0,.56
 2,14.1,0,0,0,0,0,0,0,0,.55
 3,15.9,0,0,0,0,0,0,0,0,.57
HOM
 1,22.2,0,0,0,0,0,0,0,0,.62
 2,26.0,0,0,0,0,0,0,0,0,.65
 3,30.2,0,0,0,0,0,0,0,0,.69
```

```
048 1985
TAL
 1,51.2,0,0,0,0,0,0,0,0,.90
 2,44.0,0,0,0,0,0,0,0,0,.82
 3,40.6,0,0,0,0,0,0,0,0,.79
JAC
 1,48.3,0,0,0,0,0,0,0,0,.87
 2,43.4,0,0,0,0,0,0,0,0,.82
 3,40.3,0,0,0,0,0,0,0,0,.78
OAI
 1,48.3,0,0,0,0,0,0,0,0,.87
 2,43.6,0,0,0,0,0,0,0,0,.82
 3,41.5,0,0,0,0,0,0,0,0,.80
TAV
 1,51.3,0,0,0,0,0,0,0,0,.90
 2,45.5,0,0,0,0,0,0,0,0,.84
 3,45.2,0,0,0,0,0,0,0,0,.83
RUS
 1,55.4,0,0,0,0,0,0,0,0,.95
 2,50.1,0,0,0,0,0,0,0,0,.89
 3,47.3,0,0,0,0,0,0,0,0,.86
ARC
 1,54.4,0,0,0,0,0,0,0,0,.94
 2,48.3,0,0,0,0,0,0,0,0,.87
 3,46.3,0,0,0,0,0,0,0,0,.85
WES
 1,56.2,0,0,0,0,0,0,0,0,.96
 2,51.5,0,0,0,0,0,0,0,0,.90
 3,48.8,0,0,0,0,0,0,0,0,.87
BEL
 1,56.2,0,0,0,0,0,0,0,0,.96
 2,50.3,0,0,0,0,0,0,0,0,.89
 3,47.4,0,0,0,0,0,0,0,0,.86
IMM
 1,51.8,0,0,0,0,0,0,0,0,.91
 2,51.4,0,0,0,0,0,0,0,0,.90
 3,48.3,0,0,0,0,0,0,0,0,.87
HOM
 1,59.7,0,0,0,0,0,0,0,0,1.0
 2,53.2,0,0,0,0,0,0,0,0,.92
 3,49.1,0,0,0,0,0,0,0,0,.88
```

REFERENCES

Anonymous. 1980. Geostationary Operational Environmental Satellite (GOES). GOES D,E,F Data Book. National Oceanic and Atmospheric Administration, Washington, D.C.

Armson, K.A. 1977. Forest Soils: Properties and Processes. University of Toronto Press, Toronto.

Aron, R.H. 1975. A method for estimating the number of hours below a selected temperature threshold. J. Appl. Meteor. 14:1415-18.

Barnett, U.R., J.D. Martsolf, and F.L. Crosby. 1980. Satellite temperature monitoring and prediction system. Proceedings of the 17th Space Congress. Cocoa Beach, Fla. May. Ch.4, pp. 9-20.

Bartholic, J.F., and J.D. Martsolf. 1979. Site selection. In: Modification of the Aerial Environment of Crops. B.J. Barfield and J.F. Gerber, Eds. American Society of Agricultural Engineers, St. Joseph, Mich. pp. 281-290.

Bartholic, J.F., and R.A. Sutherland. 1978. Future freeze forecasting. Proc. Fla. State Hort. Soc. 91:334-336.

Blackadar, A.K. 1976. Modeling the nocturnal boundary layer. Preprint from the Third Symposium on Atmospheric Turbulence, Diffusion, and Air Quality. Raleigh, N.C. Oct. 9-12. pp. 46-70.

Blackadar, A.K. 1979. High-resolution models of the planetary boundary layer. In: Advances in Environmental Science and Engineering. Vol. 1. J.R. Pfafflin and E.N. Ziegler, Eds. Gordon and Breach, New York. pp. 50-85.

Blackadar, A.K., and H. Tennekes. 1968. Asymptotic similarity in neutral baratropic planetary boundary layers. J. Atmos. Sci. 25:181-189.

Brady, N.C. 1974. The Nature and Properties of Soils. Macmillan Publishing Co., New York.

Burden, R.L., J.D. Faires, and A.C. Reynolds. 1978. Numerical Analysis. Prindle, Weber, and Schmidt, Boston.

Cahir, J.J., T.N. Carlson, and J.D. Lee. 1978. A Laboratory Course in Synoptic Meteorology. Department of Meteorology, The Pennsylvania State University.

Carlson, T.N., and F.E. Boland. 1978. Analysis of urban-rural canopy using a surface heat flux/temperature model. J. Appl. Meteor. 17:998-1013.

Charney, J.G. 1949. On a physical basis for numerical prediction of large-scale motions in the atmosphere. J. Meteor. 6:371-385.

Chen, E., L.H. Allen, Jr., J.F. Bartholic, and J.F. Gerber. 1983. Comparison of winter-nocturnal geostationary satellite infrared-surface temperature with shelter-height temperature in Florida. Remote Sensing of Environment. 13:313-327.

Clarke, R.H., A.J. Dyer, R.R. Brook, D.G. Reid, and A.J. Troup. 1971. The Wangara Experiment: Boundary Layer Data. Division of Meteorological Physics Technical Paper no. 19. CSIRO, Australia. pp. 3-21.

Deardorff, J.W. 1977. A parameterization of ground-surface moisture content for use in atmospheric prediction models. J. Appl. Meteor. 16:1182-5.

Gaby, D.C. 1980. Comments on "A real-time satellite data acquisition, analysis, and display system--a practical application of the GOES network." J. Appl. Meteor. 19:341.

Georg, J.G. 1971. A Numerical Model for Prediction of the Nocturnal Temperature in the Atmospheric Surface Layer. M.S. Thesis: University of Florida, Gainesville, Fla.

Gerber, J.F., and D.S. Harrison. 1964. Sprinkler irrigation for cold protection of citrus. Trans. Amer. Soc. Agr. Eng. 7:464-468.

Haltiner, G.J. 1971. Numerical Weather Prediction. John Wiley and Sons, New York. pp. 128-147.

Hansen, J.E., and D.M. Driscoll. 1977. A mathematical model for the generation of hourly temperatures. J. Appl. Meteor. 16:935-48.

Heinemann, P.H., and J.D. Martsolf. 1984. Prediction of frost night temperatures through use of GOES East satellite data and temperature prediction models. Proceedings of the Conference on Satellite/Remote Sensing and Applications. American Meteorological Society. Clearwater Beach, Fla. June 25-29. pp. 240-241.

Heinemann, P.H., J.D. Martsolf, and J.F. Gerber. 1985. Development and dissemination of temperature predictions for the Satellite Frost Forecast System. Proceedings of the 17th Conference on Agricultural and Forest Meteorology. American Meteorological Society. Scottsdale, Az. May 21-24. pp. 65-67.

Heinemann, P.H., J.D. Martsolf, J.F. Gerber, and D.L. Smith. 1984. Development of manually digitized radar and GOES IR composite products. Proceedings of the Conference on Satellite/Remote Sensing and Applications. American Meteorological Society. Clearwater Beach, Fla. June 25-29. pp. 242-244.

Holton, J.R. 1979. An Introduction to Dynamic Meteorology. Academic Press, New York. pp. 173-213.

Iribarne, J.V., and W.L. Godson. 1973. Atmospheric Thermodynamics. D. Reidel Publ. Co., Boston.

Jackson, J.L., and F. Ferguson, Jr. 1983. An experimental computer network for growers. Proc. Fla. State Hort. Soc. 96:5-7.

Jedlovic, G.J. 1985. An evaluation and comparison of vertical profile data from the VISSR atmospheric sounder (VAS). NASA Technical Paper #2425. National Aeronatics and Space Administration, Greenbelt, Md.

Kerr, R.A. 1985a. Forecasting the weather a bit better. Science. 228:40-41.

Kerr, R.A. 1985b. The next lap in the race. Science. 228:705.

Kolsky, H.G. 1972. An Introduction to Computer Simulation in Applied Science. Plenum Press, New York. pp. 173-213.

Little, T.M., and F.J. Hills. 1978. Agricultural Experimentation. John Wiley and Sons, Inc., New York. pp. 167-194.

Martsolf, J.D. 1979a. Frost protection: A rapidly changing program. Fla. State Hort. Soc. 92:22-25.

Martsolf, J.D. 1979b. Heating for frost protection. In: Modification of the Aerial Environment of Crops. B.J. Barfield and J.F. Gerber, Eds. American Society of Agricultural Engineers, St. Joseph, Mich. pp. 291-314.

Martsolf, J.D. 1980. An improved satellite frost warning system. Proc. Fla. State Hort. Soc. 93:41-44.

Martsolf, J.D. 1981. About our cover: Satellite Frost Forecast System. HortScience. 16:586.

Martsolf, J.D. 1982. Satellite thermal maps provide detailed views and comparisons of freezes. Proc. Fla. State Hort. Soc. 95:14-20.

Martsolf, J.D. 1983a. Florida frost information and dissemination system. Proceedings of the Conference on Cooperative Climate Services. NOAA National Climate Program Office. Tallahassee, Fla. March 22-24. pp. 209-227.

Martsolf, J.D. 1983b. Satellite Frost Forecast System, Phase VI. Final report to NASA/KSC. Contract No. NAS10-9892. April 14.

Martsolf, J.D., and J.F. Gerber. 1981. Florida Frost Forecast System documents freezes of January, 1981, and is refined for future seasons. Proc. Fla. State Hort. Soc. 94:39-43.

Martsolf, J.D., P.H. Heinemann, and J.F. Gerber. 1985. Demonstration: Personal computer interrogation of the Satellite Frost Forecast System. Proceedings of the 17th Conference on Agricultural and Forest Meteorology. Amercian Meteorological Society. Scottsdale, Az. pp. 185-188.

Martsolf, J.D., P.H. Heinemann, J.F. Gerber, F.L. Crosby, and D.L. Smith. 1984. Rapid weather information dissemination in Florida. Proceedings of the 10th Conference on Weather Forecasting and Analysis. American Meteorological Society. Clearwater Beach, Fla. June 25-29. pp. 208-210.

McIntosh, D.H. 1972. Meteorological Glossary. Chemical Publishing Co., New York.

Merva, G.E. 1975. Physioengineering Principles. AVI Publishing Company, Inc., Westport, Conn.

Miller, R.G. 1981. GEM: A statistical weather forecasting procedure. NOAA Technical Report NWS 28. The National Oceanic and Atmospheric Administration, Silver Spring, Md.

Monteith, J.L. 1980. Principles of Environmental Physics. Edward Arnold, Ltd., Whitstable, Kent, England.

Parton, W.J., and J.A. Logan. 1981. A model for diurnal variation in soil and air temperature. Agricul. Meteor. 23:205-216.

Perry, K.B., C.T. Morrow, A.R. Jarrett, and J.D. Martsolf. 1982. Evaluation of sprinkler rate application models used in frost protection. HortSci. 17:884-885.

Petersen, E.L. 1976. A model for the simulation of atmospheric turbulence. J. Appl. Meteor. 15:571-87.

Petterssen, S. 1956. Weather Analysis and Forecasting. McGraw-Hill Book Co., New York. 371-387.

Pielke, R.A. 1974. A three-dimensional numerical model of the sea breezes over south Florida. Month. Weath. Rev. 102:115-139.

Priestly, C.H.B. 1959. Turbulent Transfer in the Lower Atmosphere. The University of Chicago Press, Chicago.

Richardson, L.F. 1922. Weather Prediction by Numerical Process. Cambridge University Press, London.

Rosenberg, N.J. 1974. Microclimate: The Biological Environment. John Wiley and Sons, New York.

Sellers, W.D. 1965. Physical Climatology. University of Chicago Press, Chicago.

Shaw, R. 1981. Comments on "A short-range objective nocturnal temperature forecasting model." J. Appl. Meteor. 20:95-96.

Shuman, F.G., and J.B. Hovermale. 1968. An operational six-layer primitive equation model. J. Appl. Meteor. 7:525-547.

Sutherland, R.A. 1980. A short-range objective nocturnal temperature forecasting model. J. Appl. Meteor. 19:247-255.

Sutherland, R.A. 1981. Reply. J. Appl. Meteor. 20:96-97.

Sutherland, R.A., J.L. Langford, J.F. Bartholic, and R.G. Bill, Jr. 1979. A real-time satellite data acquisition, analysis, and display system--A practical application of the GOES network. J. Appl. Meteor. 18:355-360.

Sutton, O.G. 1953. Micrometeorology: A Study of Physical Processes in the Lowest Layers of the Earth's Atmosphere. McGraw-Hill Book Co., New York.

Tiedtke, M. 1983. Winter and summer simulations with the ECMWF model. In: Workshop on Intercomparison of Large Scale Models Used for Extended Range Forecasts. Reading, England. June 30-July 2. pp. 263-313.

Van Wijk, W.R. 1963. Physics of Plant Environment. North-Holland Pub. Co., Amsterdam.

Waggoner, P.E., G.M. Furnival, and W.E. Reifsnyder. 1969. Simulation of the microclimate in a forest. For. Sci. 15:37-45.

Welles, J.M., J.M. Norman, and J.D. Martsolf. 1979. An orchard foliage temperature model. J. Amer. Soc. Hort. Sci. 104:602-610.

Welles, J.M., J.M. Norman, and J.D. Martsolf. 1981. Modelling the radiant output of orchard heaters. Agricul. Meteorol. 23:275-286.

Wierenga, P.J., and C.T. de Wit. 1970. Simulation of heat flow in soils. Soil Sci. Soc. Amer. Proc. 34:845-848.

Willmott, C.J. 1984. On the evaluation of model performance in physical geography. In: Spatial Statistics and Models. G.L. Gaile and C.J. Willmott, Eds. D. Reidel Publishing Co., Dordrecht, Holland. pp. 443-460.

BIOGRAPHICAL SKETCH

Paul Heinz Heinemann was born next to the easternmost range of the Blue Ridge Mountains in Frederick, Maryland, on April 16, 1958. After living in several places during his first seven years of life, including Hagerstown, Maryland, Norristown, Pennsylvania, Charleston, West Virginia, and Fredericksburg, Virginia, he finally stayed in one place for a while after moving to Wyncote, Pennsylvania in 1965. Although brought up in a suburban Philadelphia environment, he always felt compelled to return to the mountains whenever possible.

Paul began his college career in the fall of 1976 as a forestry major at the Penn State University branch campus known as Mont Alto. Mont Alto was originally the Penn State Forestry School, and is a beautiful location set in the mountains, woods and orchards of south central Pennsylvania. It was here, however, that Paul decided to become a meteorologist.

Paul transferred up to the University Park Campus of Penn State in the fall of 1978. It was there that he found out what meteorology was really all about. The opportunity arose to do some agricultural meteorological instrumentation work with the Agricultural Engineering Department in the spring of 1979, which got him interested in the field of agricultural meteorology.

After graduating with a B.S. in meteorology in May of 1980, Paul switched over to the Agricultural Engineering Department to pursue a Master of Science degree working in frost protection. He received the M.S. degree in November, 1982.

The opportunity to work in the University of Florida's Climatology lab, along with the chance to see what it was like to live in another part of the country, persuaded Paul to move south and begin an assistantship in the Fruit Crops Department. He worked on boundary layer modeling to predict temperatures during frost nights for his doctorate research, and expects to graduate from the University of Florida in December, 1985, with a Ph.D.

Paul spends his free time playing soccer, playing guitar and singing in a band, and involving himself with church activities. As of this writing he is single and eligible, but doesn't intend to stay that way forever.

I certify that I have read this study and that in my opinion it conforms to acceptable standards of scholarly presentation and is fully adequate, in scope and quality, as a dissertation for the degree of Doctor of Philosophy.

J. David Martsolf, Chairman
Professor of Horticultural
Science

I certify that I have read this study and that in my opinion it conforms to acceptable standards of scholarly presentation and is fully adequate, in scope and quality, as a dissertation for the degree of Doctor of Philosophy.

John F. Gerber
Professor of Horticultural
Science

I certify that I have read this study and that in my opinion it conforms to acceptable standards of scholarly presentation and is fully adequate, in scope and quality, as a dissertation for the degree of Doctor of Philosophy.

James W. Jones
Professor of Agricultural
Engineering

I certify that I have read this study and that in my opinion it conforms to acceptable standards of scholarly presentation and is fully adequate, in scope and quality, as a dissertation for the degree of Doctor of Philosophy.

James A. Henry
Associate Professor of
Geography

This dissertation was submitted to the Graduate Faculty of the College of Agriculture and to the Graduate School and was accepted as partial fulfillment of the requirements for the degree of Doctor of Philosophy.

December 1985

Jack L. Fry
Dean, College of Agriculture

Dean, Graduate School